CHALMERS
UNIVERSITY OF TECHNOLOGY

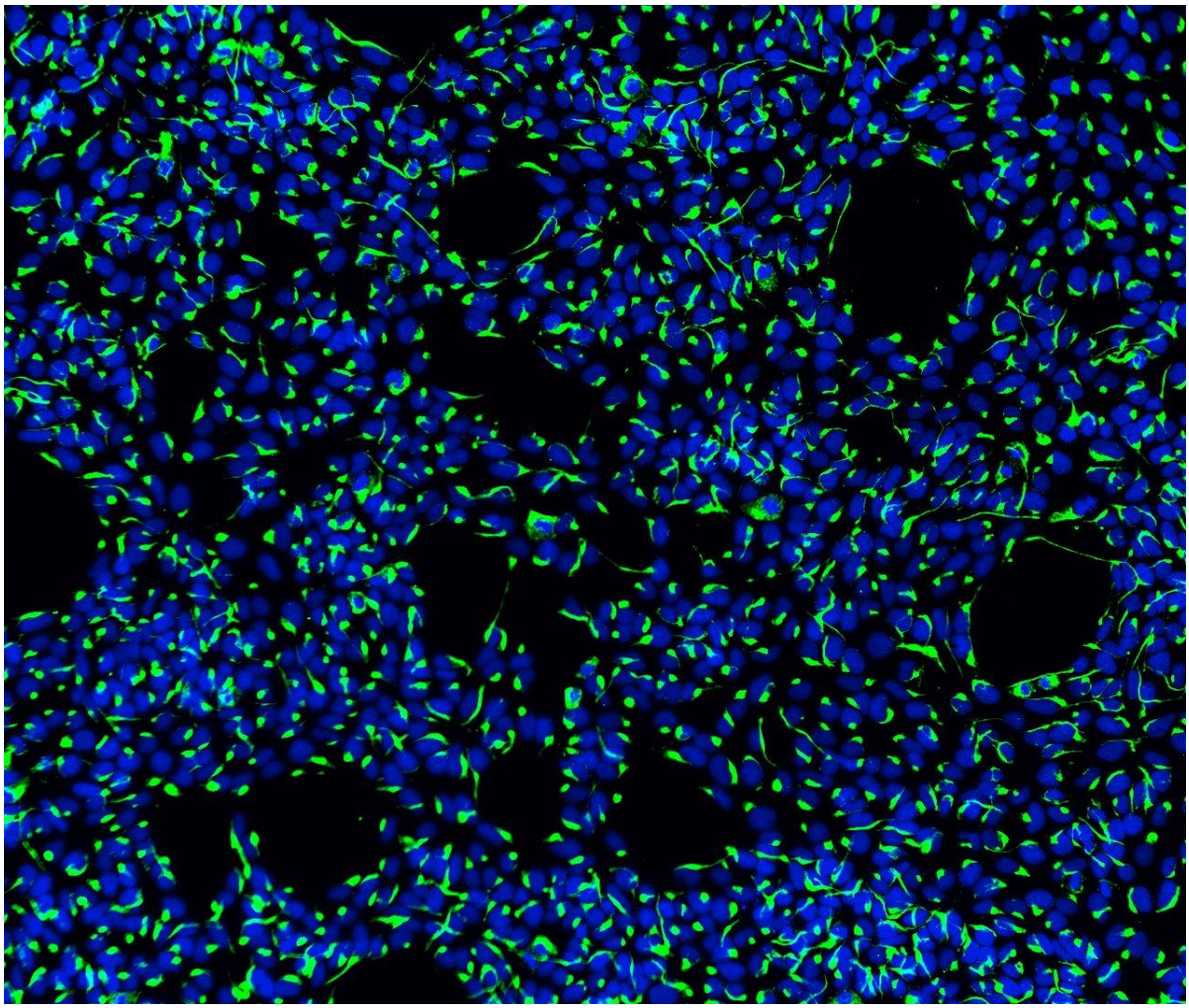

Evaluation of Small Molecules for Neuroectoderm differentiation & patterning using Factorial Experimental Design

Master Thesis in Applied Physics
For the degree of Master of Science in Biotechnology

DIMITRIOS VOULGARIS

Department of Physics, Division of Biological Physics
CHALMERS UNIVERSITY OF TECHNOLOGY
Göteborg, Sweden 2016

Master thesis in Applied Physics

Evaluation of Small Molecules for Neuroectoderm differentiation and patterning using Factorial Experimental Design

Dimitrios Voulgaris

Department of Physics
Division of Biological Physics
CHALMERS UNIVERSITY OF TECHNOLOGY
Göteborg, Sweden 2016

Evaluation of Small Molecules for Neuroectoderm differentiation and patterning using Factorial Experimental Design
DIMITRIOS VOULGARIS

Supervisor: Anders Lundin, Industrial PhD candidate, Astra Zeneca and Karolinska Institutet

Examiner: Julie Gold, Associate Professor, Division of Biological Physics, Department of Physics, Chalmers University of Technology

Master thesis for the degree of M.Sc. in Biotechnology
Division of Biological Physics
Department of Physics
Chalmers University of Technology
SE-142 96 Göteborg
Sweden
Telephone +46 (0)31-722 1000

Cover: hiPSCs differentiated for 4 days on LN-521 in neural induction N2B27 medium stained with DAPI (blue) and the intermediate filament Nestin (green).

Printed by Chalmers Reproservice
Göteborg, Sweden 2016
Evaluation of Small Molecules for Neuroectoderm differentiation and patterning using Factorial Experimental Design
DIMITRIOS VOULGARIS
Department of Physics
Chalmers University of Technology

Evaluation of Small Molecules for Neuroectoderm differentiation and patterning using Factorial Experimental Design

DIMITRIOS VOULGARIS
Department of Physics
Chalmers University of Technology

ABSTRACT

Screening for therapeutic compounds and treatments for diseases of the Brain does not only encompass the successful generation of iPS-derived homogenous neural stem cell populations but also the capacity of the differentiation protocol to derive on-demand region-specific cells. Noggin, a human recombinant protein, has been extensively used in neural induction protocols but its high production costs and batch-to-batch variation have switched the focus to utilizing small molecules that can substitute noggin. Resultantly, the aim of this study was to optimize neuroepithelial stem cell generation in a cost-efficient fashion as well as to evaluate the impact that patterning factors (i.e. small molecules or proteins that enhance the emergence of type-specific neuronal populations) have on the regionality of the neural stem cell population. Findings in this study suggest that DMH1 is indeed a small molecule that can replace noggin in neural induction protocols as previously documented in literature; DMH1 appears also to have a ventralizing effect on the generated neural population.

Keywords: induced pluripotent stem cells, neuroectoderm differentiation, small molecules, factorial experimental design.

Acknowledgements

Firstly, I would like to express my gratitude to my thesis advisor, PhD candidate, Anders Lundin (Karolinska Institutet and AstraZeneca), for his continuous guidance, motivation and excellent support throughout this thesis, his inspirational tutoring was pivotal to the successful completion of this thesis.

I would also like to thank my academic thesis advisor Associate Professor, Julie Gold (Department of Physics, Chalmers University of Technology), for her guidance in the writing of this thesis as well as her comments which always posed a source for improvement of my thought process and academic writing.

I am deeply grateful to Cecilia Boreström and Anna Jonebring for all the scientific discussions throughout my thesis. Moreover I would like to express my sincere appreciation to Louise Stjernborg, Anette Kry-Persson and Anna Svensson for their advice and support in the lab.

I would like to thank Josefina Kristensson, Märta Jansson, Louise Delsing and Cecilia Graneli for the wonderful company in the office during my stay at AstraZeneca and Ryan Hicks and the rest of the iPSC team for welcoming me into the team.

Last but not least I would like to thank my family for believing in me and for all the support they have provided me throughout the years, the greatest gift I have ever and will ever receive. I dedicate this thesis to my father.

Abbreviations

hiPSCs: Human Induced pluripotent stem cells
hESCs: Human embryoid stem cells
TGFβ: Transforming growth factor beta
BMPs: Bone morphogenetic proteins
SMAD: Portmanteau of the protein SMA (Caenorhabditis Elegans) and the Drosophilia protein Mothers Against Decapentaplegic (MAD)
R-SMAD: Receptor-regulated SMAD
co-SMAD: Common-mediator SMAD
ICC: Immunocytochemistry
PCR: Polymerase Chain Reaction
EB: Embryoid Body
ECM: Extracellular Matrix
ICM: Inner Cell Mass
GW: Gestational week
PNS: Peripheral Nervous System
SHH: Sonic Hedgehog
MHP: Median Hinge Point
NES cells: Neuroepithelial stem cells
Wnt: Wingless-related integration site
NI: Neural Induction
SMs: Smalls Molecules
FED: Factorial Experimental Design
ALK: activin receptor-like kinase
Fz: Frizzled

Table of Contents

Chapter 1: Purpose and Significance of the Study

1.1 Introduction

The emergence of induced pluripotent stem cells (iPSCs) via the reprogramming of somatic cells in response to external stimuli (Takahashi and Yamanaka 2006, Takahashi, Tanabe et al. 2007) represent a milestone in the way scientists approached the concept of personalized medicine and drug screening.

The reprogramming of somatic cells to iPSCs can be carried out with the introduction of the Yamanaka factors (Oct4, Sox2, cMyc and Klf4) using lentiviruses (Yu, Vodyanik et al. 2007). Integration-free approaches have been also shown to facilitate the reprogramming of somatic cells to iPSCs using sendai viruses (Fusaki, Ban et al. 2009) and miRNA techniques (Judson, Babiarz et al. 2009).

Out of the many organs of the human body, the brain is arguably one of the most complicated organs. Brain development is a complicated process and its predominant feature lies in the orchestration of distinct, yet interactive, variables such as intrinsic and extrinsic signals that generate concentration gradients of morphogens/growth factors. The interplay between these signals imparts region-specific cellular functionality which gives rise to the structure of the mature brain.

Understanding the underlying mechanisms of brain development and simulating in vitro these extrinsic and intrinsic signals would contribute greatly to the generation of in vitro models. These models can be used for drug screening for neurodegenerative and neurodevelopmental diseases.

A plethora of applications were rendered feasible by utilizing hiPSCs whilst avoiding the controversy and the ethical restrictions that revolved around the use of human embryonic stem cells (hESCs). As a result, exhaustive studies focusing on the induction of hiPSCs to the three germ layers have been undertaken by the scientific community aiming at optimizing differentiation protocols and yields as well as the evaluation whether hiPSCs do indeed pose an alternative to hESCs.

Recent studies have focused on generating robust and highly efficient protocols which can give rise to homogenous cell populations via the differentiation of hiPSCs towards the neuroectoderm. A vital stimulus in neural induction is the failure of the Bone Morphogenetic Proteins (BMPs) -4 to bind to their cell membrane receptors rendering the downstream activation of genes associated with non-neural germ layers not possible. The BMP-4 inhibition is mediated by proteins such as noggin which act by masking the active site of BMP-4.

In 2009, Chambers et al utilized noggin, a BMP-4 inhibitor, and SB431542, a small molecule that has been documented to enhance neural conversion, in a single chemically defined protocol yielding a high neural conversion. However, noggin is a human recombinant protein which entails high production costs and, more importantly, batch-to-batch variation tampering the robustness of protocols (Neely, Litt et al. 2012, Surmacz, Fox et al. 2012). Hence, small molecules (SMs) that can simulate noggin's action have been investigated in literature.

1.2 Aim

Neuroectoderm differentiation, in other words, the generation of neuroepithelial stem cells (NES, also referred to as neural stem cells) that are characterized by homogeneous neural conversion of hiPSCs (and hence avoiding the tedious mechanical isolation of colonies of interest) would greatly improve the scaling up of assays in a time- and cost-effective manner. Therefore, highly efficient neuroectoderm differentiation protocols are constantly being developed.

The aim of this master thesis is to evaluate and optimize the neuroectoderm differentiation protocol based on Chambers et al (2009). What this optimization entails is the replacement of the BMP-4 inhibitor, noggin, with pharmacological BMP-4 inhibitors (small molecules). The evaluation of the alternative BMP-4 inhibitor will be performed by employing a Factorial Experimental Design.

Variables that were considered and evaluated for their implications in the differentiation are: the seeding density, the type and concentrations of proteins/small molecules implicated in the neuroectoderm induction to evaluate the cell's progression from a pluripotent to a more fate-restricted cell state.

Small molecules – unlike human recombinant proteins such as noggin – are manufactured with high purity and therefore batch-to-batch variations are almost negligible. Moreover, costs associated with SMs are greatly reduced compared to that of human recombinant proteins, hence, there is a need to evaluate the capacity of SMs ,whose performance imitates that of noggin's, to drive hiPSCs into the neuroectoderm.

1.3 Limitations

The factor of time was one of the greatest limitations as there are seemingly endless combinations of the abovementioned variables. To validate and derive sufficient data in order to validate how one variable affects the other and vice versa would exceed the time required for a one year master thesis.

In this project, only one culturing system was used; LN521-Nutristem® with the r-IPSC 1j line. How and to which extend different culturing systems affect the differentiation in a whole was not evaluated. Furthermore the protocol was used on the same hiPSC line throughout this project. Different generations of hiPSCs may share different characteristics (e.g. concentrations of endogenous proteins).

The passage number of the cell line was also not considered. All differentiations were carried out in passage number less than 25 though the passage number for each differentiation was not the same.

Chapter 2: Background & Literature Overview

2.1 Embryogenesis

Embryogenesis is initiated by the fusion of an oocyte with a spermatozoon which gives rise to the totipotent zygote. After successive cleavage divisions the zygote assumes the structure of the morula at the fourth day post-conception. The morula is a 16-cell mass structure which, at 4.5 days post-conception, undergoes transformation and assumes a hollow-like spherical structure, the blastocyst (Figure 1 & Figure 2a).

In more detail, during the transformation of the Morula to the blastocyst, which is known as blastulation, cells of the outer cell layer of the morula (blastomeres) come together forming a tightly packed cell mass called Inner Cell Mass (ICM) which is supported by the formation of desmosomes and gap junctions, this process is referred to as compaction (Mercader 2008). The end structure of the compaction (blastocyst) resembles a hollow ball consisting of the ICM, the blastocyst cavity (blastocoele) and the outer cell layer, the trophoblast (Figure 1).

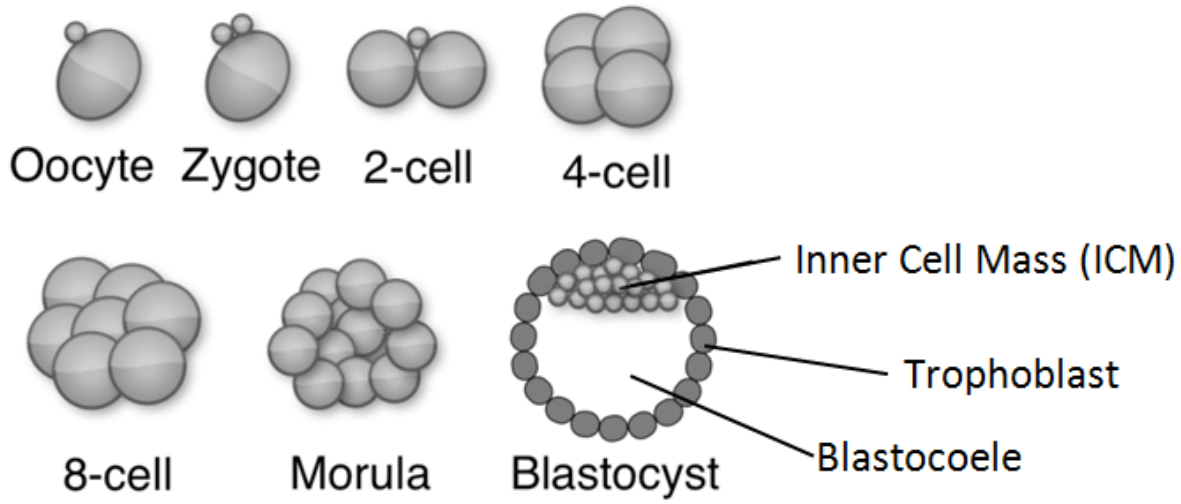

Figure 1 *Stages of early embryogenesis. After the fusion of the oocyte with the spermatozoon the resulting structure (Zygote) undergoes successive cleavage divisions assuming a 16-cell mass structure, the morula, after 4 days post-conception. The morula gives rise to the blastocyst after approximately 4.5 days post-conception. The blastocyst is now composed of a cavity with fluid called blastocoele, the ICM and the Trophoblast layer. Adapted from (Racaniello 2015).*

The two different cell lineages, cells of the trophoblast and ICM, are physically and functionally distinct; composing the first cell lineage specification in Embryogenesis. The trophoblast layer gives rise to the placenta, chorion and umbilical cord while the ICM gives rise via gastrulation to the three primary germ layers: ectoderm, mesoderm and endoderm (Gilbert 2006). The following section only focuses on the further development of the ICM.

Succeeding the blastulation, the delamination of the ICM to form the hypoblast and epiblast layers takes place in the second Gestational week (GW). Cells of the ICM which are in direct contact with the fluid in the blastocoele formulate the hypoblast while cells positioned in the exterior walls of the blastocyst (i.e. cells that are attached or are in closer proximity to the trophoblast layer) formulate the epiblast (Lewis 2007).

The epiblast and the hypoblast layers form together a disc-like structure, the bilaminar germ disc. At this point in the embryogenesis the amniotic sac and yolk sac develop (Figure 2b). The amniotic sac is formed by the delamination of some cells of the Epiblast. Cells of the hypoblast start proliferating and expanding laterally assuming the structure of the yolk sac (Figure 2b). Later on the amniotic sac hosts the embryo for further development while the yolk sac facilitates blood supply to the embryo.

The remaining cells of the hypoblast give rise to the extra embryonic tissues while the cells of the epiblast generate the three primary germ layers: the endoderm, mesoderm and ectoderm (Figure 2c). The endoderm gives rise to structures such as the interior lining of the gastrointestinal tract (e.g. liver, pancreas) (Zaret 2001) , the Respiratory tract (e.g. lungs) and thymus. The mesoderm gives rise to muscle tissue, cartilage, bone and the vascular system.

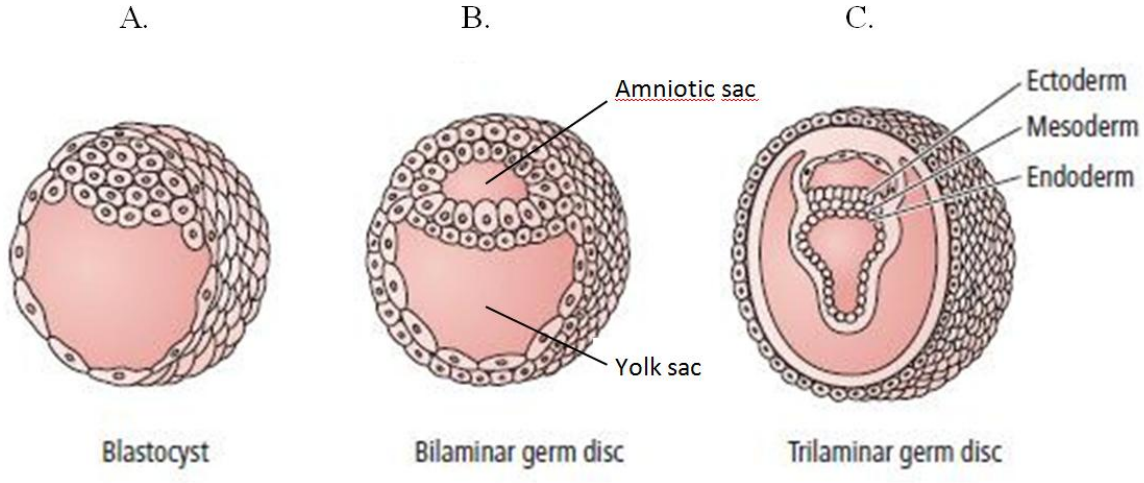

Figure 2 *The delamination of the Blastocyst results in a disc-like structure, the trilaminar germ disc.* ***a.*** *The blastocyst forms 4.5 days post-conception, resembling a hollow-ball structure.* ***b.*** *The epiblast and hypoblast layer, collectively known as the bilaminar germ disc, give rise to the amnioctic and yolk sac.* ***c.*** *The delamination of the epiblast gives rise to the trilaminar germ disc which consists of the three germ layers, ectoderm mesoderm and endoderm. Adapted from (Maria Patestas 2006).*

The ectoderm later on divides into two types of ectodermal layer stem cells: the epidermal ectodermal and neuroectodermal layer. The former gives rise to structures such as skin and nails while the latter forms the nervous system (Stiles and Jernigan 2010).

The process of Gastrulation takes place in GW2 and is initiated by the emergence of a slit-like transient structure, namely the primitive streak, which is situated dorsally of the developing embryo and extends to the anterior and posterior end, (Figure 3a). The structure of the primitive streak is formed at the point where two counter-rotating cell flows coalesce and extend anteriorly in a fashion which in 1929 Graeper referred to as polonaise movements.

The formation of the primitive streak dictates the symmetry of the developing embryo (rostral-caudal body axe). At the rostral end of the primitive streak lies a structure that is greatly implicated in cellular signalling, the primitive node (Downs 2009). The primitive node consists one of the organizers in embryogenesis called Spermann-Mangold Organizer (in amphibians) or Organizer (Sander and Faessler 2001) and greatly regulates the generation of the germ layers. The primitive node and primitive streak correspond to the rostral and caudal ends, respectively, of the developing embryo.

Cells of the epiblast layer start to ingress and migrate towards the primitive streak where ,upon arrival, detach from the epiblast and move downwards to the area between the epiblast and hypoblast layers, a process widely known as invagination (Figure 3b) (Downs 2009). The first wave of migrating cells displaces the hypoblast and forms the endoderm. Following the formation of the endoderm, cells continue to move towards the newly formed endoderm, establishing the mesoderm while the remaining cells in the epiblast form the ectoderm (Figure 3c).

The aforementioned process, the generation of the germ layers, as well as the ensuing course of events in the embryogenesis are vastly governed by the affinity between the germ layers which is coordinated by the transmembrane proteins Cadherins. The type of Cadherins and the upregulation/downregulation of the expression of Cadherins are among the variables that regulate such affinity (Gilbert 2006).

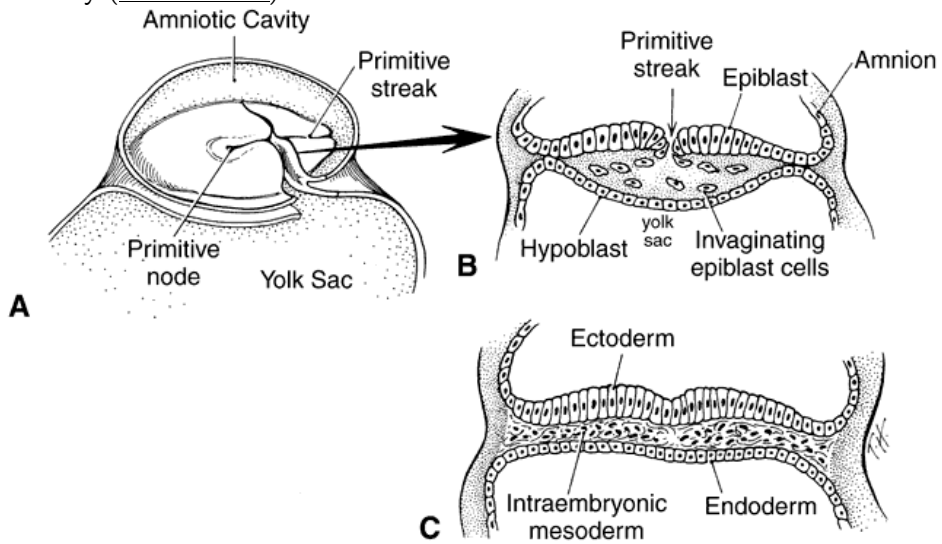

Figure 3 *The emergence of the primitive streak is the onset of gastrulation* ***a.*** *The formation of the primitive streak is pivotal for the generation of the body axes (e.g. rostrocaudal axis, the emergence of the primitive node is also of great importance since it assumes the role of the organizer in early embryogenesis.* ***b.*** *Following the formation of the primitive streak epiblast cells ingress and detach from the epiblast invaginating the space between the hypoblast and epiblast layer.* ***c.*** *Following the invagination process, the first wave of cells displace cells of the hypoblast forming the endoderm, a second wave of cells forms the mesoderm while the remaining cells of the epiblast give rise to the ectoderm. Adapted from (Duane 1993).*

2.2 Induced Pluripotent Stem Cells

Induced pluripotent stem cells - much like ESCs - are able to generate all three germ layers: ectoderm, mesoderm and endoderm. The presence, or lack thereof, of specific growth factors (e.g. Bone morphogenetic proteins) and molecules facilitate the downstream reaction cascades that result in enabling other molecules to act as transcription factors regulating gene expression.

Simulating in vitro the later parts of the early Embryogenesis and deriving on-demand specific germ layers has been a vibrant area of research over the years only to be intercepted by the various ethical issues and constraints that emerge from the clinical utilization of hESCs (Siegel 2013), an obstacle that undoubtedly put a halt in the progression of hESCs in clinical applications. Induced pluripotent stem cells paved the way for an alternative approach that altogether enabled scientists to avoid the ethical controversy of hESCs.

Induced Pluripotent Stem Cells are most commonly generated by reprogramming harvested human fibroblasts or using even less invasive procedures such as harvesting renal epithelial cells present in the urine (Zhou, Benda et al. 2012). Recent studies have suggested that there are not significant differences in the performance of hiPSCs and hESCs for when the same differentiation protocols were carried out, the end-product was the same in both cases (Spence, Mayhew et al. 2011, Emdad, D'Souza et al. 2012).

The expansion and differentiation of hESCs and hiPSCs are facilitated by Embryoid Body (EB) formation (Keller 1995), feeder layers consisting of stromal cells (Nakano, Kodama et al. 1994) or Extracellular matrix (ECM) -based culture substrates (Bhattacharyya, Kumar et al. 2012) with the addition of ROCKi which allows for single-cell growth (without EB formation) by minimizing the death associated with the dissociation of iPSCs. Utilizing ECM-based culture substrates is more favorable because it enables xeno-free and feeder-free conditions which reduce variability in the differentiation protocols as well as being cost-efficient.

2.3 Brain development

Brain development poses an extremely complicated process, hence, it is only reasonable that brain development is characterized by highly regulated mechanisms that dictate the development of the brain; such coordinated mechanisms involve molecular as well as cellular signaling.

Brain development starts in GW3 and it is postulated that molecular cues emanating from a mesoderm-derived structure, the notochord, initiates the ensuing events of brain development (Smith and Schoenwolf 1989). In a simplified overview of brain development, the ectoderm upon the presence or lack thereof of specific morphogens gives rise to the neural plate (neuroepithelium), neural folds and epidermal ectoderm.

The neural plate by altering its conformation (concurrently with the neural folds) give rises to the neural tube (Neurulation) and neural crest (Larsen 2001). The neural folds become the neural crest which later on gives rise to a number of different cell lineages such as neurons and glia of the peripheral nervous system (PNS), melanocytes, smooth muscle cells as well as cartilage and bone of the cranium and face (Huang and Saint-Jeannet 2004).

The neural tube embodies all the different types of neural progenitor cells that eventually differentiate to different neural cell populations of the CNS. These different neural cell populations have distinct functionalities and based on which they give rise to the various parts of the human brain. The neural tube constitutes the first well-defined structure in brain development.

2.3.1 Ectodermal fate

The formation of the neural plate, neural crest and epidermis is governed by the expression of morphogens by stem cell niches such as the notochord and other organizing centers (Sander and Faessler 2001) referred collectively as the organizers. The superfamily of transforming growth factor (TGFβ) ligands is a major group that is implicated in many developmental processes and constitutes a major component of stem cell niches. BMPs are morphogens of the TGFβ superfamily and are secreted during gastrulation from the trophoblast (Gilbert 2014).

The organizer's major implication is mediated by the expression of BMPs' antagonists, such as noggin, chordin and follistatin (Hemmati-Brivanlou and Melton 1997), that mitigate the influence of BMP-4 on the midline of the ectoderm (i.e. to the cells in the immediate vicinity of the notochord (Figure 4)). The lateral areas of the ectoderm that are not under the influence of the BMPs' inhibitors render the binding of BMP-4 and -7 to their receptors possible and therefore activating genes associated with the epidermal ectoderm fate.

Cells of the ectoderm overlying the notochord give rise to the neural plate. The edges of the neural plate give rise to the neural crest and finally the rest of the ectoderm turns into the epidermal ectoderm (Figure 4).

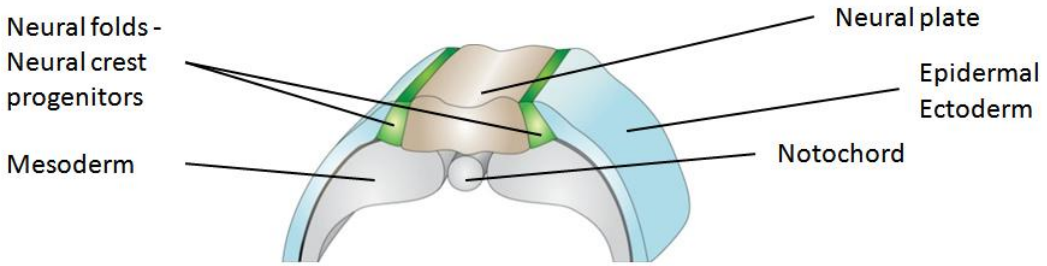

Figure 4 *The neural plate is formed due to the inhibitory effect of various BMPs antagonists (e.g. noggin) possibly emanating from the notochord, while cells residing laterally in the ectoderm are susceptible to BMPs' binding and thus, giving rise to the epidermal ectoderm. Cells in-between the neural plate and epidermal ectoderm are the neural crest progenitors. Adapted from (Mayor and Theveneau 2014).*

2.3.2 Primary & Secondary neurulation

As previously mentioned, in GW3 the ectoderm creates two folds called neural folds, in-between the folds cells occupying this area start thickening giving rise to a neural structure, the neural plate (Figure 4).

The midline of the neural plate is referred to as the median hinge point (MHP) (Figure 5 left a), this part of the neural plate gets anchored to the notochord and gradually deepens forming the neural groove (primary Neurulation, Figure 5 left b), the folds rise in tandem with the deepening of the MHP and eventually merge, the structure now resembles a hollow tube (secondary Neurulation Figure 5 left c).

During GW3 the closure of the neural tube in central regions takes place with the anterior neuropore closing first followed by the posterior neuropore. The anterior neuropore of the tube, prior to its closure, expands and forms the three primary vesicles; the prosencephalon (forebrain), the mesencephalon (midbrain) and the rhombencephalon (hindbrain). The prosencephalon gives rise to the telencephalon and diencephalon while the rhombencephalon gives rise to the metencephalon and myelencephalon. The mesencephalon does not experience further division (Figure 5 right).

The aforementioned vesicles are referred to as the secondary brain vesicles and are situated along the rostral-caudal axis of the developing embryo and are responsible for the establishment and further development of the central nervous system (Stiles 2008, Stiles and Jernigan 2010).

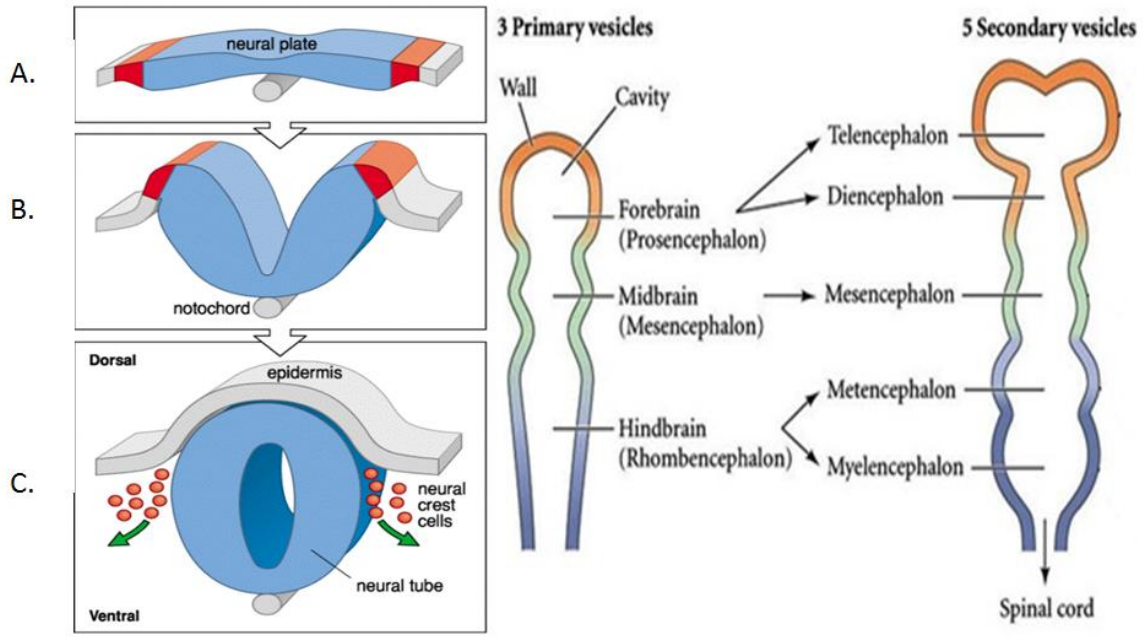

Figure 5 Left: *Transformation of the neural plate to the neural tube.* ***a.*** *The area overlying the notochord starts thickening giving rise to the neural plate.* ***b.*** *The primary Neurulation consists of the deepening of the MHP and the formation of the neural groove.* ***c.*** *The closure of the tube (centrally) is referred to as secondary Neurulation (Shrestha 2010).* ***Right:*** *the three primary vesicles: the prosencephalon, mesencephalon and rhombencephalon delineate the rostral-caudal axis. The prosencephalon and rhombencephalon experience further division, the prosencephalon gives rise to the telencephalon and dienceplalon and the rhombencephalon gives rise to the metencephalon and myelencephalon. The Mesencephalon does not undergo further division. These five vesicles constitute the secondary brain vesicles. Adapted from (Gilbert 2014).*

2.3.3 Dorsal-ventral polarization

Two signaling centers are fundamental to the transformation of the neural plate to the neural tube. The one being the notochord by secreting the morphogen Sonic Hedgehog (SHH) (Jessell 2000, Gilbert 2014) and the other one is the epidermal ectoderm by secreting BMP4 and -7 (Chizhikov and Millen 2005, Gilbert 2014).

Morphogens' impact on cell fate which is concentration- and time-depended can be visualized by the "French flag" model (Wolpert 1969) (Figure 6). Based upon this model there are two opposing diffusion gradients of BMP4 and SHH in which high expression of the former or the latter or the same expression level of both influence cell fate.

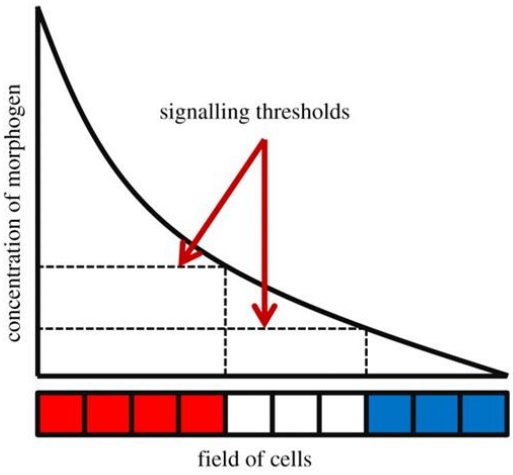

Figure 6 *The French flag model illustrates the effect the morphogens exert on cell fate, morphogens usually create a concentration gradient by which cell fate is determined. High concentration of a morphogen dictates cells to assume the "red" cell fate, intermediate concentration the "white" cell fate and low concentrations the "blue" cell fate. Although a simplified model depicting the effect of one morphogen, the same principle holds when opposing concentration gradients of two or more morphogens are in effect. Adapted from (Karim, Buzzard et al. 2012).*

The synergistic effect of the concentration gradients of such morphogens has a pivotal impact on the neuronal fate of cells occupying the neural tube. As the five secondary vesicles are generated from the neural tube, cells occupying the various brain vesicles have assumed an even more restricted fate associated with the respective part of the brain they occupy. Hence, the molecular cues neural stem cells are exposed to dictate the functionality and therefore regionality of the generated neuronal populations.

The effect of morphogens when the neuronal fate is shifted towards cells which accommodate functionalities associated with the myelencephalon is referred to as caudalization while the opposite (shift towards the telencephalon) as rostralization. Cells occupying brain regions situated towards the back of the embryo are due to the dorsalizing effect of morphogens while the opposite effect is referred as ventralization (Figure 7).

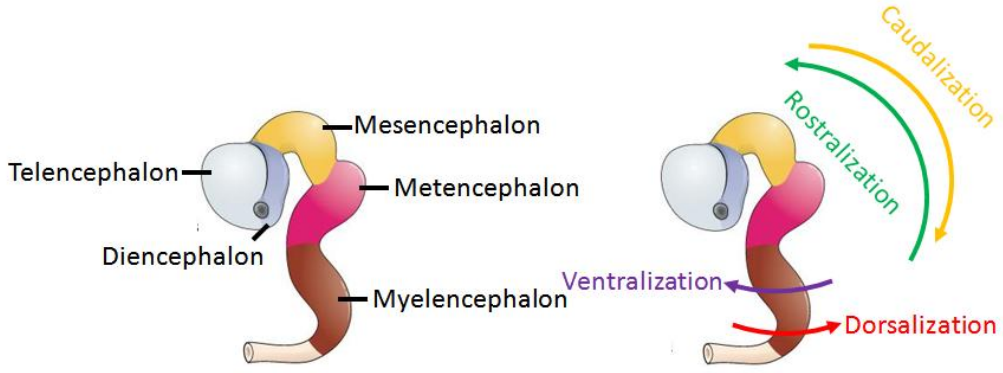

Figure 7 *Lateral view of the embryo in GW5.The regional identities of the neuronal populations are dictated by the combined concentration gradients of different morphogens. The rostrocaudal and dorsoventral axis are formed due to the ability of morphogens to impart different cell fates. Rostralization is referred to as the process by which cells are shifted towards the telencephalon while the process shifting cell fates towards the myelencephalon as caudalization. The process by which morphogens impart cell fates towards the back of the embryo is referred as dorsalization while the opposite effect as ventralization.*

In more detail regarding the dorsal-ventral polarization of the neural tube, the dorsal region of the neural tube is called the roof or alar plate and it exerts its effect by expressing BMP4 and forming a gradient along the dorsal-ventral axis. Cells in the ventral region (floor plate) of the neural tube express SHH and form a concentration gradient along the ventral-dorsal axis in an opposing fashion of BMPs'. The concentration gradients of the two aforementioned morphogens act in concert imparting the dorsal-ventral regionality of the developing brain (Figure 8) (Wilson, Lagna et al. 1997, Patten and Placzek 2000).

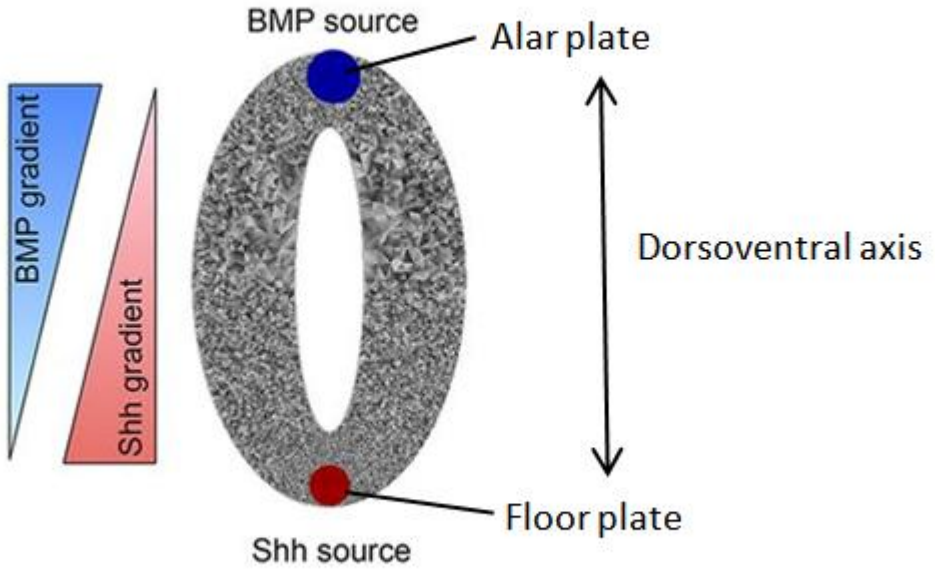

Figure 8 *Two opposing concentration gradients are responsible for generating the dorsoventral polarization of the neural tube. The notochord by expressing SHH affects the ventral part of the neural tube stimulating the area in the immediate vicinity of the notochord to express SHH itself, thus, giving rise to the floor plate in the ventral region of the neural tube. While in the dorsal region of the neural tube the alar plate is formed, which expresses BMPs presumably under the effect of the epidermal ectoderm overlying the neural tube. Adapted from (Quiñinao, Prochiantz et al. 2015).*

Resultantly, Shh's effect on ventralizing the neural tube is reflected in the generation (in order of increasing ventral identity) of V0, V1, V2 interneurons, motor neurons and V3 interneurons *(Ericson, Briscoe et al. 1997)*. Neuronal populations in the dorsal region are subdivided into 6 types (dI1-dI6) and only the most dorsal neuronal populations (dI1-dI3) are influenced by the presence of BMPs in the alar plate (Lee, Dietrich et al. 2000), the rest (dI4-dI6) are generated regardless of the presence of BMPs (Müller, Brohmann et al. 2002).

The inclination of neural stem cells to assume different regional identities and hence functionalities can be linked to region-specific gene products, the same holds for cells occupying the neuroectoderm. Cells occupying the neuroectoderm (i.e. the neural plate) express, among others, Pax6, Sox1 and Sox2 genes. Pax6 and Sox1 are the earliest genes to be expressed in the neuroectoderm denoting a neural commitment of the ESCs/iPSCs (Simona Casarosa 2013). Pax6 is also associated with different brain regions. Characteristic genes of the neural stem cells are: Nestin, MmrN1, Plagl1, PLZF and ZIC2.

In order to characterize the regional identity of neural populations certain genes have been associated exclusively with each of the three primary vesicles. However, there are genes that their

expression is overlapping in the three primary vesicles such as Pax6 and OTX2. Genes associated with the various regions of the brain are presented in Figure 9.

Neuroectoderm Markers	Neural Stem Cell Markers	Regionality Markers
Sox2 Sox1 Pax6	Nestin PLZF MmrN1 Plagl1 ZIC2	Forebrain FoxG1 OTX2 Pax6 Midbrain LMX1A OTX2 Hinbrain GBX2 HOXB4 Pax6

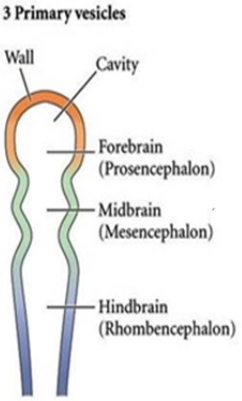

Figure 9 *Genes associated with different brain regions as well as genes denoting neural commitment of ESCS/hiPSCs. The earliest markers of cells occupying the neuroectoderm (neural plate) are Pax6 and Sox1. The pluripotency gene Sox2 is also expressed in this type of cells. Genes associated with specific brain regions are, among others: FoxG1 (forebrain) LMX1A (midbrain) and GBX2-HoxB4 (hindbrain). The expression of Pax6 and OTX2 is present in more than one primary vesicle.*

2.4 Neuroectoderm Induction

Neural induction in vitro as well as the evaluation of various patterning methods to impart neuronal cells with distinct functionality, and hence regionality, has been studied extensively (Perrier, Tabar et al. 2004, Koch, Opitz et al. 2009, Krencik and Zhang 2011, Emdad, D'Souza et al. 2012, Espuny-Camacho, Michelsen et al. 2013, Maroof, Keros et al. 2013). On the quest to induce the generation of region-specific neuronal cell populations scientists aim to simulate the in vivo environment (stem cell niche) during brain development, and more specifically the autocrine and paracrine signaling that drive neuroectoderm induction and direct cells to assume a region-specific identity.

Neural stem cells populations were generated as a pure cell population (without contamination of cells from other germ layers) from hESCs in 2001 (Reubinoff, Itsykson et al. 2001, Zhang, Wernig et al. 2001). Nevertheless a long-term self-renewing neural stem cell population that exhibited the plasticity to generate different neural stem cell lineages was not yet established and hence the on demand generation of neuronal or glial population was not possible.

Initially, neural inductions were carried out on stromal cells which contaminated cell cultures leading to biased differentiation and highly variable results, thus hampering the differentiation efficiency. The culturing system was greatly improved by the introduction of coated well plates. Coated well plates pose a better alternative than stromal layers since they provide a more robust culturing system under xeno-free conditions.

Neural stem cells that exhibited long-term capacity for self-renewal were ultimately differentiated from human ES cells on feeder-free coated well plates (Koch, Opitz et al. 2009). The isolated neural stem cell population exhibited capacity for self-renewal as well as typical structural characteristics and markers of the neuroepithelium (Koch, Opitz et al. 2009).

Prior to 2009, neural inductions were mostly carried out by the introduction of BMP-4 inhibitors such as noggin (since BMP-4 inhibition is essential for neural induction). In 2009 the differentiation yield to neural stem cells was greatly improved by the combined activity of noggin and SB431542 (Chambers, Fasano et al. 2009) a pharmacological inhibitor of the TGFβ pathway. The combination of the two molecules inhibited the two smad-mediated pathways in the TGF-b signaling pathway. Resulting data suggested that these two molecules work synergistacally in a complimentary fashion, directing efficiently both hESCs and hiPSCs to a neuroectodermal lineage.

Owing to the advent of hiPSCs, neuroectoderm induction protocols were carried out in both hESCs and hiPSCs to verify that the progression from a pluripotent state to a more fate-restricted one exhibited similar patterns in both cases and the transition from hESCs to hiPSCs as a starting material gained ground (Chambers, Fasano et al. 2009, Emdad, D'Souza et al. 2012, Falk, Koch et al. 2012).

2.5 TGFβ signaling pathway

TGFβ ligands play a crucial role in the induction to specific germ lineages and thus the manipulation of the TGFβ pathway results in the differentiation of hiPSCs to different germ layers (Dupont, Zacchigna et al. 2005).

The mechanism of TGFβ pathway revolves around the phosphorylation of a TGFβ type I receptor (a serine/thionine transmembrane receptor kinase) which is catalyzed by a TGFβ type II receptor (Figure 10). The binding of a TGF beta superfamily ligand activates the TGFβ type II receptor. (Alberts B 2002). Proteins/growth factors of the superfamily of TGFβ ligands are among others: BMPs, Activin, Nodal and TGFβ (Bioinformatics).

Following the activation of the transmembrane TGFβ type I receptor the intracellular SMAD proteins, namely receptor-regulated SMAD (R-SMAD) and common-mediator SMAD (co-SMAD), are activated and are able to modulate gene expression.

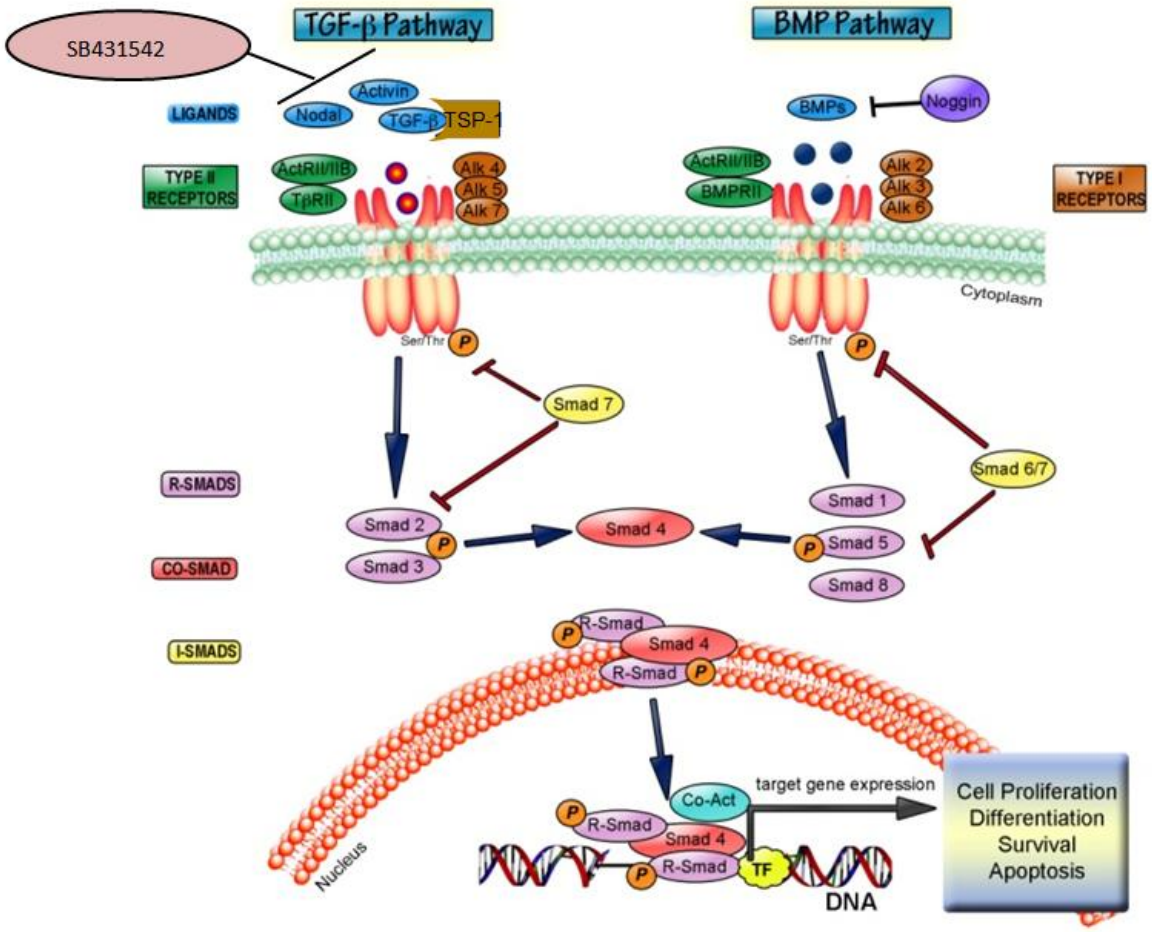

Figure 10 *TGFβ and BMP-4 pathway inhibition by small molecules/proteins such as SB431542 and noggin. The failure of TGFβ ligands to bind to their TGFβ type I receptors alters the expression of genes. Resultantly, cell fate is coupled to the accessibility of the transmembrane TGFβ type I receptors. Adapted from (Villapol, Logan et al. 2013).*

Numerous ventures have been undertaken in order to elucidate the signaling mechanism in the TGFβ pathway and how it is coupled to the downstream regulation of gene expression. The interplay of molecules extra- and intracellularly (Xu 2006, Ross and Hill 2008) and the impact of different growth factors on the TGFβ pathway are among the variables that greatly influence the induction of germ layers (Massagué and Xi 2012).

Many molecules have been documented to play a major role in the neuroectoderm induction; such molecule are the proteins noggin, chordin and follistatin (Hemmati-Brivanlou and Melton 1997). Noggin is a protein which is a natural antagonist of BMP-4 (Hemmati-Brivanlou and Melton 1997), the inhibition of which averts ESCs from differentiating into the mesoderm and has been used in many neuroectoderm induction protocols (Lee, Shamy et al. 2007, Elkabetz, Panagiotakos et al. 2008). Moreover, SB431542, another candidate molecule that has been explored for its implication in the TGFβ pathway, has been utilized in neuroectoderm induction protocols (Smith, Vallier et al. 2008). SB431542 inhibits the Activin/Nodal pathway by blocking the phosphorylation of TGFβ type I receptors.

2.6 Wnt signaling pathway

The activation of the Wingless-related integration site (Wnt) pathway has been postulated to enhance neural commitment and promote the self-renewal of neural stem cells therefore it has also been used in neuroectoderm differentiation protocols (Li, Sun et al. 2011, Lu, Liu et al. 2013).

Wnt pathway is an evolutionary conserved pathway implicated in cell mobility, cell polarity, regulation of calcium inside the cell (Gilbert 2014) and stem cell renewal (Nusse 2008). Moreover it plays a pivotal role in the formation of body axis during embryonic development (van Amerongen and Nusse 2009).

The Wnt pathway can be divided into the canonical or Wnt/β-catenin depended pathway and the non-canonical or Wnt/β-catenin independent. The non-canonical pathway can be further divided into the Planar Cell Polarity and the Wnt/Ca^{2+} pathways (Habas and Dawid 2005). In this study, only the canonical pathway will be discussed and considered (Figure 11).

Gene expression is regulated by the translocation and accumulation of the cytoplasmic protein β-catenin into the nucleus which is mediated by the activation of the Wnt pathway. Wnt proteins are extracellular glycoproteins that bind to the extracellular receptor complex consisting of the protein Frizzled (Fz) and the low-density-lipoprotein-related protein 5/6 (LRP 5/6).

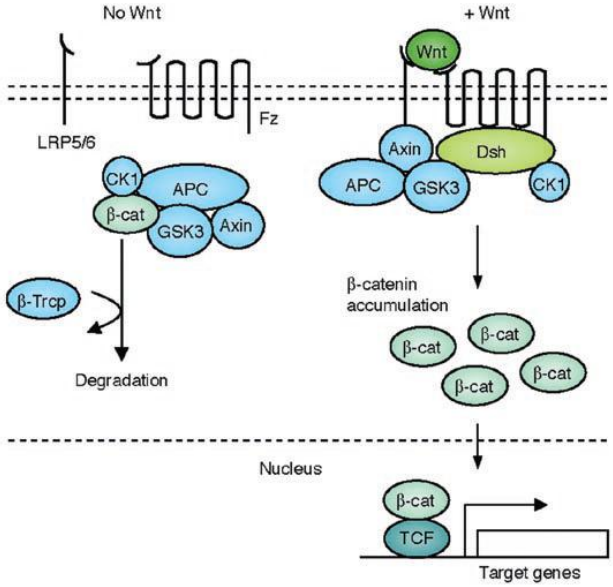

Figure 11 *Schematic representation of the Canonical Wnt pathway. Without the activation of the Fz – LRP 5/6 complex, b-catenin is degraded by the proteosomal machinery (β-TrCP). On the contrary, activation of Fz – LRP 5/6 by Wnt glycoproteins imparts conformational changes to the destruction complex that ultimately prevents the degradation of β-catenin. The accumulated of β-catenin act in a co-transcriptional capacity to transcriptional factors such as TCF activating target genes (Komiya and Habas 2008).*

The protein Fz is a transmembrane protein that gets activated concurrently with the recruitment of LRP 5/6 by Wnt glycoproteins. Fz and LRP 5/6 synergistic action transduces signals to the prosphoprotein Dishvelled which renders the β-catenin destruction complex (composed of Axin, Adenomatosis Polyposis Coli (APC), glycogen synthase kinase 3 (GSK3) and casein kinase 1a (CK1a) (Gordon and Nusse 2006) unable to target β-catenin.

The targeting and consequent degradation of β-catenin is implemented by its phosphorylation from the destruction complex which flags it for ubiquitination and eventual degradation by the proteosomal machinery (β-TrCP).

To simulate the Wnt pathway in vitro, pharmacological inhibitors (e.g. CHIR99021) of GSK3 have been employed which imitate the activation of Dsh resulting in the accumulation of β-catenin and hence activation of the Wnt pathway downstream genes.

2.7 Small Molecules

The 3D structure of BMP-4 antagonist noggin is vital to its ability to inhibit BMP-4 since its mode of action lies in the binding of noggin to the active site of the BMP-4 protein (Groppe, Greenwald et al. 2002), thus batch-to-batch variations and structural instability of recombinant proteins in general lead to noggin's attenuated activity(Neely, Litt et al. 2012). Moreover, another drawback of noggin is that noggin is a recombinant protein which entails high production costs (Surmacz, Fox et al. 2012). Consequently, ventures were undertaken to explore new candidate molecules that are relatively stable, cost-efficient and manufactured with high purity.

These traits, structural stability and cost-efficiency, are addressed by SMs. SMs that can inhibit BMP-4's action have been evaluated in various protocols, some of them that have been used in literature and will be evaluated in this study are: Dorsomorphin, LDN193189 and DMH1 (Figure 12).

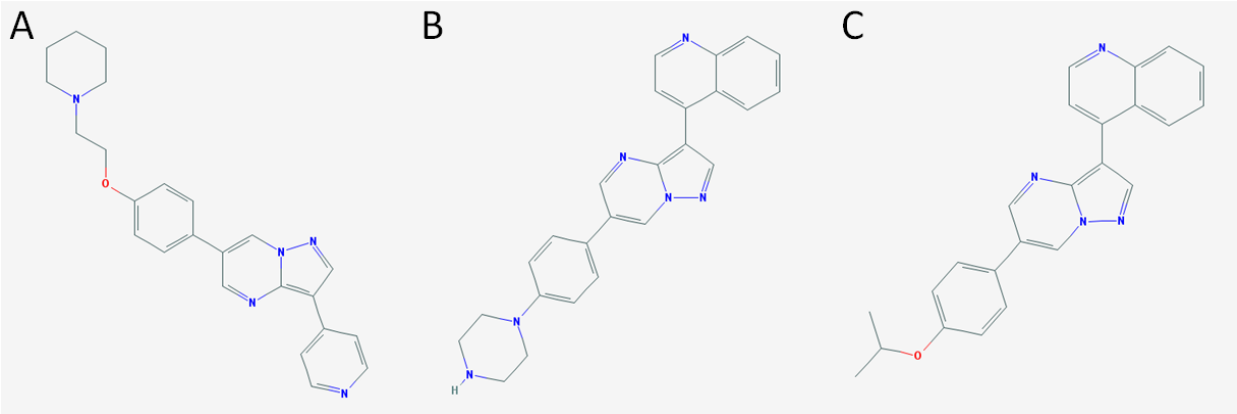

Figure 12 *2D structures of the pharmacological BMP-4 inhibitors a) Dorsomorphin b) LDN193189 and c) DMH1. LDN193189 and DMH1 are chemical analogues of Dorsomorphin. Structures retrieved from PubChem Compound Database.*

Small molecules have a different mode of action than noggin. While noggin intercepts the activation of TGFβ type I receptors - the activin receptor-like kinases (ALK) (ALK2, ALK3 and ALK6) - by binding to the active site of the ligand that is responsible of the eventual activation of type I receptors (via type II receptors), small molecules on the other hand bind directly to the TGFβ type I receptors, preventing their activation. Hence, noggin and small molecules are preventing the activation of the BMP-4 pathway at different levels (Figure 13).

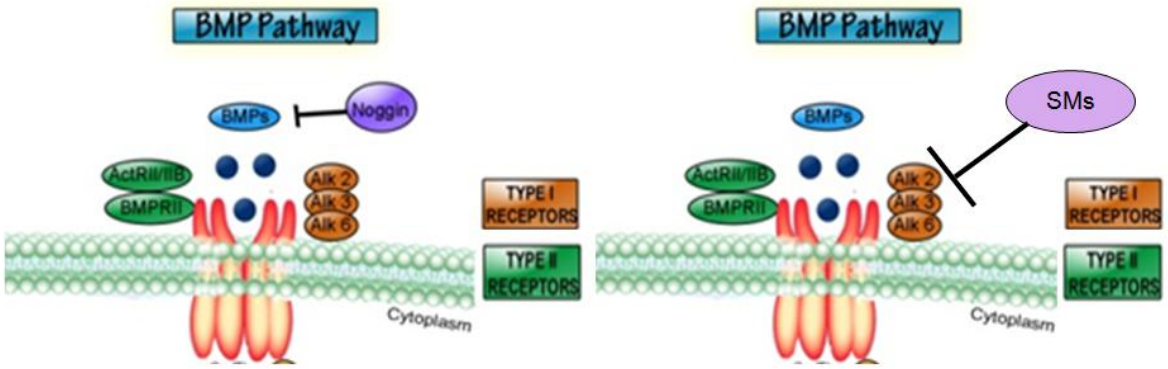

Figure 13 *Inhibition of the BMP-4 pathway by Noggin/SMs at different levels.* ***Left****: Noggin inhibits the activation of the BMP-4 pathway by masking the active site of BMP-4 proteins rendering BMP-4 proteins unable to activate the TGFβ type II receptors.* ***Right:*** *Small molecules target the TGFβ type I receptors (ALK2, ALK3 and ALK6) masking them from BMP-4 proteins.*

Dorsomorphin has been used in neural induction protocols with same strategy as in Chambers et al. (2009), which employs both BMP-4 and TGFβ1 inhibition. Dorsomorphin has been shown to suppress the differentiation to the trophoectoderm mesoderm and endoderm in hESCs and enhance neuroectoderm differentiation. However its mode of action has been documented to vary; in one study (Zhou, Su et al. 2010) it is postulated that dorsomorphin alone is able to inhibit type I receptors in both pathways (TGFβ1 and BMP-4) rendering the presence of SB431542 insignificant. Whereas in other studies (Reinhardt, Glatza et al. 2013) they employ both molecules for a neuroectoderm differentiation with high efficiency.

LDN193189 is a chemically modified small molecule that is the result of a structure-activity relationship study aiming at improving the potency of Dorsomorphin (Cuny, Yu et al. 2008). Since LDN193189 is a chemical analogue of Dorsomorphin it follows similar mode of action as Dorsomorphin. The TGFβ1 and BMP-4 inhibition duo was also employed with this type of BMP-4 inhibitor (Kriks, Shim et al. 2011, Chambers, Qi et al. 2012, Vazin, Ball et al. 2014).

Another study focusing on structure-activity relationship of Dorsomorphin aiming at minimizing the "off target" effects of Dorsomorphin (Hao, Ho et al. 2010) resulted in the identification of DMH1 as another small molecule, chemical analogue of Dorsomorphin. A notable difference between DMH1 and the other two BMP-4 inhibitors is that DMH1 is highly selective towards ALK2 and ALK3 but not ALK6. Comparative studies revealed that Noggin and DMH1 have the same potency in neuralizing hiPSCs (Neely, Litt et al. 2012, Du, Chen et al. 2015).

Even though the aforementioned SMs have been used successfully in neural induction protocols with hiPSCs/ESCs as a starting material, different iPSC lines exhibit different traits e.g. different concentrations of endogenous proteins. Therefore protocols should be re-evaluated and concentrations of SMs should be optimized when using different hiPSC lines.

Chapter 3: Materials & Methods

Evaluation of the protocol (standard protocol) based on the published protocol in Chambers et al was initially addressed in this study as it would serve as the reference differentiation to the differentiation in which SMs would be used as BMP-4 inhibitors, replacing noggin. All protocols can be seen in Figure 14, top.

Furthermore, the Wnt pathway was activated by the pharmacological GSK-3 inhibitor CHIR99021 (which constitutes the only deviation between the protocol used in this thesis and the one used in Chambers et al.) since Wnt activation has been documented to enhance neural commitment (Li, Sun et al. 2011).

Characterization of the differentiation utilizing the standard protocol (Chambers protocol + CHIR99021) was carried out by performing immunocytochemistry (ICC), real-time quantitative polymerase reaction (qPCR) and imaging (brightfield and widefield fluorescent microscopy).

ICC was utilized in order to characterize the differentiation process at different time points. Antibodies to specific proteins of interest were used in ICC experiments, such as pluripotency markers (e.g.Oct4/Nanog) as well as proteins which are associated with a neural fate (e.g. Sox1, PAX6). Real-time qPCR was used to reveal the mRNA expression of genes associated with neural commitment and with different regions of the human brain.

SMs were evaluated using factorial experimental design by which the best combination of molecules and concentration were identified. The readouts for FED analysis were based on ICC experiments (in 96-well plate format) for Pax6 and Sox1 proteins (Pax6 and Sox1 genes are the earliest genes to be expressed in the neuroectoderm). The samples were visualized using wide-field fluorescent microscopy in order to quantify data from the experiments. The intensity was regarded as an indicator of how potent the growth factor/SM was in neuralizing hiPSCs. More cells with signal intensity above the background would indicate a more potent neural induction.

When the ideal SMs were identified the neural induction containing the SMs was up-scaled to a 12-well format. The evaluation of SMs in the neural induction protocol (optimized protocol) was based on mRNA expression analysis of Pax6 and Sox1 genes between the standard and optimized protocol (Figure 14, below). The upregulation of these genes as well as the downregulation of pluripotency genes such as Oct4 and Sox2 would be an indicator of whether SMs can indeed replace noggin in this hiPSC line.

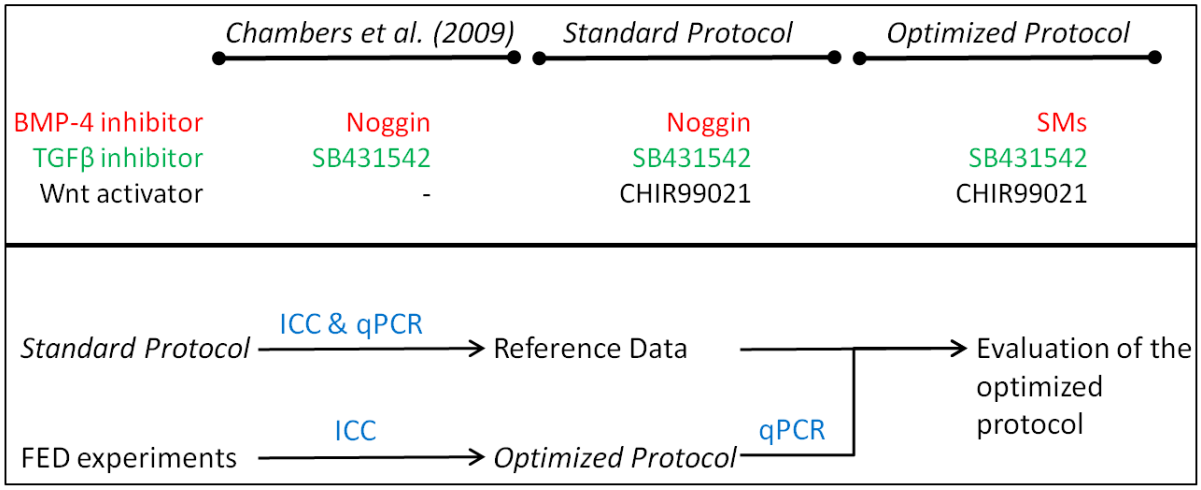

Figure 14 *The various protocols and methods that were employed in this study.* ***Top****: The standard protocol used in this study to generate the reference data contains in the neural induction medium noggin (BMP-4 inhibitor) SB431542 (TGFβ inhibitor) and CHIR99021 (Wnt activator). CHIR99021 is the only compound that was not used in Chamber et al. In the optimized protocol SMs replaced noggin.* ***Bottom:*** *The evaluation of the optimized protocol was carried out by comparing the qPCR data from the neural induction of the standard (reference data) and optimized protocol.*

ICC and qPCR would act in a complementary fashion since ICC may occasionally exhibit false positive samples on account of unspecific binding, degradation of the primary/secondary antibodies etc. On the other hand qPCR alone reveals information on the transcriptome level and does not infer any information on the translation of proteins. Interpreting data by taking into account the findings both of these methods lead to safe conclusions.

Furthermore, it was also evaluated whether SMs have the capacity to shift the regional identity of the differentiated cells in comparison to the regional identity of cells generated with the standard protocol (Chambers et al. + CHIR99021).

3.1 Cell culture

The iPS cell line that was used in this study is the r-iPSC-1j line and it was reprogrammed from skin fibroblasts utilizing the Stemgent mRNA reprogramming kit. Cell culture of hiPSCs is performed on LN-521™ coated well plates and Nutristem® culturing medium. Nutristem® medium facilitates a xeno- and feeder-free culturing system and laminin contributes to the recreation of the natural stem cell niche. The combination of the culturing medium and the coated well plates provides a suitable vessel for hiPSCs' survival and expansion as well as retaining their differentiation capacity without the usage of apoptosis inhibitors.

Well plates were coated using 10 μg/ml LN-521™ and cells were seeded out at seeding densities varying between 35-50K cells/cm^2 depending on the experimental setup. Dissociation of hiPSCs was carried out enzymatically every 3-4 days (depending on confluency) using TrypLE™ and cells were dissociated once they had reached 90-100% confluency. Overconfluency was avoided during expansion to maintain their pluripotency features. Medium change was performed on a daily basis and cell counting was performed using a flow-based cell counter, CedexHiRes (AB Ninolab). Cells were incubated at 37° C under 20% (v/v) O_2, 5% (v/v) CO_2.

3.1.1 Neuroectoderm Induction protocol

The protocol that was followed (standard protocol, Figure 15) in order to induce a neuroectoderm fate was based on the protocol used in Chambers et al. 2009. Cells were seeded out at 150K cells/well (2 wells in a 12-well format) and cultured in Nutristem® medium (day -1) for 24h with the addition of 10μM ROCK inhibitor in order to minimize dissociation-induced apoptosis for 24h. The following day (day 0), Nutristem® was switched to N2B27 medium, DMEM/F12 + Glutamax: Neurobasal (1:1), noggin (500ng/ml), SB431542 (10 μM), CHIR99021 (3.33 μM), N2 supplement (1:200), B27 supplement (1:100) and β-mercaptoethanol (91 μM) (Table 1) which was replenished daily.

On day 4, cells were passaged into laminin 521-coated wells at different seeding densities ranging from 20-60 %, in more detail, from the first well 20% 30% and 50% of the cultured cells were passaged to 3 new wells in a 12-well plate format while 40% and 60% of the cultured cells of the remaining well were passaged to 2 new wells resulting in 5 wells in a 12-well format with increasing seeding densities (20-60%) in order to identify the optimal seeding density for neuroectoderm induction.

From day 4 onwards SB431542 was removed from the N2B27 medium (Figure 15, d4). On day 10, noggin was also withdrawn from the N2B27 medium (Figure 15, d10). The cell cultures were split into 1:3 and 2:3 ratios on day 11 in double coated Poly-L-Ornithine-Laminin 2020 well plate (PLO-L2020, 20 μg/ml PLO and 1 μg/ml L2020) and from this day onwards cells were cultured in NES propagation medium (Figure 15).

ICC and qPCR performed on samples taken on day 4 and day 11 for characterization of the neural induction.

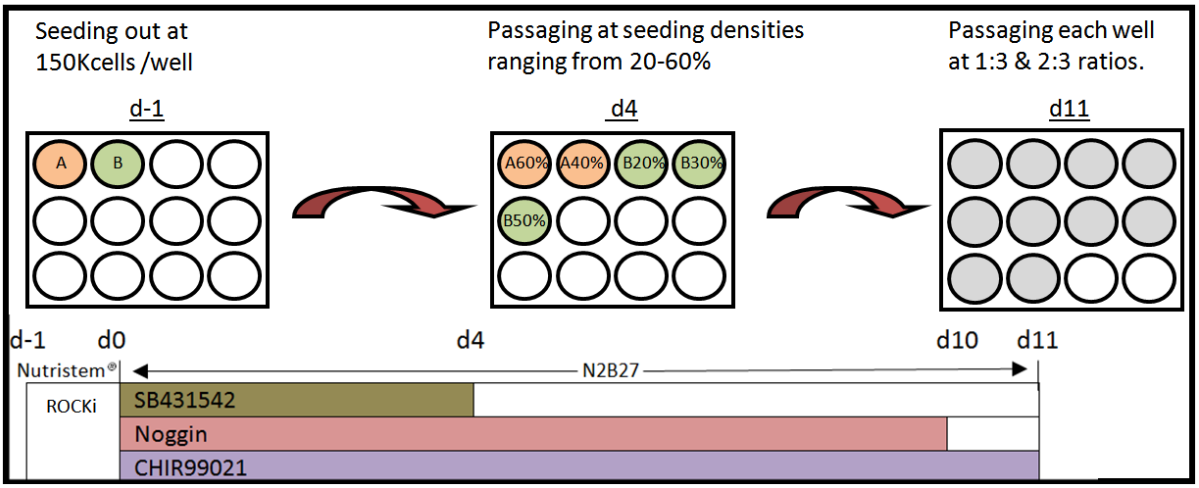

Figure 15 *Schematic representation of the neuroectoderm induction protocol used in this study. Cells were cultured in Nutristem® medium (d-1) in the presence of ROCKi for 24h and then the culturing medium was switched to N2B27 (d0) with subsequent withdrawals of SB431542, noggin on day 4 (d4) and day 10 (d10), respectively.*

Compound	N2B27	NES propagation medium
DMEM/F12 + Glutamax	1:1	✓
Neurobasal		-
N2	1:200	1:100
β-mercaptoethanol	91 μM	-
B27	1:100	1:1000
Noggin	500 ng/ml	-
SB431542	10 μM	-
CHIR99021	3.33 μM	-
b-FGF	-	10ng/ml
EGF	-	10ng/ml

Table 1 *Media formulations used in this study. Initially, noggin was used as BMP-4 inhibitor, but was eventually replaced by SMs that act as BMP-4 inhibitors.*

Bright field images were captured on various days using a Nikon Eclipse TE2000-U microscope with Zyla sCMOS camera, operated by NIS elements software (Nikon Corporation, Tokyo, Japan).

3.2 Immunocytochemistry

ICC employs primary antibodies that bind specifically to the epitope on the target antigen; primary antibodies are raised in different species other than the target antigens in order to avoid cross-reactivity. The secondary antibodies that are introduced bind to the primary antibodies as they have been raised against the host species of the primary antibody. Secondary antibodies are conjugated with a fluorochrome and thus antigens/proteins of interest can be visualized under a fluorescent microscope.

3.2.1 Data credibility and ICC controls

Data derived from ICCs are sometimes too compelling often leading to misleading observations, misinterpretation of data, and hence inaccurate conclusions. Consequently some controls must be performed and taken into account in order to minimize unspecific binding of either the primary or secondary antibody. Three types of controls have been suggested (Burry 2011): primary antibody controls, secondary antibody controls and label controls. Due to time limitations not all controls have been explored.

One of many methods to ascertain the specificity of the primary antibody is colocalization with the primary antibody of interest and a different primary antibody as to verify that they bind to the same structure. This is carried out by having two primary antibodies targeting the same antigen but with a different epitope specificity (Burry 2011). Moreover, primary antibodies are prone to reacting non-specifically which is minimized by introducing isotype controls.

Secondary antibody control tests the specificity of the secondary to the primary antibody. This can be carried out by introducing secondary antibodies to fixed cells without primary antibodies. Ideally, a signal should not be detected since secondary antibodies would not have an antigen to bind to. However, due to the fixation procedure that is not usually the case and a blocking solution e.g. milk proteins or serum depending on the type of primary antibody used as well as its binding capacity.

Fetal Bovine Serum (FBS) is introduced in this study after the fixation in order to minimize the unspecific binding of secondary antibodies e.g. to aldehydes. Label controls refer to the rare case in which the samples exhibit autofluorescence. In this case fixed cells without introducing any primary/secondary antibody should suffice in order to rule out endogenous fluorescence (Burry 2011).

3.2.2 ICC in this study

On days 4 and 11 of the differentiation cells were seeded out at 50-70K cells/well in 96-well plate in order to characterize the progression of hiPSCs to a neural-restricted lineage. After 24h incubation cells were fixed using formaldehyde 4% for 15 min.

Following the fixation, blocking buffer (10% FBS 0.1% Triton X-100 in PBS (+/+)) was introduced to the fixed cells for 60 min. Primary antibodies were diluted to working concentrations (Table 2) in dilution buffer (1% FBS 0.01% Triton X-100 in PBS (+/+)) and incubated overnight at 4° C. Secondary antibodies were diluted (x400) in dilution buffer at ambient temperature for 60 min. Finally DAPI (x2000) in dilution buffer was introduced and incubated at ambient temperature for 10min. Between each step and after the addition of DAPI, the fixed cells were washed with PBS (+/+) 2-3 times for 5 min.

Primary antibody	Company	Catalog #	Working Concentration (µg/ml)
Sox1	R&D Systems	AF3369	10.0
Sox2	Millipore	AB5603	5.0
Nestin	R&D Systems	MAB1259	2.5
PLZF	Santa Cruz	sc-28319	2.0
FoxG1	Abcam	Ab18259	2.0
TRA-1-60	Stemgent	09-0010	5.0
Oct4	Stemgent	09-0023	100x
Nanog	Cell signaling	D73G4	800x

Table 2 *Working concentrations of primary antibodies used in ICC.*

Samples from day 4 and day 11 were treated with the abovementioned procedure and images were collected via the ImageXpress Micro XLS System (Molecular Devices, Sunnyvale, California, USA).

3.3 Polymerase Chain Reaction

Polymerase chain reaction is a technique that has been widely used in molecular biology for various applications such as DNA cloning, gene expression analysis etc. It exploits DNA's bases complementary affinity in order to generate multiple DNA copies. The reaction is usually carried out in small tubes containing the DNA sample, nucleotides, primers specific to the region of interest and DNA polymerase.

PCR consists of three stages the exponential amplification, the leveling off stage and the plateau. The exponential amplification can be divided in a series of repeated temperature changes, called cycles; each cycle is initiated by the denaturation of the DNA template strand usually at 94°C followed by the annealing step during which the primers bind to the DNA strand and the DNA synthesis step in which the DNA polymerase synthesizes a complementary to the DNA template strand.

3.3.1 Real-time quantitative PCR

In this study the real-time quantitative PCR (qPCR) version of PCR was used in order to quantify the expression of genes of interest. In qPCR fluorescent reporter probes complementary to the sequence of interest are used, these probes are fluorescently labeled at their 5'end and a quencher is positioned at their 3'end. The quencher, when in proximity to the fluorophore, absorbs the energy of the excited fluorophore preventing its emission and hence detection (Ishmael and Stellato 2008).

The emission and detection of the probe is only possible under the 5' nuclease activity of Taq DNA polymerase which cleaves oligonucleuotide probes during PCR. The proximity of quencher to the fluorophore is altered enabling unquenched emission. The signal increases proportionally with the release of the fluorophores. In that way quantification of the initial sample is rendered possible, the quantification can be either absolute or relative.

Absolute quantification requires the use of standard curves of the diluted starting material so that a direct comparison can be made. Relative quantification requires the normalization of the cycle threshold (Ct) of the gene of interest to the reference gene i.e. genes that are used for cell maintenance and their expression is not affected by treatments (e.g. GAPDH). Ct represents the cycle number and is inversely proportional to the concentration of the sample.

In this study relative quantification was used, and the Double Delta Ct method was utilized, The Double Delta Ct method calculates the fold change to be equal to $2^{-\Delta\Delta Ct}$, where ΔCt is the difference in Ct between the gene of interest and the reference gene, and ΔΔCt is the difference between the ΔCt of the treated and the untreated sample (Livak and Schmittgen 2001). In this study GAPDH was used as a reference gene and the untreated group was hiPSCs, NES cells were also included in the experiments for comparison.

3.3.2 Sample Preparation

On days 4 and 11 of the differentiation cells were harvested (500-1000K) and RNA was isolated. RNA cannot be used as a template for qPCR therefore isolated RNA was reversely transcribed to complimentary DNA (cDNA) in order to be analyzed with qPCR. In all qPCR runs a reference cell line, namely long-term neuroepithelial cells (ltNES), was also included for a direct comparison between the differentiated cells and the reference line.

RNA isolation was carried out using the RNeasy micro kit (Qiagen). Cell pellets from days 4 and 11 were disrupted by adding 350-600 µl RLT buffer (10 µl/ml β-mercaptoethanol was included to inactivate RNAses) and lysate was homogenized by using a GIAshredder spin column. The homogenized lysate was transferred to an RNAease spin column placed in a collection tube which has a silica-base membrane. An equal volume of ethanol was added and that in combination with the

high-salt containing RLT buffer facilitates appropriate binding conditions for the RNA to bind to the membrane.

The spin column membrane was washed with RW1 (1X) and RPE (2X) buffers to remove any cell debris by centrifuging. Finally, the RNeasy spin column was transferred into a new collection tube and RNA was collected by elution using 30 µl of RNAse-free water directly to the spin column membrane followed by centrifugation. RNA concentration was measured using NanoDrop 2000.

Reverse transcription was carried out utilizing the High Capacity cDNA Synthesis kit (Applied Biosystems). To prepare the samples, 10 µl of 2XRT master mix (Table 3) was placed in a PCR tube along with 10 µl of the RNA sample. According to the protocol, the maximum amount of RNA that should be used is 2µg therefore dilutions were made when RNA concentration was higher than 200 ng/µl. The final solution was loaded on a thermal cycler. The setting of the program of the thermal cycler followed 4 steps: Step 1 25°C for 10 min, step 2 37°C for 120 min, step 3 85°C for 10 min and on hold at 4°C until the sample was recovered.

Component	Volume (µl)
10 X RT Buffer	2.0
25 X dNTP Mix	0.8
10 X RT Random Primers	2.0
MultiScribe™ Reverse Transcriptase	1.0
Nuclease-free water	3.2
Total	**10**

Table 3 *Volumes for the 2XRT Master mix per reaction.*

All cDNA samples were diluted to 3ng/µl. Each sample for PCR analysis was prepared (in duplicates) by adding 3 µl of cDNA, 5 µl of Taqman® Fast Advanced Master Mix 1.5 µl of H_20 and 0.5 µl of Taqman® Gene Expression Assay (Table 4, Life technologies). qPCR data were visualized using TIBCO® Spotfire® v. 6.5.3.

Taqman® Gene Expression Assay	Assay-ID	Gene Description
FOXG1	Hs01850784_s1	Regionality Marker
OTX2	Hs00222238_m1	Regionality Marker
LMX1A	Hs00892663_m1	Regionality Marker
GBX2	Hs00230965_m1	Regionality Marker
PAX6	Hs00240871_m1	Regionality Marker
OLIG2	Hs00300164_s1	Regionality Marker
Sox1	Hs01057642_s1	Neuroectoderm marker
Sox2	Hs01053049_s1	Neuroectoderm marker
PLZF	Hs00957433_m1	Neural Stem Cell Marker
GAPDH	Hs04420697_g1	Reference Gene
MmrN1	Hs00201182_m1	Neural Stem Cell Marker
Plagl1	Hs00414677_m1	Neural Stem Cell Marker
ZIC2	Hs00600845_m1	Neural Stem Cell Marker

Table 4 *Genes used in qPCR for mRNA expression analysis.*

3.4 Factorial Experimental Design

Factorial Experimental Design (FED) is favorable when optimizing assays. Assay optimization requires the exploration of factors that elicit specific responses. Data generated though the conventional one-factor-at-a-time (OFAT) method can miss the optimal setting of the factors (Figure 16 Left), is time consuming and cannot provide any information regarding the interaction between the factors.

Therefore utilizing FEDs can generate data in an efficient way especially when there are many factors at multiple levels. Moreover, it is possible to evaluate the effect of the interaction of factors which would not be possible in an AFAT method. Information on the direction of future experiment is attained by a strategic experimental outline ensuring the optimization of assays (Figure 16 Right).

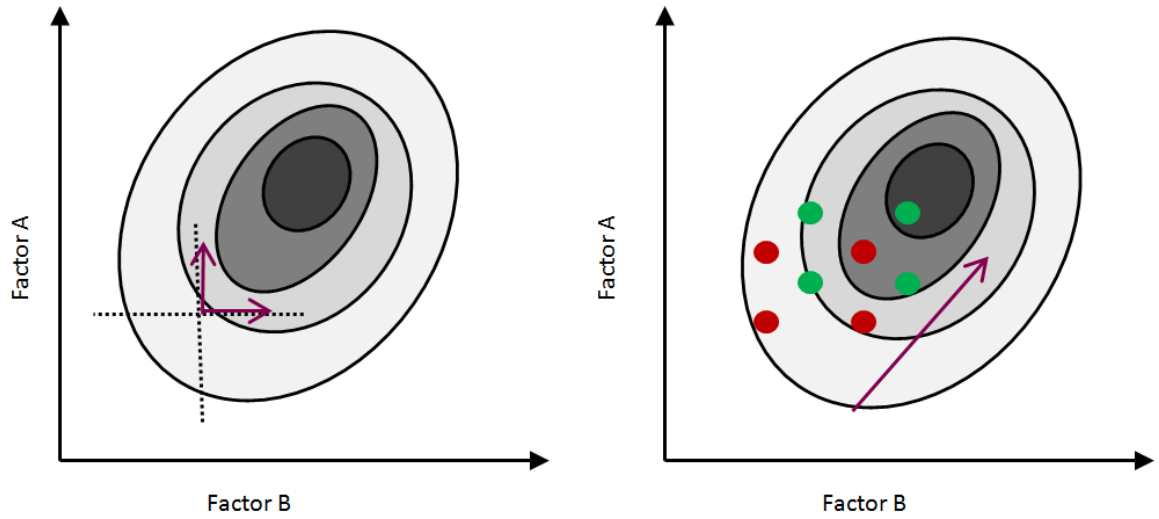

Figure 16 *A hypothetical response model **Left**: Readouts from OFAT method (dashed lines).When altering one variable at a time a seemingly maximum response will be reached, however, the settings of factors that give the true optimum readout (dark area) will not be explored with this strategy. According to the readouts that are generated from the OFAT design; the direction of new experiments (purple arrow) for optimization will not lead to the true optimum settings. **Right:** Readouts generated from FED method (red dots), the design space of this method allows for a more accurate direction (purple arrow) for future optimization experiments (green dots) reaching true optimum settings.*

The readouts for FED analysis were generated by ICC analysis. HiPSCs were cultured for 4 days using the same approach and medium as described in Ch 3.1.1, the only difference being the exchange of noggin with pharmacological BMP-4 inhibitors. On day 4 cells were fixed and ICC was performed.

The Sox1/Pax6 protein markers were chosen as the readout for the FED experiments; Pax6 and Sox1 are the earliest markers to be expressed in stem cells that have been fate-restricted to the neuroectoderm. The fluorescent intensity (above the background) was used as an indicator of the capacity of the various BMP-4 inhibitors to induce neutralization, hence, the more signal from the cells the more potent the neural induction ICC is a reliable method as a readout considering that protein translation would be monitored and not mRNA expression.

Data (Readouts) were generated utilizing the MetaXpress® High-Content Acquisition & Analysis software (Molecular Devices, Sunnyvale, California, USA), 4 sites per well were collected for statistical purposes. The analysis of data from FED experiments was carried out in TIBCO® Spotfire® v. 6.5.3 and FED models were generated in Umetrics MODDE v. 11.

Dorsomorphin, LDN193189 and DMH1 were the main BMP-4 inhibitors evaluated in this study. Different levels (i.e. concentrations) of each factor were selected according to literature.

In FED experiments all possible combinations of all levels between the factors are performed, e.g. for 3 factors each at the 3 levels produces 3^3= 27 combinations per FED experiment. In this study an additional factor was used at 2 levels resulting in 54 combinations per FED experiment. When optimal conditions were met, these conditions (Factors & Levels) were re-evaluated in a 12-well format.

For evaluation of the generated model R2 and Q2 values are calculated from the readouts and are always between 0 and 1. The R2 values reflect the goodness of fit, how good the model fits the data with 1 representing a perfect fit. The Q2 value estimates the predictive ability of the model i.e. its ability to predict data outside the experimental values. R2 and Q2 are calculated automatically in Modde 11 and are derived from the following formulas.

$$R^2 = 1 - \frac{SS_{res}}{SS_{tot}} = 1 - \frac{\sum_{i=1}^{n}(y_i - \hat{y}_i)^2}{\sum_{i=1}^{n}(y_i - \bar{y})^2}$$

$$Q^2 = 1 - \frac{PRESS}{SS_{tot}} = 1 - \frac{PRESS}{\sum_{i=1}^{n}(y_i - \bar{y})^2}$$

Where SS_{res} is the sum of squares of the residual corrected for the mean and SS_{tot} is the total sum of squares of the readouts corrected for the mean. PRESS is calculated in a cross validation procedure i.e. one of the readouts is left-out of the model and the rest of the data are used to predict that left out response.

$$PRESS = \sum_{i=1}^{n}(y_i - \hat{y}_i^{CV})^2$$

Where $\hat{y}_i^{CV}$ is the predicted left-out readout calculated from the rest of the data.

.

Chapter 4: Results

4.1 Evaluation of the standard noggin-containing protocol

Bright-field images of the neural induction using the standard noggin containing protocol collected on days 0, 4, 5 and 11 (Figure 17). On day 4 as mentioned in Ch 3.1.1 5 different seeding densities were used in a new 12-well plate. Images presented here are for the 40% sample (127 K cells/cm^2).

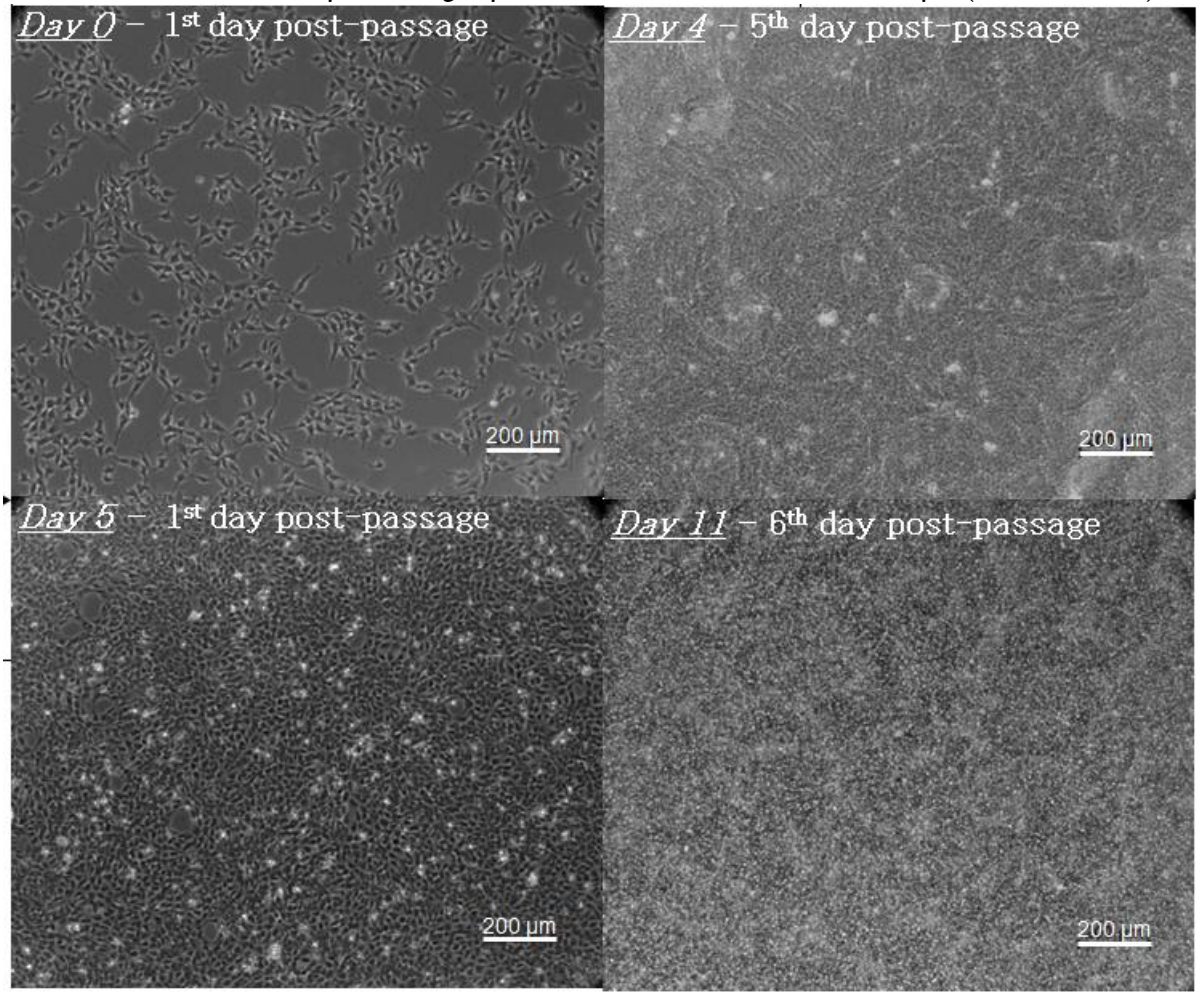

Figure 17 *Bright field images (10x) collected on days 0 4,5 and 11 of the neural induction for the standard noggin-containing protocol for the 40% sample corresponding to 127K cells/cm^2 seeding density on day 4.*

4.1.1 Immunocytochemistry and qPCR

ICC images for days 4 and 11 (Figure 18) for the 40% sample, seeding density on day 4: 127K cells/cm^2.

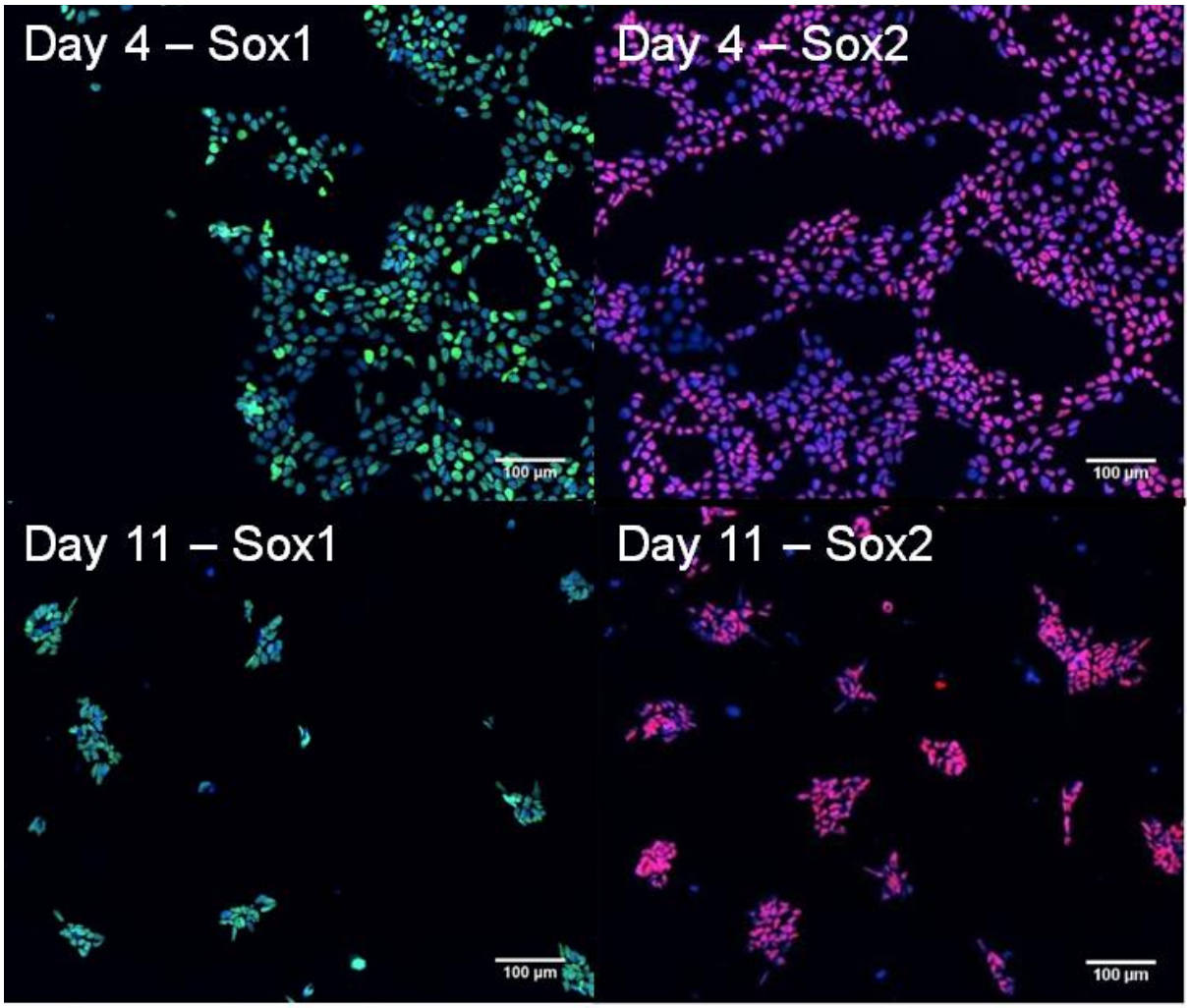

Figure 18 *ICC images for Sox1 (green) and Sox2 (red) antibodies for Days 4 and 11 of the neuroectoderm induction, DAPI staining is in blue.*

From the ICC staining it can be seen that there is a signal for both Sox1 and Sox2. Sox1 translation is also backed up by the upregulation of Sox1 expression (Figure 19) hence verifying both expression and translation of Sox1 and Sox2.

Sox1 is one of the earliest markers to be expressed (along with Pax6) in the neuroectoderm, and thus its expression denotes neural fate commitment (Pevny, Sockanathan et al. 1998). However its expression is transient and does not persist in the differentiated neural stem cells.

By day 4, Sox1 expression was upregulated and the expression by day 11 varied depending on the seeding density suggesting that the seeding density on day 4 has an effect on regulating Sox1 expression by day 11 (Figure 19). The sample that exhibited the highest Sox1 upregulation was the sample 50% (seeding density 159K/cm^2). Sox1 upregulation is in accordance with published data (Chambers, Fasano et al. 2009, Thomson, Liu et al. 2011).

Even though Sox2 is indeed a gene associated with the maintenance of pluripotency of hiPSCs (Chambers and Tomlinson 2009). Sox2 expression is also postulated to promote neural commitment by inhibiting the expression of genes associated with other cell lineages (Thomson, Liu et al. 2011) rendering Sox2 expression vital for neural commitment. Furthermore, Sox2 expression is also associated with maintaining the multipotent traits of neural stem cells (Graham, Khudyakov et al. 2003) and its suppression is correlated with neuronal differentiation (Hutton and Pevny 2011). Moreover, it has been documented that the upregulation of Oct4 repressors results in the repression of Sox2 (Masui, Nakatake et al. 2007). The aforementioned trends of Sox2 are reflected by the slight downregulation of Sox2 expression during the differentiation.

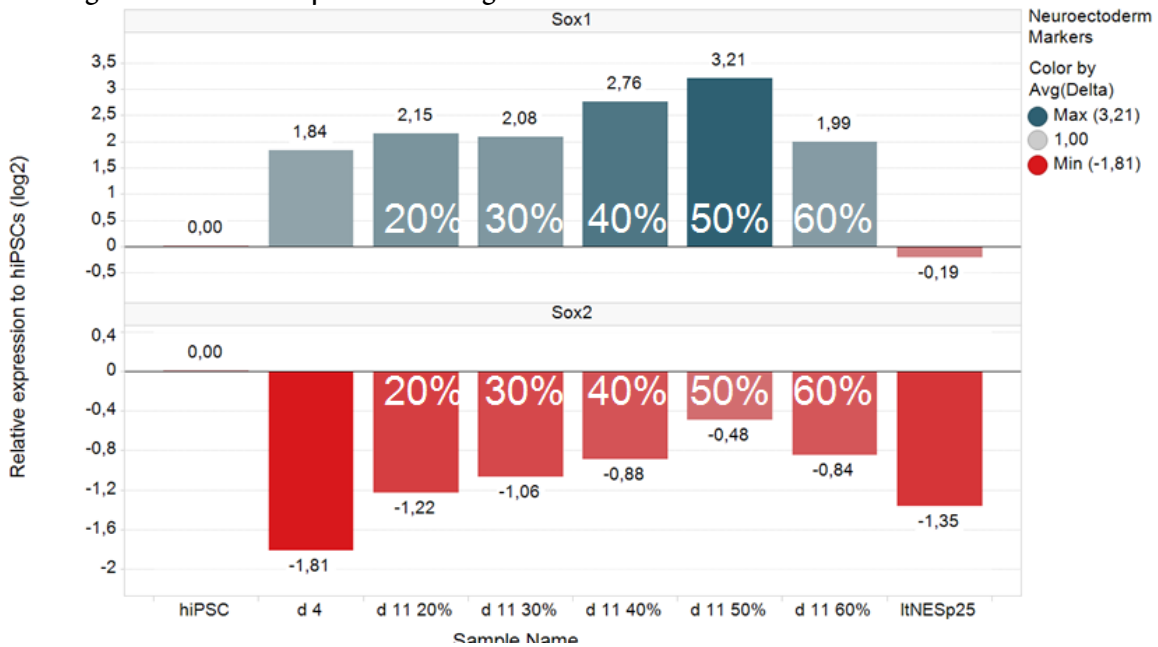

Figure 19 *Gene Expression Analysis of neuroectoderm markers Sox1 & Sox2 for the long-term neuroepithelial stem cells at p. 25 (ltNESp25), hiPSCs and the differentiated cells from day 4 (d 4) & 11 (d 11). For day 11 samples from different seeding densities on day 4 are also presented (d 11 20%-60%). Sox2 expression is slightly downregulated by day 4 but exhibits upregulation trends by day11. Sox1 expression is upregulated by day 4 and by day 11 denoting neural fate restriction.*

Furthermore, when looking closely at the various samples of day 11 (d 11 20%-60%) another observation that surfaces through mRNA expression analysis is that the more Sox1 was upregulated the less Sox2 expression was suppressed. That comparison between these samples is possible since these samples are all referring to the same day of differentiation (day 11) and the only difference between the samples lies in the seeding density on day 4.

Hence, it can be argued (considering that correlation does not necessarily imply causation), that the less Sox2 is repressed the more Sox1 expression is upregulated, even though the exact opposite effect may be true. The former explanation may be more likely taking into consideration that the expression of Sox2, as previously mentioned, suppresses markers associated with other cell lineages paving the way for expression of the neuroectoderm marker Sox1.

Data regarding markers associated with neural stem cells and regionality makers are presented in Figure 20, Figure 21 & Figure 22. From the ICC images presented in Figure 20, it can be seen that there is a signal for both Nestin and FoxG1 and a weak signal from PLZF on day 11 in yellow, overlapping of FoxG1 (red) and PLZF (green). Nestin is an intermediate filament that is expressed in undifferentiated neural stem cells and its expression is vital for the self-renewal of neural stem cells (Park, Xiang et al. 2010).

FoxG1 is a gene expressed in the forebrain and, according to literature, forebrain is the default identity of neural stem cells without introducing any patterning factors (Lupo, Bertacchi et al. 2014).Therefore the generated cells seem to assume a forebrain identity which also in line with the findings in Chambers et al (2009).

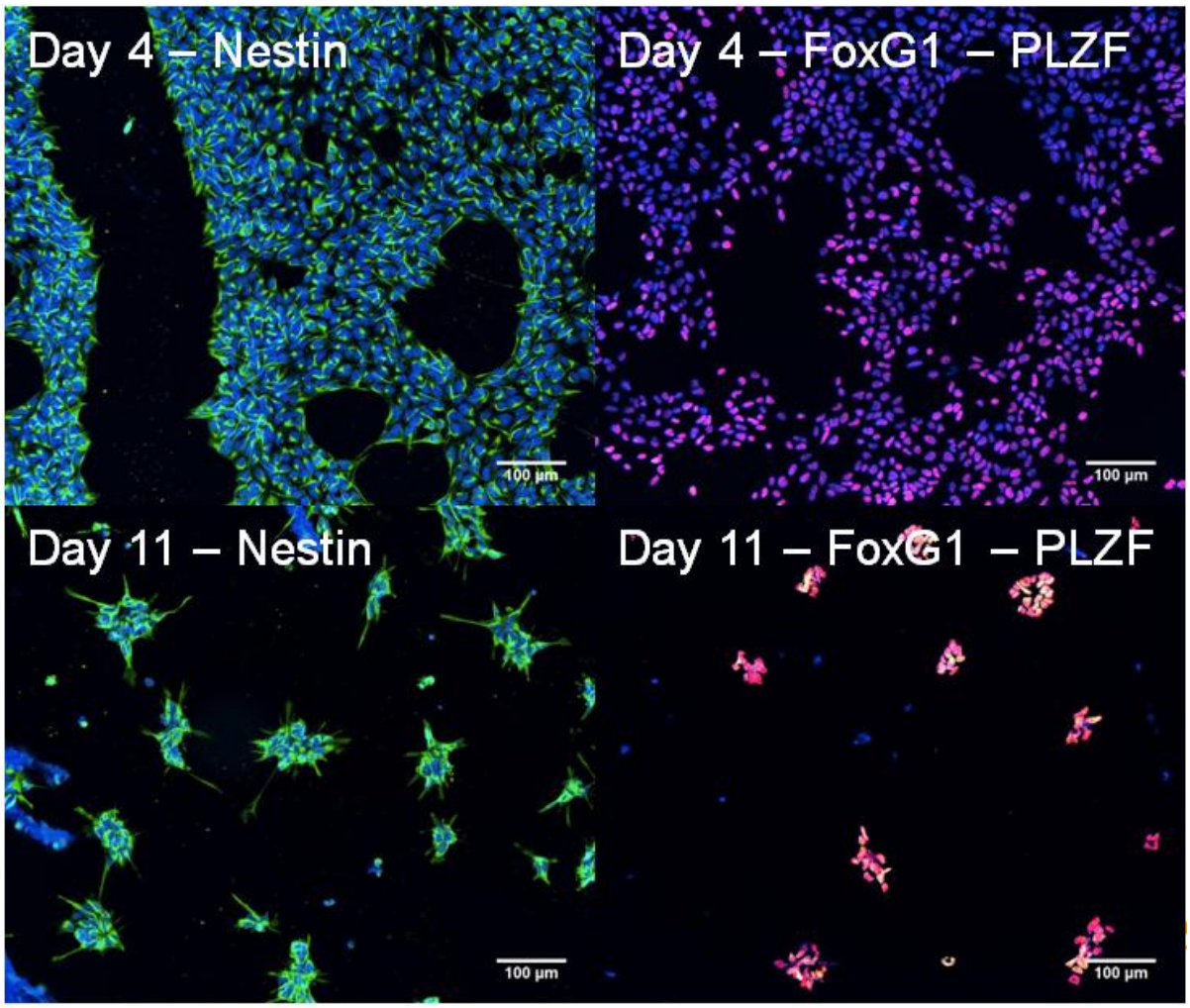

Figure 20 *ICC images for Nestin (green), FoxG1 (red) and PLZF (green) antibodies for days 4 and 11 of the neuroectoderm induction. Signal from FoxG1 suggests forebrain regionality. DAPI staining is in blue.*

A closer look at the ICC images (Figure 18 & Figure 20) reveals that on day 11 cells are considerably less than on day 4 even though the seeding densities before the ICC was approximately the same (50 k/cm^2). That may be attributed to the fact that as the differentiation progresses the differentiated cells lose the affinity to the initial coating LN-521 (i.e. expression of different proteins responsible for cell attachment) According to the protocol on day 11 cells are passaged on double coated Poly-L-Ornithine-Laminin 2020 well plates (PLO-L2020, 20 µg/ml PLO and 1 µg/ml L2020) while all the ICC experiments were done in LN-521.

Regarding the neural stem cell markers (MmrN1, PLZF, Plagl1 and ZIC2), qPCR data (Figure 21) reveal that by day 11 all but ZIC2 genes were expressed at approximately the same level as in the reference line ltNES. PLZF protein translation is also evident in Figure 20 verifying the expression and translation of PLZF. Furthermore the seeding density on day 4 (20-60%) does not seem to have an impact on gene expression of the neural stem cell markers.

MmrN1 PLZF and Plagl1 are genes associated with neuroepithelial stem cells (Falk, Koch et al. 2012). Results from studies on mice embryos have suggested that ZIC2 may be a pluripotency marker since its expression pattern is overlapping with Oct4 expression in mouse embryogenesis (Brown and Brown 2009). Furthermore ZIC2 expression during brain development is crucial since mutations in this gene causes holoprosencephaly (Houtmeyers, Souopgui et al. 2013). Consequently ZIC2 expression is essential for both cell populations (Neural stem cells and hiPSCs).

ZIC2 expression remained stable throughout the differentiation while the pluripotency gene Sox2 was slightly downregulated during the differentiation (Figure 19). A finding that contributes to the fact that the differentiated cells have assumed a neuroectoderm fate considering that ZIC2 is only expressed, apart from the developing embryo, in the brain and testis (Gure, Stockert et al. 2000) and thus its downregulation would imply a commitment to germ layers other than the neuroectoderm.

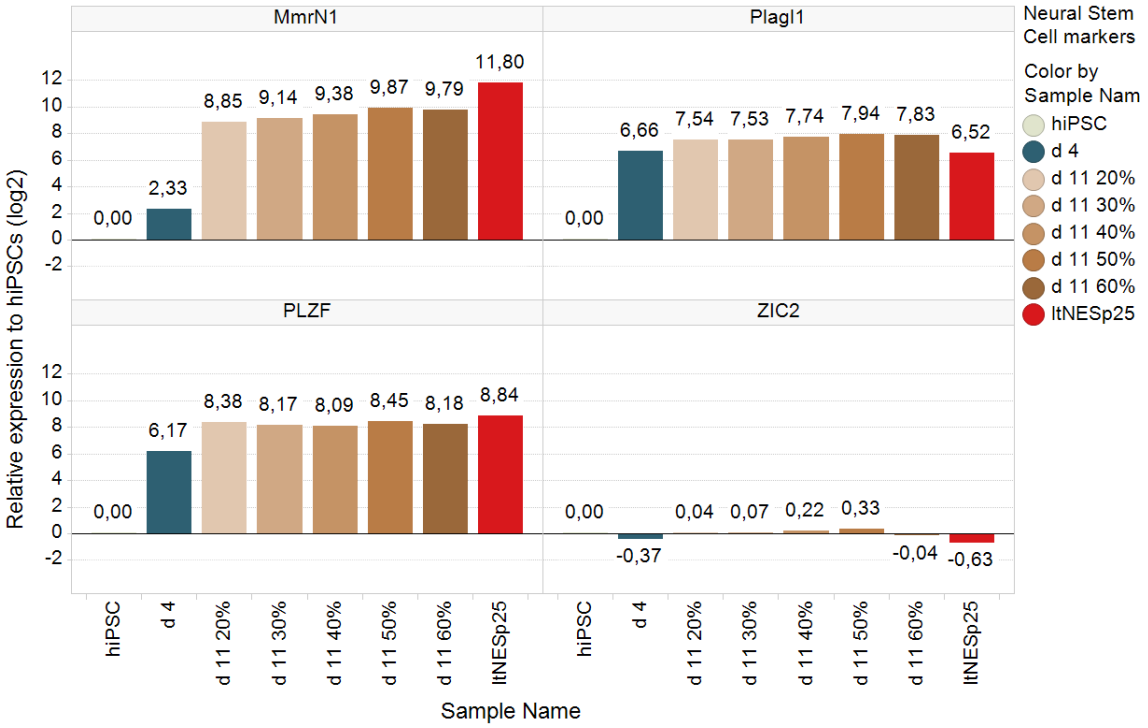

Figure 21 *Gene expression analysis of genes associated with Neural Stem Cell markers for ltNES cells, hiPSCs and cells from day 4 and 11 of the differentiation. Expression of MMRN1 PLZF and PLAGL1 are highly upregulated while* ZIC2 expression does not experience notable changes in the differentiation.

The various genes associated with different parts of the brain are presented in Figure 22.

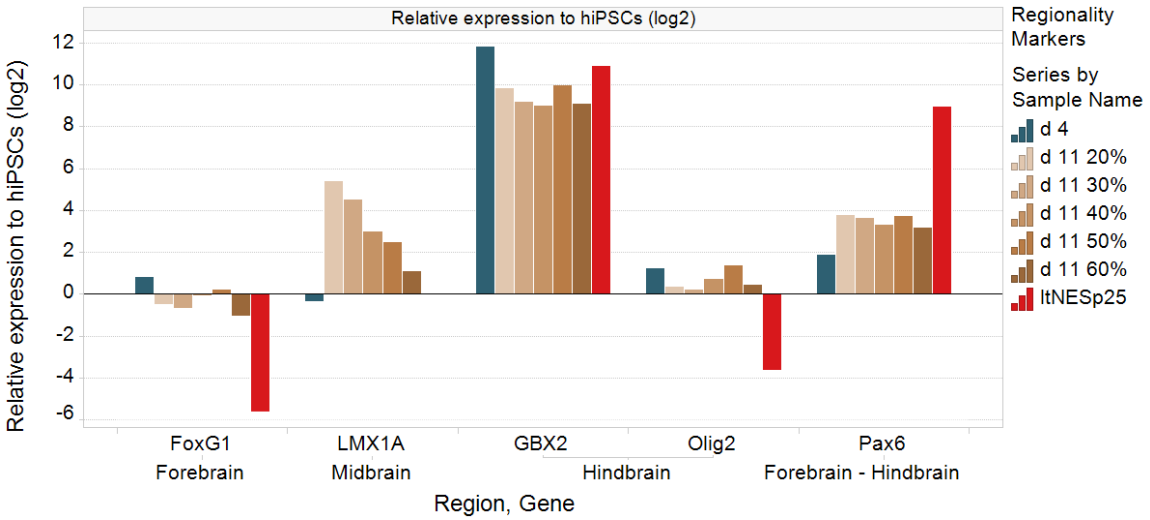

Figure 22 *Gene expression analysis for markers associated with different brain regions. The hindbrain marker GBX2 is highly upregulated by day 4 (d 4) while its upregulation persists by day 11 (d 11). Seeding density seems to have an impact on the expression of the midbrain marker LMX1A. Pax6 expression is also evident and not subject to the seeding density on day 4.*

Pax6 is an early neuroectoderm marker that its expression persists in the neural stem cells and its expression is restricted to the dorsal telencephalon (forebrain) (Kageyama 2013) and to the ventral hindbrain (Koch, Opitz et al. 2009). Pax6 is upregulated by day 4 and remained stable by day 11. Due to the fact that is expressed in both forebrain and hindbrain its expression cannot be used as an indicator of a specific regionality.

The seeding density seems to have a strong impact on the expression of the midbrain marker LMX1A while it does not seem to have an impact on the expression of the rest regionality markers. In more detail, the seeding density on day 4 seems to be inversely related to the upregulation of LMX1A.

GBX2 is a gene associated with hindbrain regionality (Wassarman, Lewandoski et al. 1997) and it is highly upregulated by day 4 and its expression persists by day 11 suggesting that the differentiated cells have a more hindbrain than forebrain identity.

According to the data (Figure 22) FoxG1 (forebrain marker) expression is either slightly downregulated or remained stable. However, data from the ICC (Figure 20) indicate that a signal from FoxG1 protein was detected, suggesting that the FoxG1 expression in ICC may be a false positive.

However, the data presented in qPCR analysis are relative expression to hiPSCs (ΔΔCt) taking a closer look at the ΔCt values (difference between reference gene and gene of interest) of the hiPSCs and the differentiated cells it can be seen that the ΔCt value for the FoxG1 gene in the hiPSCs is 7.395 (the smaller the Ct value the more a gene is expressed), as a reference to that, ΔCt value of the GBX2 gene which was highly upregulated in the differentiated cells is 6.753 and in hiPSCs is 16.554.

To put some words behind the numbers, the analysis monitors to what extend certain genes are upregulated or downregulated in reference to the genes in the hiPSCs, consequently the fact that a change in FoxG1 expression was not documented it does not mean FoxG1 is not already expressed in hiPSCs and the differentiated cells and, in fact, FoxG1 is highly expressed in both hiPSCs and the differentiated cells.

4.2 Factorial Experimental Design: Evaluation of alternative BMP-4 inhibitors.

In the first FED experiment the levels that were used are indicated in Table 5. The selection of the levels was done based on literature review.

BMP-4i	Levels (µM)
Dorsomorphin	0, 1, 2.5
LDN193189	0, 0.1, 1
DMH1	0, 2, 5

Table 5 *Factors and levels used in FED #1.*

Data from Factorial Experimental Design #1 (FED # 1) presented in Figure 23 suggest that high concentrations of DMH1 and dorsomorphin completely inhibited cell viability; a FED model could not be generated due to the lack of available factors/levels. Nevertheless, from the remaining factor/levels in can be seen that for example the settings DMH1 2 µM and LDN 0.1 µM contributed to 75% $Sox1^+$ cells and the cell viability was not hampered dramatically while the standard protocol (corresponding to DMH1/LDN193189/Dorsomorphin/Noggin 0µM/0µM/0µM/500ng/ml generated 35% $Sox1^+$ cells suggesting that combination of SMs is better at neuralizing hiPSCs. ICC images from the standard protocol and the one with only SMs present are presented inFigure 24.A signal from Pax6 was not detected.

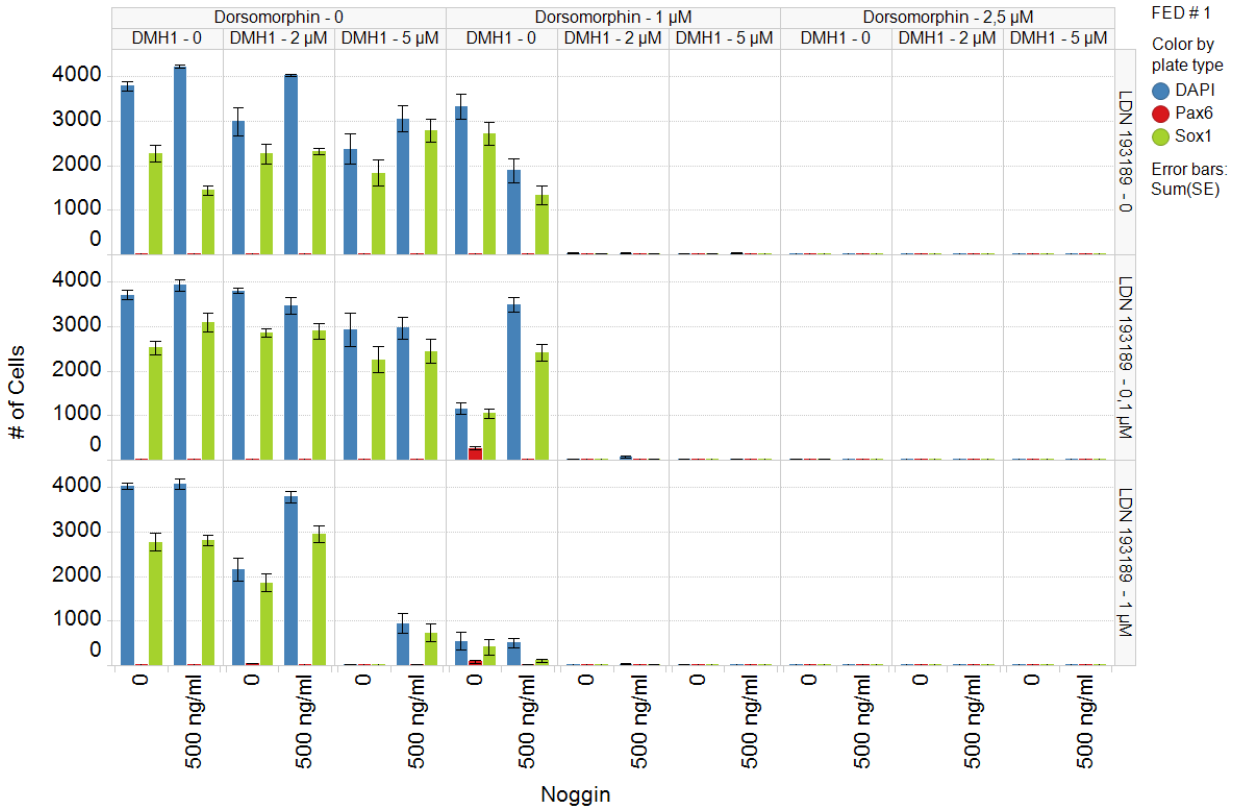

Figure 23 *Data collected from FED # 1. Cell toxicity was noted at high concentrations of DMH1 and Dorsomorphin. Nevertheless, data from the remaining wells suggest that there is a signal from Sox1 protein when either of the BMP-4 inhibitors is introduced in the absence of noggin.*

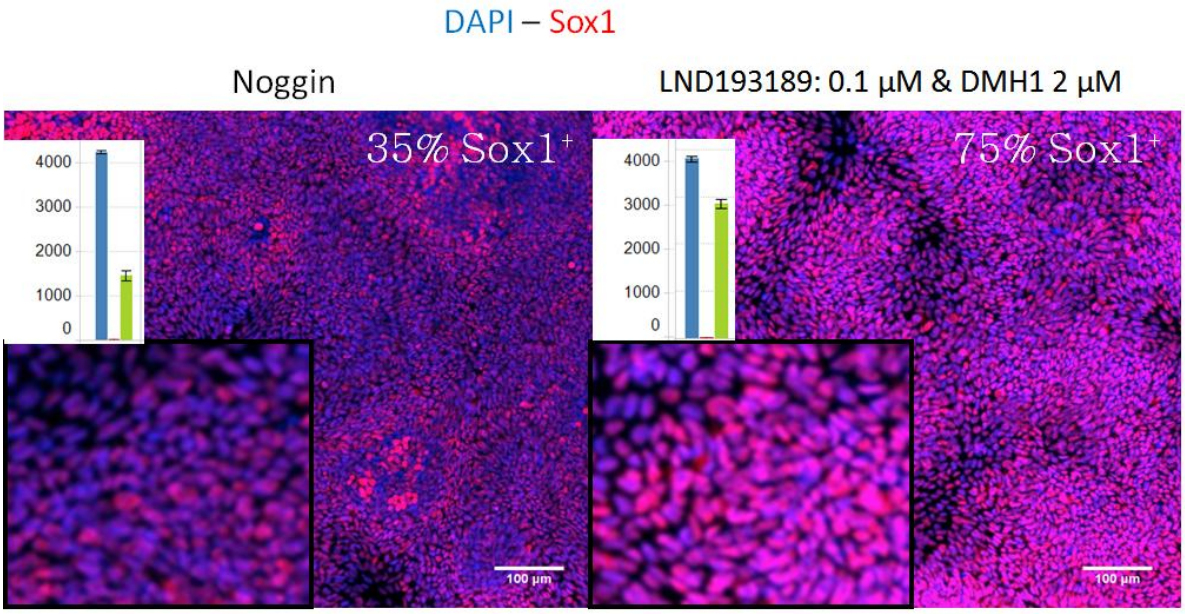

Figure 24 *ICC images for the standard protocol containing noggin (Left) and the combination of SMs (Right). More Sox1$^+$ cells are observed with the use of SMs compared to the noggin-containing protocol. The y-axis units are number of cells while the blue bar chart denotes DAPI$^+$ cells and the green bar chart Sox1$^+$ cells. The % of Sox1$^+$ cells is derived from the ratio Sox1$^+$ cells/DAPI$^+$ cells × 100%.*

Dorsomorphin has been postulated to inhibit receptors in both pathways, TGFβ and BMP-4 (Zhou, Su et al. 2010) and it may be that TGFβ pathway is highly repressed due to the presence of high concentrations of both SB431542 and dorsomorphin. Therefore FED # 2 was performed with exactly the same settings but with a lower SB431542 concentration (2 µM, previously 10 µM) (Figure 25) in order to assess whether that would rescue the cytotoxicity which was the main theme of the previous FED. Data presented in Figure 26.

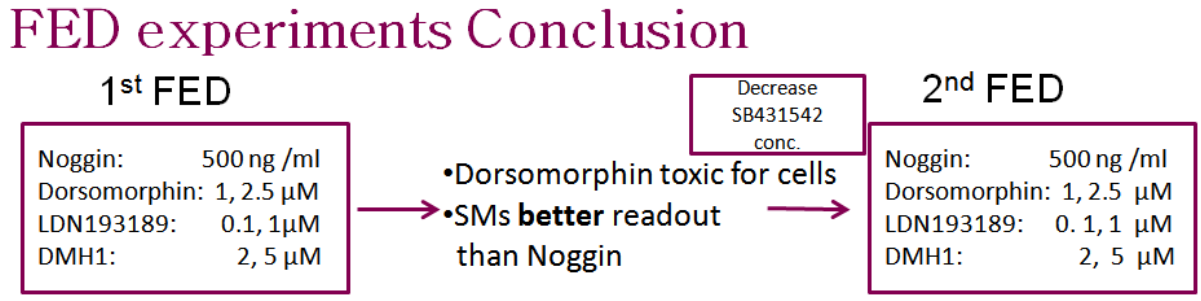

Figure 25 *The main conclusions drawn from the first FED was that high concentration of Dorsomorphin is toxic regardless of the addition of other SMs. While there were settings (LDN193189 0.1 µM & DMH1 2 µM) that gave a better readout than noggin alone, a FED model could not be generated due to the lack of available data from the various factors/levels. The strategy behind the next FED was to evaluate whether by lowering the concentration of SB431542 would improve cell viability.*

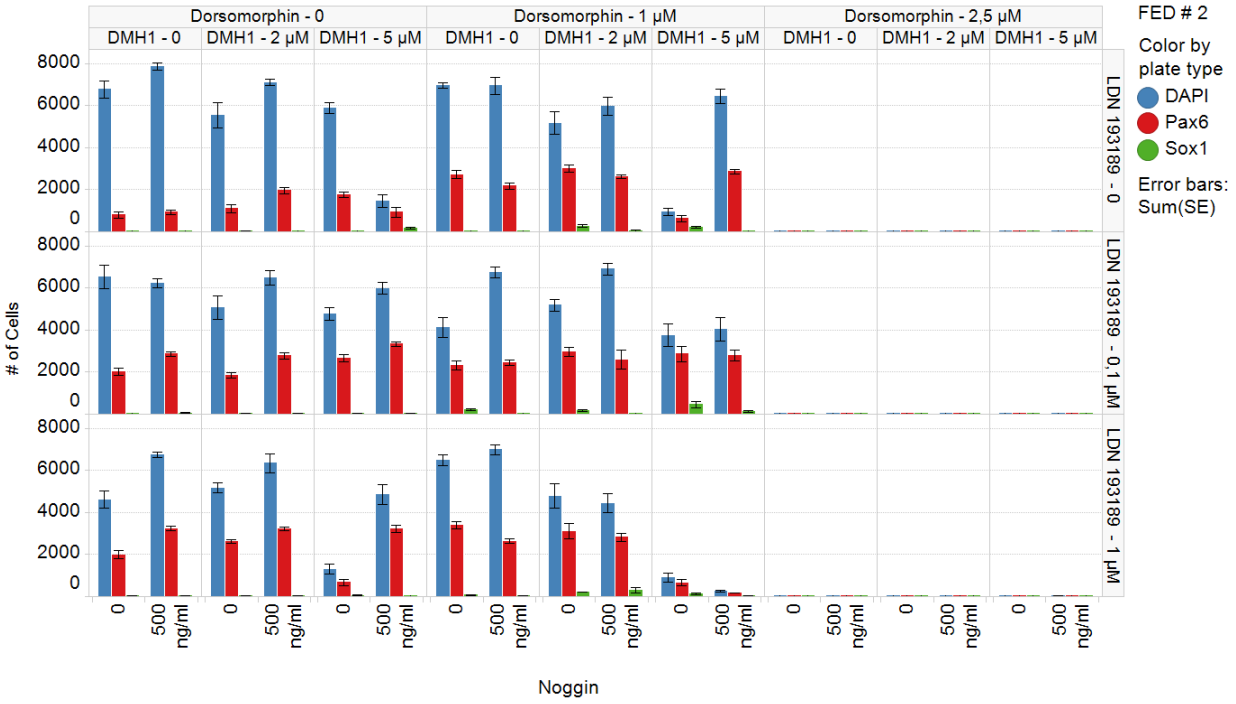

Figure 26 *Data from FED #2. Cell viability was improved with the lower concentration of SB431542 (2 µM). The high concentration of Dorsomorphin seemed to still contribute to cell death. Pax6 signal was detected in this FED instead of Sox1.*

Interestingly in this FED, PAX6 signal was detected while Sox1 had a really weak signal. The opposite pattern was noted in the first FED. The only difference in the second FED was the lower concentration of SB431542.

The cell viability was still hampered in high concentration of SMs suggesting that lowering the concentration SB431542 did not improve cell viability and that cell toxicity may be a response of the combination of high concentrations of SMs.

ICC images of the medium containing noggin and SMs are presented in Figure 27. The settings that appear more favorable (dorsomorphin/LDN193189/DMH1 1/0.1/5 µM) were chosen for re-evaluation in a 12-well format for qPCR analysis, however, on day 3 the cells died suggesting a difference between the 96-well format that FED experiments were carried out and the 12-well formal that neural inductions were carried out.

Even though both FED #1 and FED #2 failed to generate a model, they revealed that the combination of various SMs generates in a better readout that noggin alone (Figure 24 & Figure 27), thus noggin was not included in the next FED.

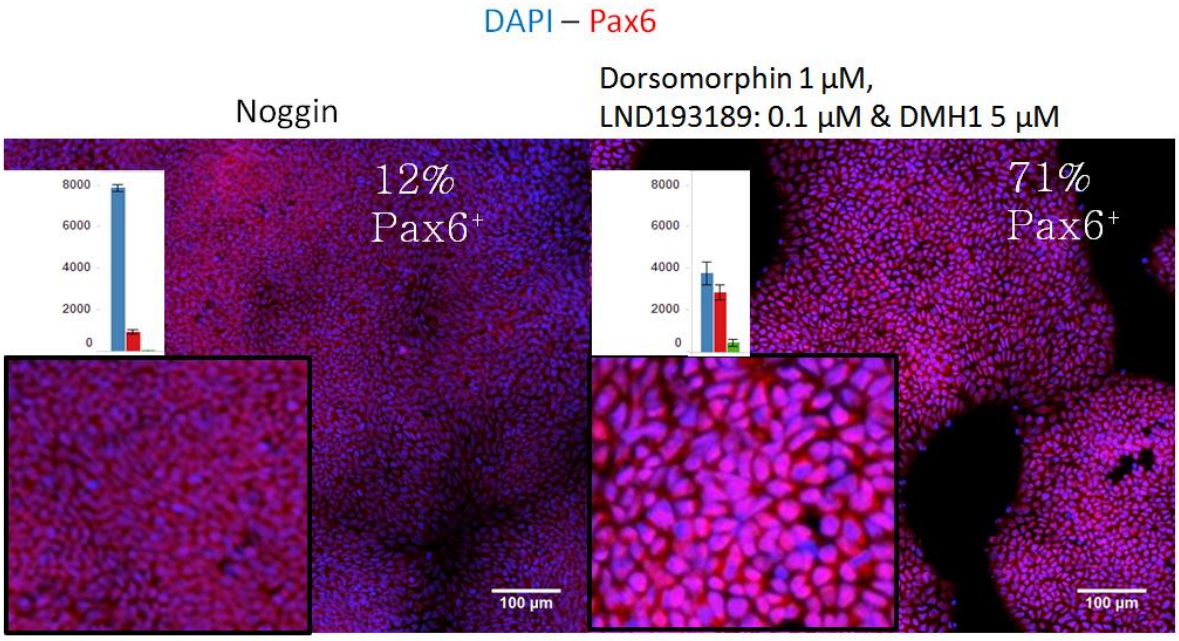

Figure 27 *ICC images for the standard protocol containing noggin (Left) and the combination of SMs (Right). With the use of SMs Pax6$^+$ cells increased to 71% although the cell viability was slightly hampered there are considerably more Pax6$^+$ cells in the neural induction with the SMs. The y-axis units are number of cells while the blue bar and red charts denote DAPI$^+$ and Pax6$^+$ cells, respectively. The % of Pax6$^+$ cells is derived from the ratio Pax6$^+$ cells/DAPI$^+$ cells × 100%.*

For the next FED (FED #3) the concentrations (levels) of Dorsomorphin were shifted to lower concentrations (Figure 28). It was also deemed interesting to evaluate if different concentrations of SB431542 have an impact on the Pax6-Sox1 protein expression since FED #1 has Sox1 signal and FED#2 Pax6 signal and ,more importantly, to find an optimum concentration for SB431542, therefore SB31542 was included as a factor (many levels) instead of a constant (one level).

Moreover β-FGFi (PD0325901) was also introduced as a factor replacing LDN193189 since it has been documented that β-FGF signaling inhibits neural conversion (Greber, Coulon et al. 2011).

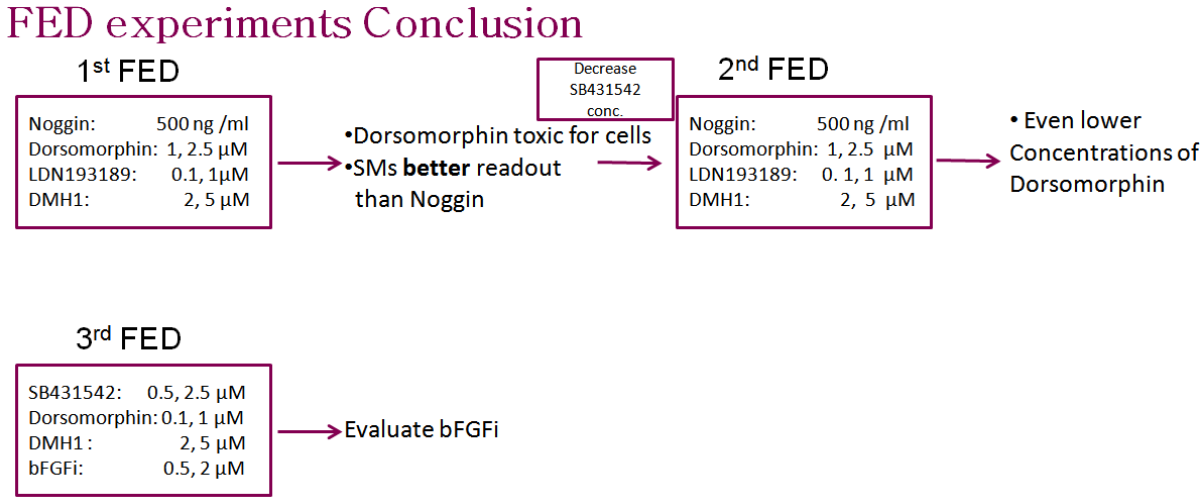

Figure 28 *Summary of the conclusions of the first two FED #1 & #2 as well as the settings of FED # 3. FED #1 & #2 exhibited cell toxicity and a FED model could not be generated due to the lack of available data. The conclusion from FED #2 suggests that Dorsomorphin should be at lower levels. Moreover, bFGFi was introduced as a factor replacing LDN193189.*

In FED # 3 (Figure 29) Sox1 protein signal was documented as in FED #1. Representative images of the least and most favorable readouts are presented in Figure 30.

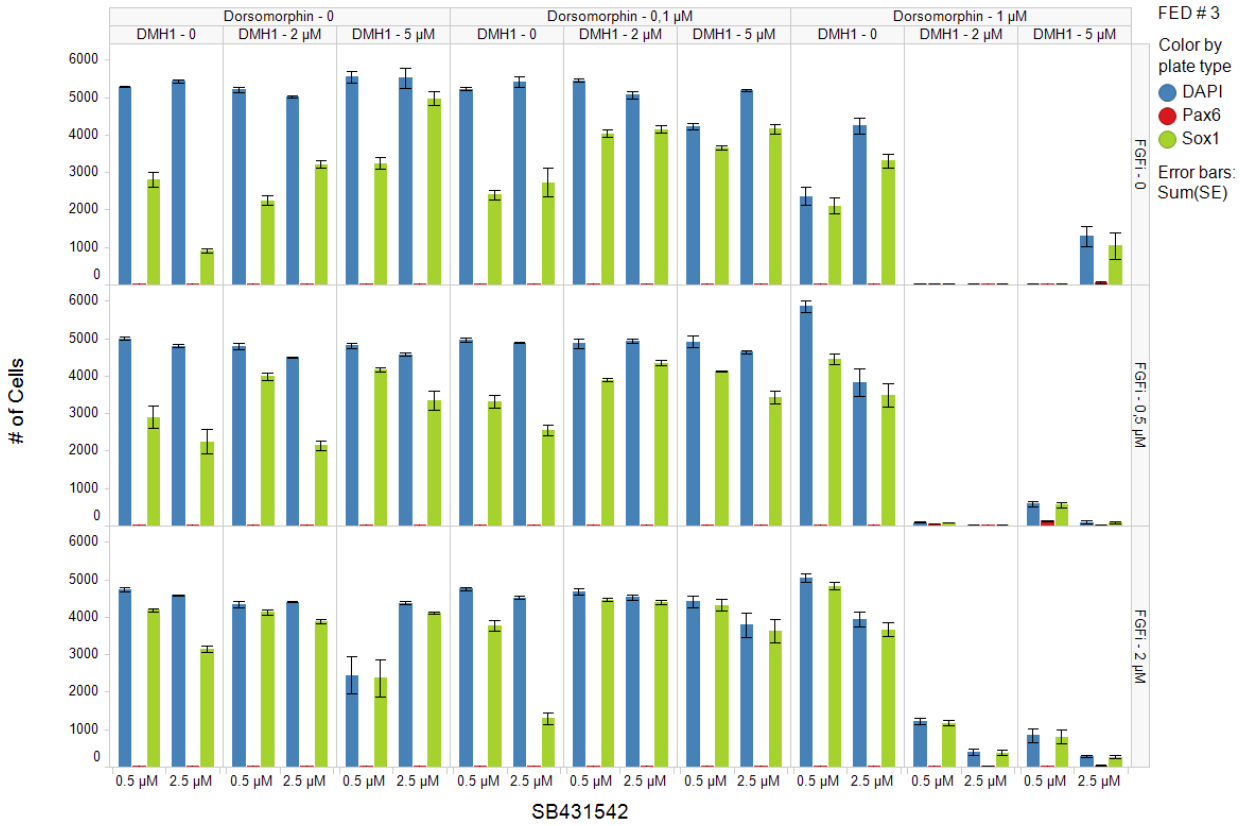

Figure 29 *Data from FED # 3. Cell viability was greatly improved with the lower concentrations of Dorsomorphin. Sox1 protein expression was evident while Pax6 was not detected, findings are in accordance with FED # 1 but not with FED # 2*.

In Figure 30 (right) 90% Sox1$^+$ cells were generated using DMH1/SB421542 5/2.5 µM while in Figure 27 (Left, FED #1) the standard protocol (containing only noggin and SB421542 10 µM) was able to generate 35% of Sox1$^+$ cells indicating once again that SMs do in fact perform better than noggin in neuralizing hiPSCs.

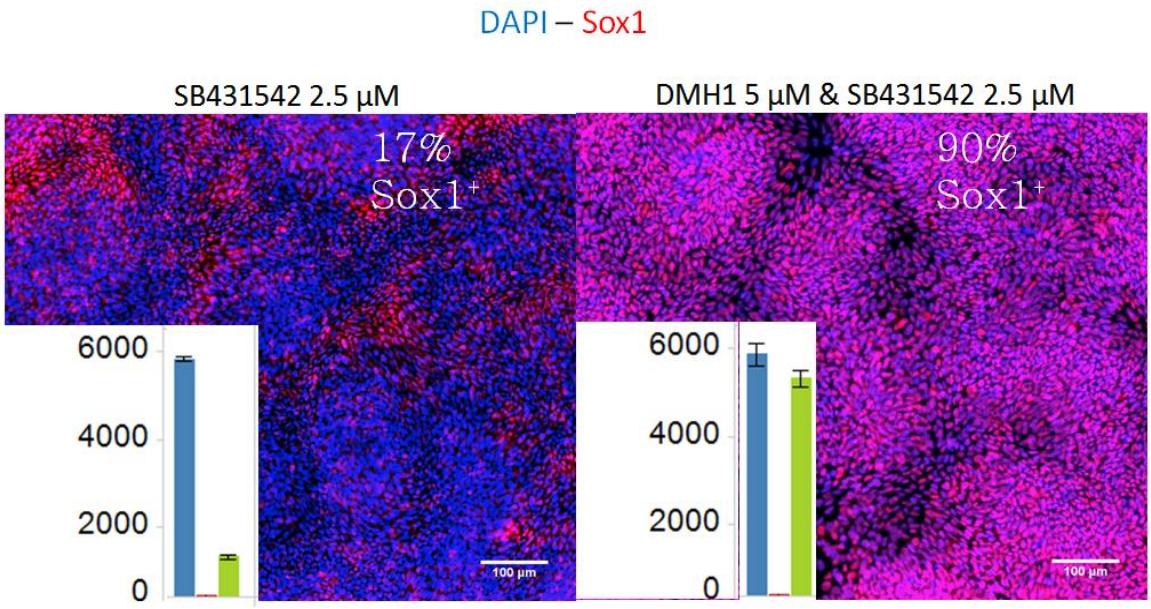

Figure 30 *ICC images for the least optimum readout (Left) and one of the optimum readouts containing the small molecule DMH1 at 5µM (Right). The y-axis units are number of cells while the blue bar chart denotes DAPI$^+$ cells and the green bar chart Sox1$^+$ cells. The % of Sox1$^+$cells is derived from the ratio Sox1$^+$ cells/DAPI$^+$ cells × 100%.*

In FED #3 cell viability was improved rendering possible the generation of a FED model (Figure 31). However, high concentration of dorsomorphin (1µM) was toxic when combined with other small molecules and thus that concentration of dorsomorphin was excluded from the model.

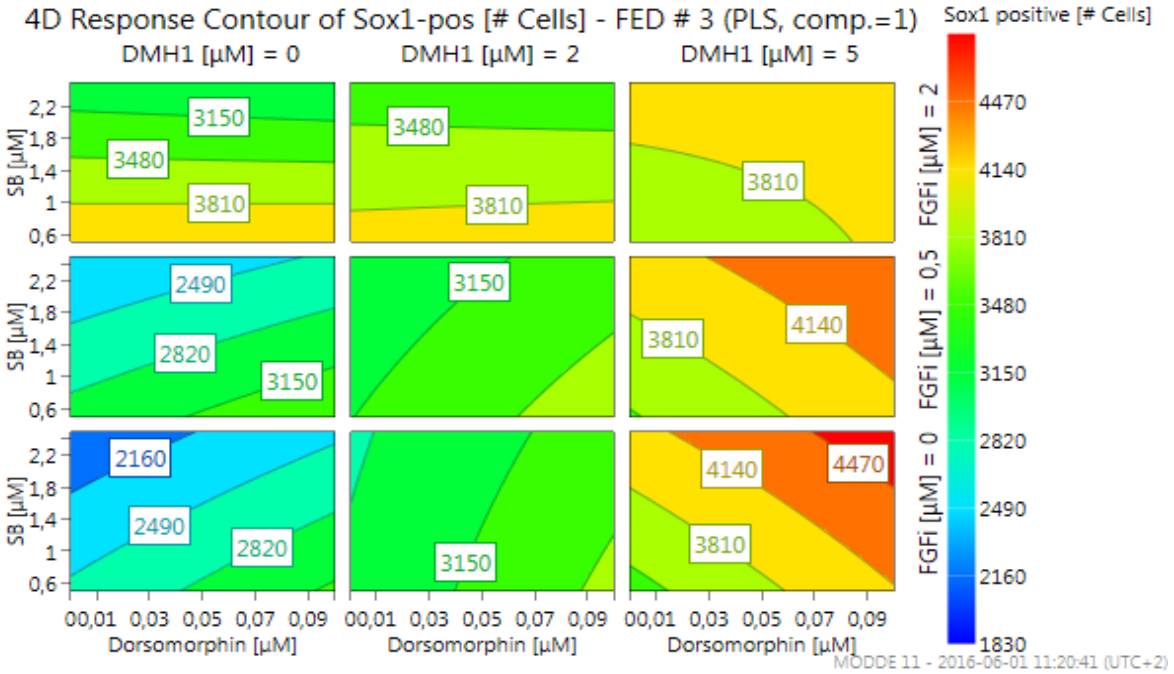

Figure 31 *Generation of FED model with MODDE 11. This image depicts the capacity of various combinations of SMs (factors) and their concentrations (levels) to generate Sox1$^+$ cells for FED # 3. The size of Sox1$^+$ populations is color-coded with blue and red denoting lower and higher, respectively, amounts of Sox1$^+$ cells. In this image, four variables can be identified: SB431542 (SB), dorsomorphin, DMH1 and bFGFi (FGFi). The contour plots depict the possible outcome in the amount of Sox1$^+$ cells by plotting the concentration of SB431542 against the concentration of dorsomorphin. Each contour plot refers to a specific concentration of DMH1 and bFGFi. From left to right, the concentration of DMH1 increases, and from bottom to top, the concentration of bFGFi increases. Readouts from dorsomorphin 1µM were excluded from the generation of this model due to the cell toxicity.*

The contour plots that were generated with the observed readouts from FED # 3 represent the predicted readouts generated by the various combinations of SB431542 (SB), dorsomorphin, DMH1 and bFGFi (FGFi). Each contour plot refers to a specific concentration of DMH1 and bFGFi and the variables in each contour plot are the concentrations of SB431542 (SB) and dorsomorphin. As previously mentioned, the concentration of dorsomorphin (1μM) at which cell toxicity was documented was excluded as it would interfere with the model.

Plotting the concentration of SB431542 (SB) against the concentration of dorsomorphin reveals how the combination of the various concentrations of these molecules affects the amount of Sox1$^+$ cells. Moreover each contour plots is coupled to a specific concentration of DMH1 and bFGFi. From left to right, the concentration of DMH1 increases. The concentration of bFGFi increases from bottom to top. The various amounts of Sox1$^+$ cells are color-coded with blue denoting lower numbers of Sox1$^+$ cells and red higher numbers of Sox1$^+$ cells. Consequently, the best combination of SMs, and hence the direction of new FED experiments, to neuralize can be easily identified in the red areas in the contour plots.

According to the contour plots (Figure 31) the highest number of Sox1$^+$ cells is attributed to the combination of SB431542 2.5 μM, dorsomorphin 0.1 μM, DMH1 5 μM and bFGFi 0 μM. However, taking a look at the observed readouts (Figure 32 right) it can be seen that the generated FED model has failed to predict the highest possible number of Sox1$^+$ cells since according to the observed values SB431542 2.5 μM and DMH1 5 μM is the settings with the highest number of Sox1$^+$ cells (circled dot no 31, number 31 assigned by Modde corresponding to SB431542 2.5 μM and DMH1 5 μM, data not shown).

These contradictive results can be explained from (Figure 32 left) it can be inferred that the generated model is not only of rather low importance (R2=0,486) but its predictive power i.e. its ability to predict data outside of the experimental values, is near zero (Q2=0.063), rendering any deductions from Figure 31 unreliable.

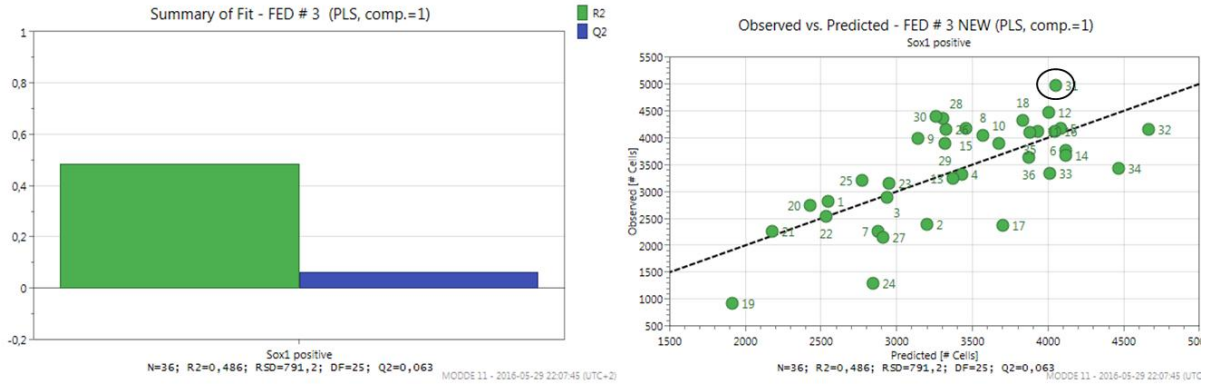

Figure 32 *Summary of fit and Observed vs. Predicted readouts.* ***Left****: Summary of fit with a rather low R2 and an almost 0 Q2.* ***Right:*** *The model generated (Predicted readouts) denoted with a dashed line while the green dots represent the actual (observed) readouts from the third FED.*

One possible reason behind the really poor R2 and Q2 values of the FED model, 0.486 and 0.063, respectively, is that for the generation of the model only two levels of dorsomorphin were included (dorsomorphin 0 and 0.1, basically one level) possibly limiting the reliability and predictive power of the model. To that end, a FED model was generated again (Figure 33) without the readouts of dorsomorphin.

This new generated mode suggests two strategies for neural induction. The red areas in the contour plots in Figure 33 indicate that DMH1/SB431542 5/2.5 μM would be one possible strategy (right contour plot in Figure 33) and bFGFi/SB431542 (SB) 2/0.5 μM (left contour plot in Figure 33) would be the other. DMH1/SB431542 5/2.5 μM was elected for up scaling to a 12-well format, constituting the optimized protocol. Characterization of the optimized protocol was carried out via qPCR analysis and comparison with the qPCR data obtained in for the standard protocol

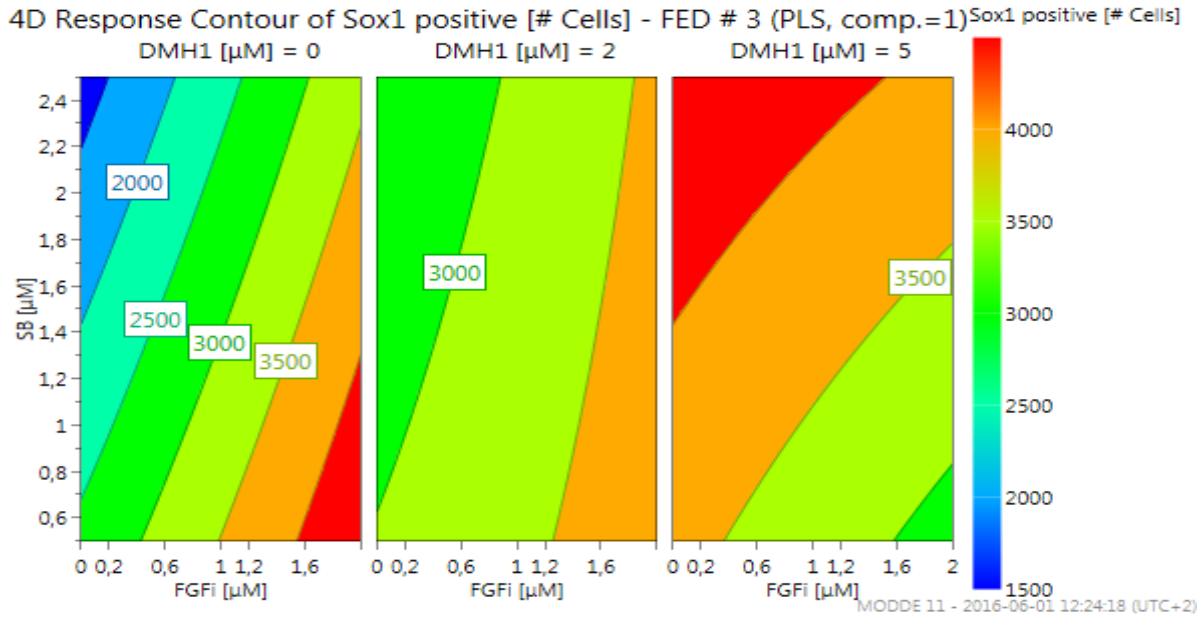

Figure 33 *Generated FED model with the exclusion of dorsomorphin. Model generated with MODDE 11. This image depicts the capacity of various combinations of SB431542 (SB), DMH1 and bFGFi (FGFi) (factors) and their concentrations (levels) to generate Sox1$^+$ cells for FED # 3 without introducing the data from dorsomorphin. The size of the Sox1$^+$ population is color-coded with blue and red denoting a lower and higher, respectively, number of Sox1$^+$ cells. In this image, three variables can be identified which are: SB431542 (SB), DMH1 and bFGFi. The combination of the various levels and factors give a different amount of Sox1$^+$ cells. In the contour plots SB431542 is plotted against bFGFi (FGFi). From left to right the concentration of DMH1 increases. When looking at the generated model two strategies can be identified (i.e. two red areas denoting a high number of Sox1$^+$ cells): DMH1/SB431542 (SB) 5/2.5 µM and bFGFi (FGFi)/ SB431542 (SB) 2/0.5 µM.*

Taking a look at the summary of fit between the initial and the later FED models (Figure 34) it can be seen that the R2 and Q2 values have improved for the second model suggesting that indeed the reduced levels of Dorsomorphin resulted in the unreliability of the generated model.

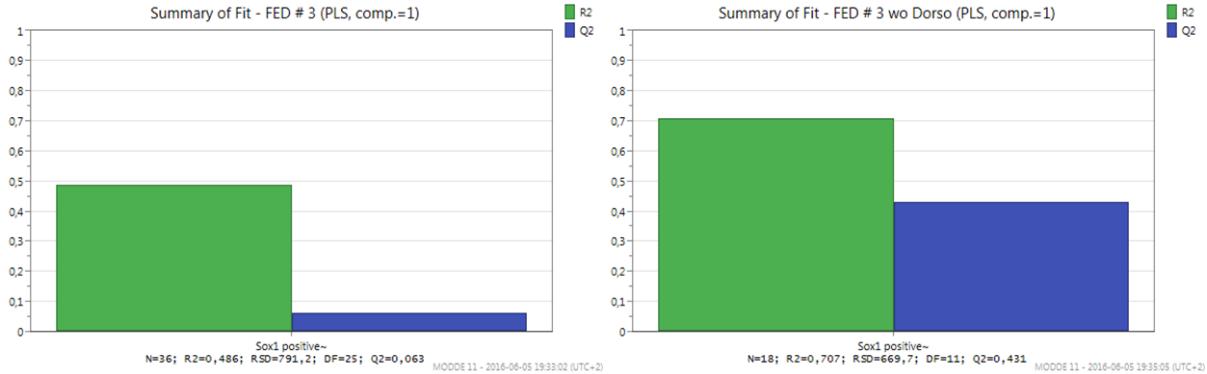

Figure 34 *Comparison between the summary of fit from the initial generated model (left) and the model generated without introducing dorsomorphin (right). The latter model has greater R2 and Q2 values suggesting that the range of levels of dorsomorphin was the limiting factor in the reliability of the first model.*

Summarizing the FED experiments (Figure 35) it can be seen that dorsomorphin in combination with other BMP-4 inhibitors was toxic at high concentrations (1 & 2.5 µM). Lowering SB431542 concentration did not improve cell viability (FED # 2). Different SB431542 concentrations were explored in FED # 3 along with the introduction of bFGFi and findings suggest that bFGFi is required depending on the concentration of SB431542.

Future experiments point to the direction of evaluating higher concentrations of SB431542 in the presence of bFGFi as well as perhaps avoiding dorsomorphin or exchanging it with LDN193189.

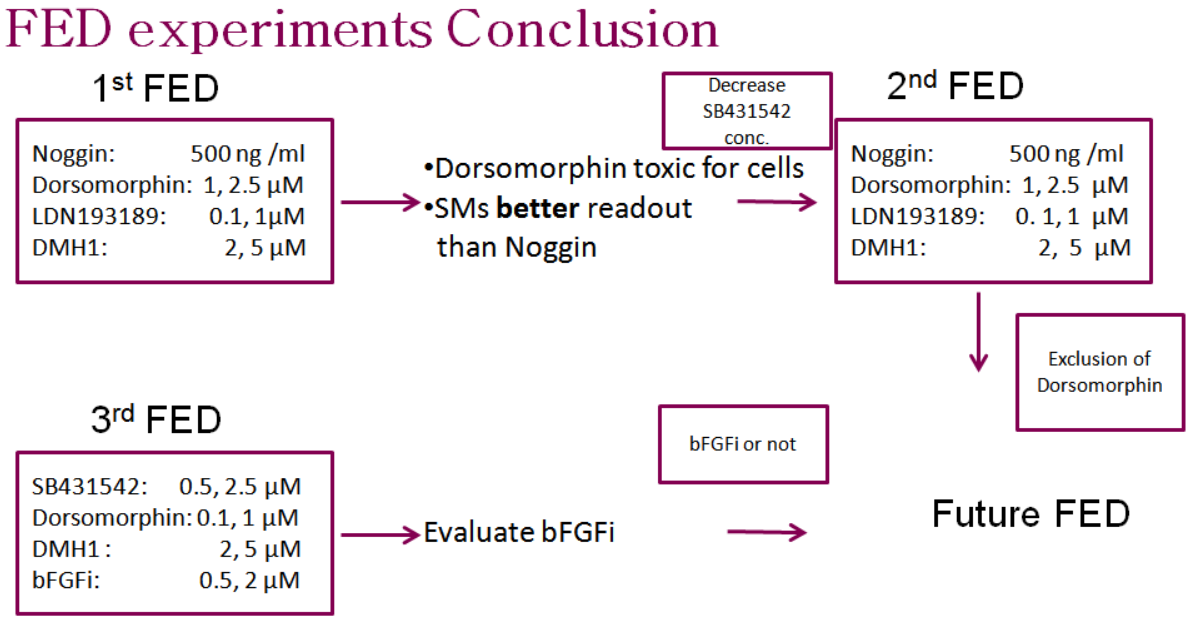

Figure 35 *Conclusion of the FED experiments summarizing the output from each experiments as well as the direction of future FED experiments for further optimization.*

4.3 Evaluation of optimized protocol and comparison to the standard protocol

Neural induction was carried out using the optimized protocol, that is, the protocol containing the SM DMH1 that was identified in the FED experiments to be able to neuralize 90% of the iPSC population (DMH1 5 µM & SB431542 µM).

From Figure 36 it can been seen that DMH1 has an effect on cell proliferation since on day 4 in the standard protocol cells have covered the whole area while in the optimized protocol cells have not. Considering the initial seeding density on day 0 seems to be approximately the same for the two protocols (40K/cm^2) the hampering of cell proliferation in the optimized protocol is probably due to the presence of DMH1.

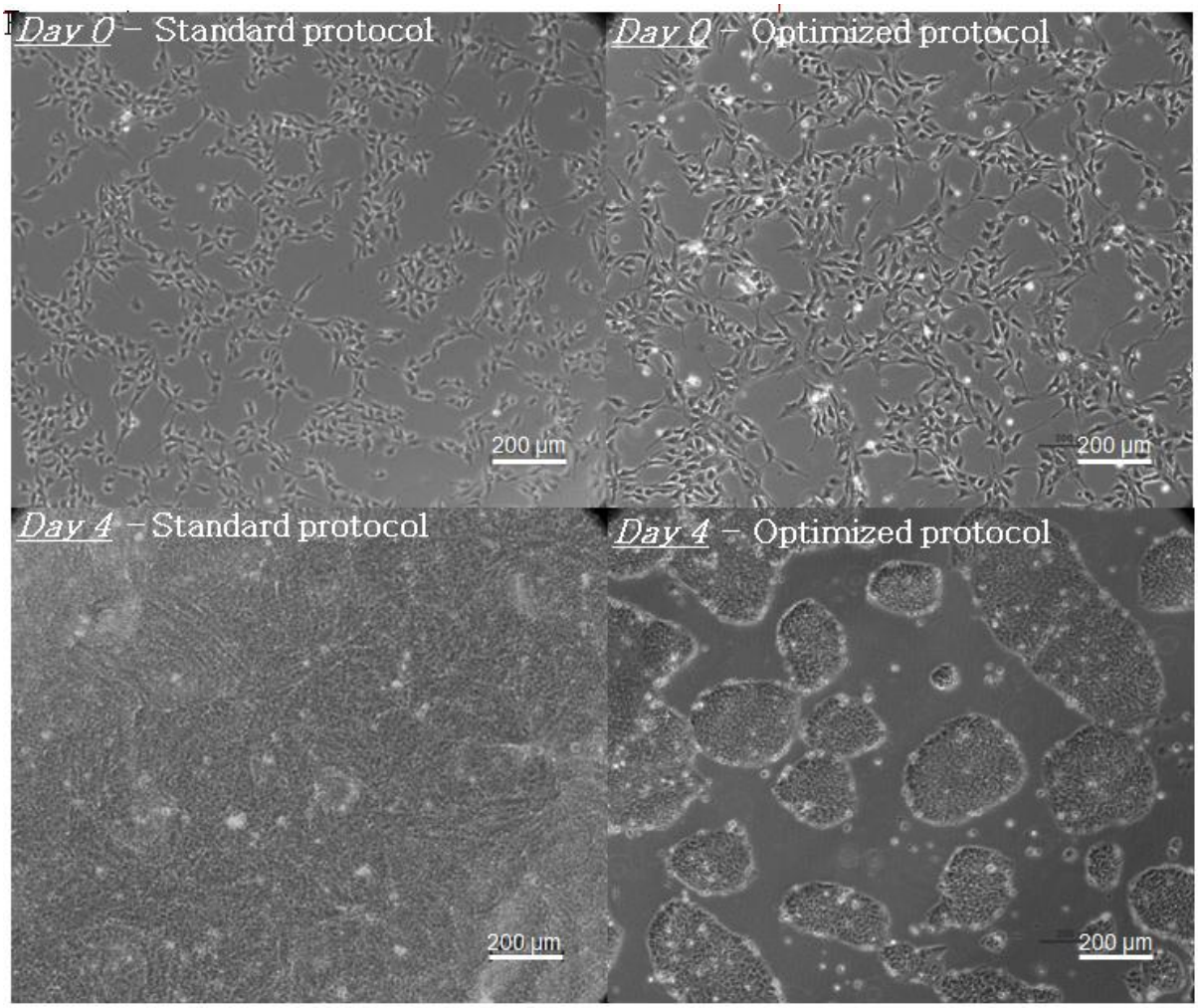

Figure 36 *Bright field images (10x) collected on days 0 and 4 of the neural induction with the standard noggin-containing protocol (noggin 500 ng/ml and SB431542 10 µM) and the optimized protocol (DMH1 5 µM and SB431542 2.5 µM).*

From the images in Figure 37 the same conclusion about DMH1 cannot be reached since the seeding densities on day 4 were different.

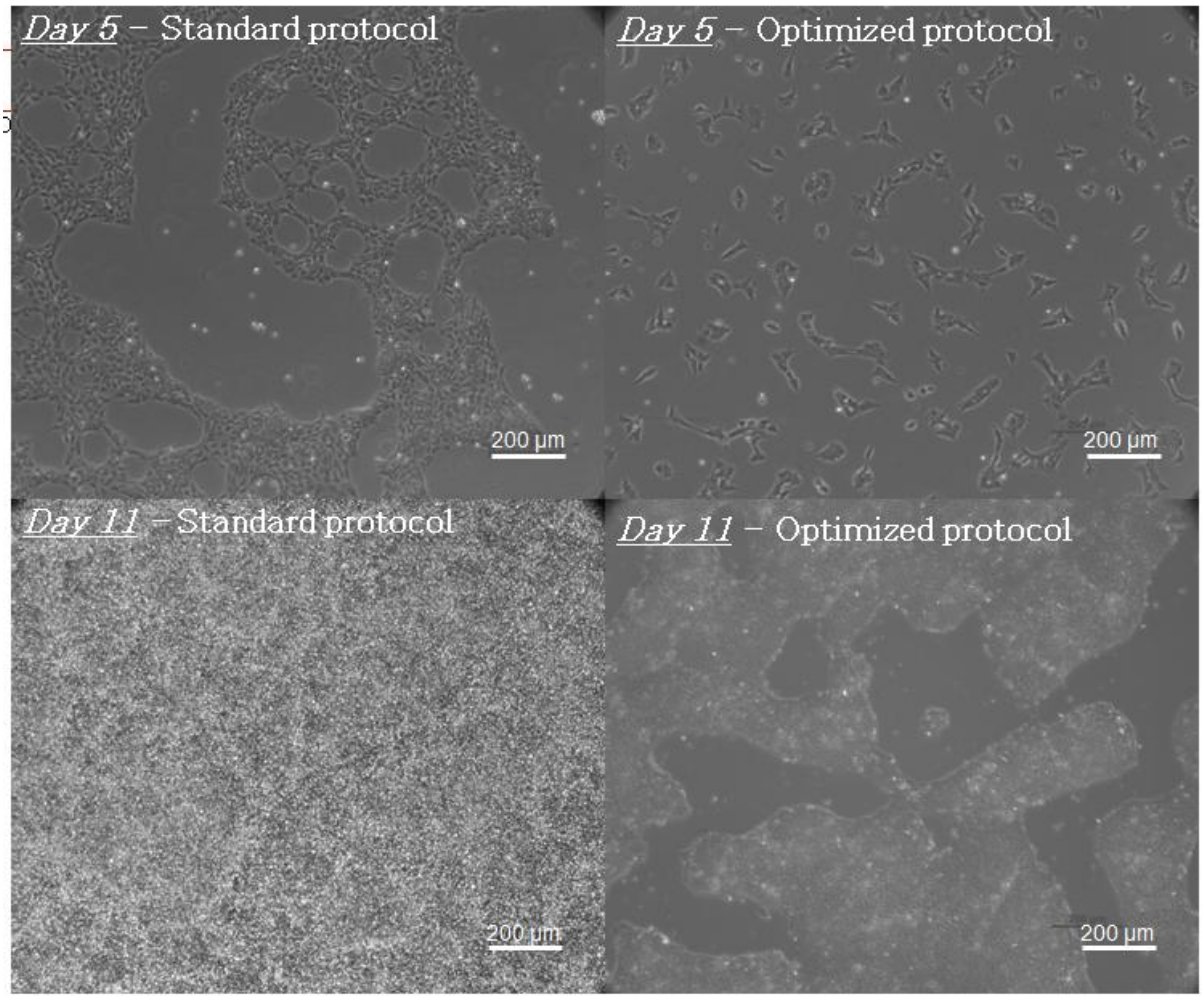

Figure 37 *Bright field images (10x) collected on days 5 and 11 of the NI #3 (standard protocol, 20% 63K/cm^2 on day 4) and NI #6 (optimized protocol, 26 K/cm^2 on day 4).*

On days 4 and 11 samples were collected and prepared for qPCR analysis. In order to compare the two protocols, the standard and the optimized one(Table 6) , the 20% sample (63 K/cm^2) from the standard protocol was used since the seeding density on day 4 was the one that was comparable to the seeding density on day 4 for the optimized protocol, 26 K/cm^2.

Compound	Standard Protocol	Optimized Protocol
DMEM/F12 + Glutamax	1:1	1:1
Neurobasal		
N2	1:200	1:200
β-mercaptoethanol	91 µM	91 µM
B27	1:100	1:100
BMP-4 inhibitor	noggin, 500 ng /ml	DMH1, 5 µM
SB431542	10 µM	10 µM
CHIR99021	3,33 µM	3,33 µM

Table 6 *Formulation of the various media used in neural induction with the standard and optimized protocol. The difference between these two is the type of BMP-4 inhibitor and the concentration of SB431542 which was lower (2.5 µM) in the optimized protocol.*

Data from qPCR for the optimized protocol are presented in Figure 38. Gene expression analysis for the pluripotency gene Oct4 suggest the commitment to a germ layer since Oct4 expression was downregulated by day 4 (Figure 38). Sox1 expression remained stable by day 4 but by day 11 it was upregulated while Sox2 expression exhibited the opposite trend, Sox2 expression was downregulated by day 4 but remained stable by day 11(Figure 38).

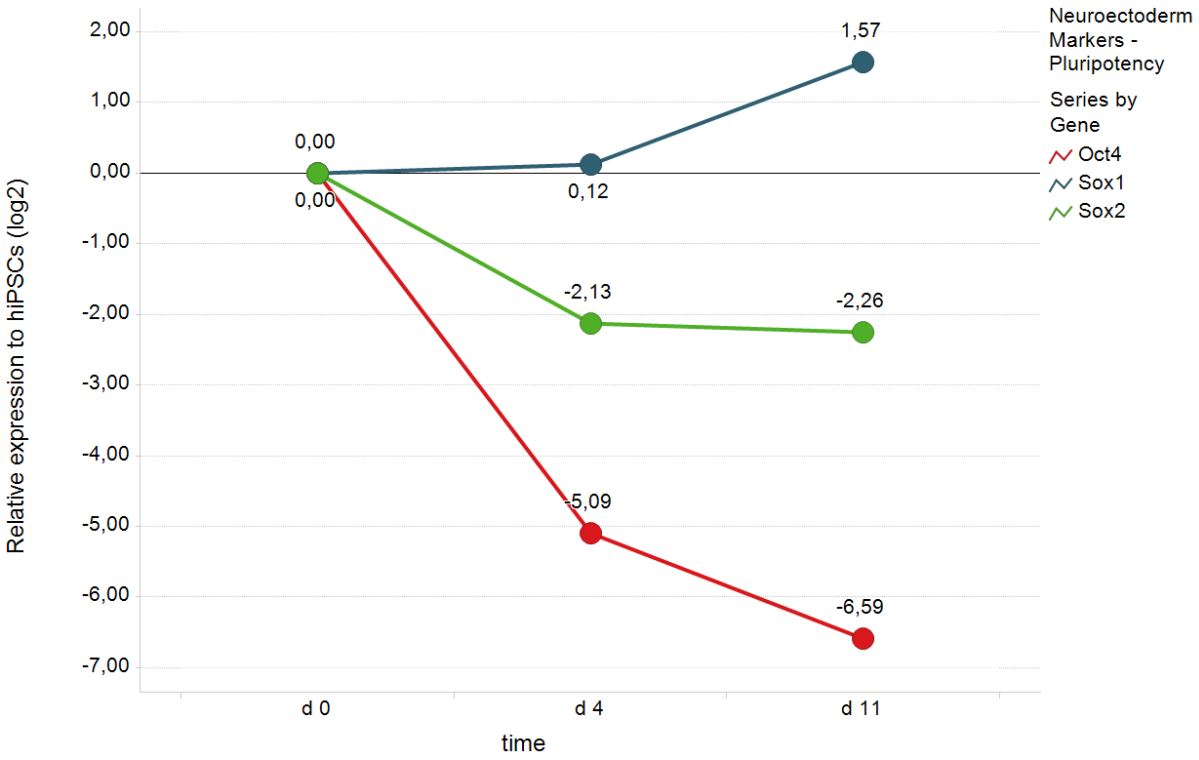

Figure 38 *Gene Expression analysis for pluripotency genes-Neuroectoderm Markers for the Optimized protocol (DMH1 5 μM and SB431542 2.5 μM). Oct4 expression was continuously downregulated. Sox1 expression was stable by day 4 (d 4) and upregulated by day 11 (d 11) while Sox2 expression was downregulated by day 4 (d 4) and remained stable by day 11 (d 11).*

Upon comparison of the qPCR data from the two protocols, the standard noggin-containing protocol and the optimized protocol, it can be seen that Sox1 and Sox2 expression trends are similar suggesting (Figure 39) that noggin's action can be simulated by DMH1.

The expression of Sox1 by day 4 is possibly the only small deviation between these protocols regarding these markers. In the standard protocol (noggin) Sox1 was upregulated by day 4 while in the optimized one (DMH1) Sox1 expression remained stable. Nevertheless by day 11 both protocols have almost similar levels of Sox1 expression.

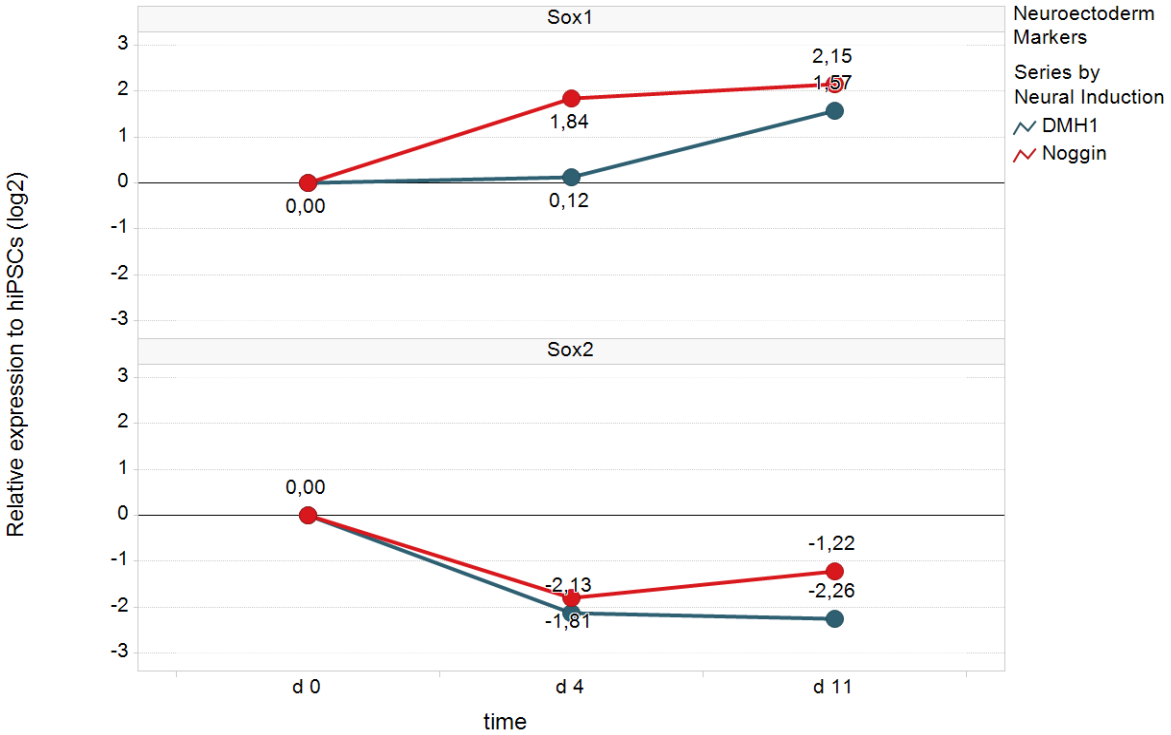

Figure 39 *Comparison of the neuroectoderm markers Sox1 and Sox2 between the standard (noggin 500 ng/ml and SB431542 10 µM) and optimized protocol (DMH1 5 µM and SB431542 2.5 µM). Expression of Sox1 and Sox2 followed the same trend in both protocols apart from the difference in Sox1 expression by day 4.*

Gene Expression analysis relieved that the expression profile for the neural stem markers was approximately the same for the two protocols (Figure 40) suggesting that the two protocols are equivalent in their capacity to impart neural stem cell characteristics to the differentiated cells.

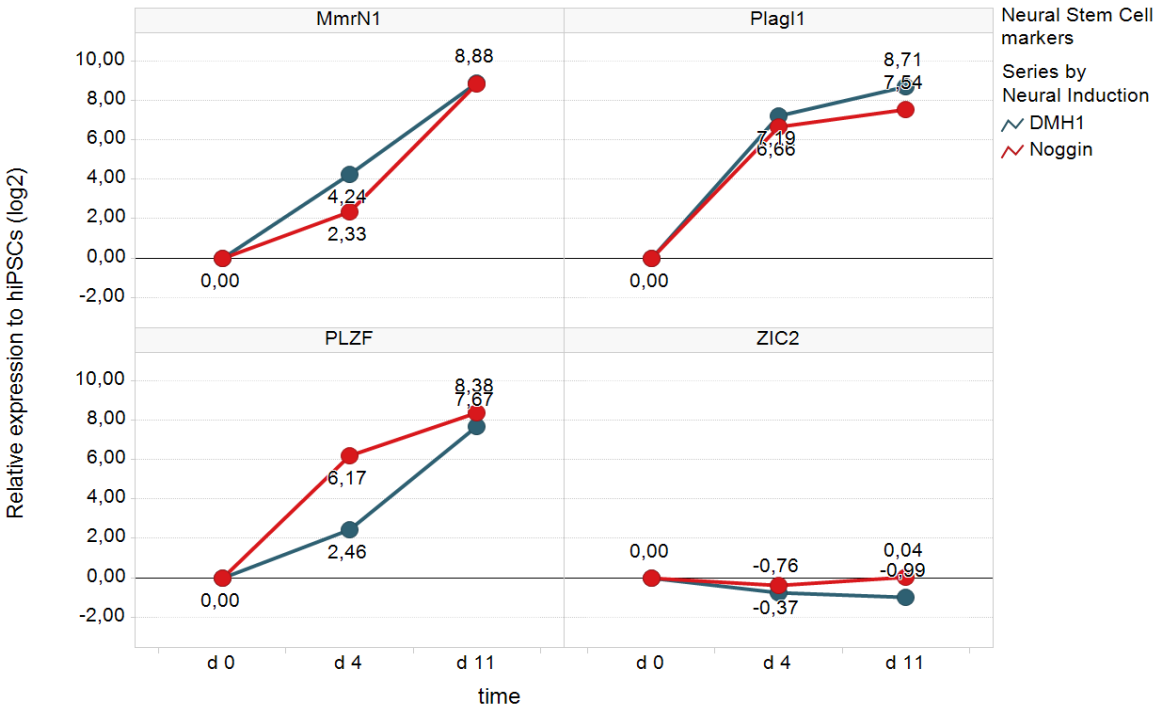

Figure 40 *Comparison of the neural stem cell markers MMrN1, Plagl1, PLZF and ZIC2 between the standard (noggin 500 ng/ml and SB431542 10 µM) and optimized (DMH1 5 µM and SB431542 2.5 µM) protocol. All genes associated with neural stem cell markers are expressed almost at the same level between the two protocols with the only difference observed in PLZF expression by day 4.*

Comparing the expression of the various regionality markers the first substantial difference in the two protocols which can be detected is the significant upregulation of Pax6 by day 11(Figure 41). GBX2 expression was almost similar between the two protocols.

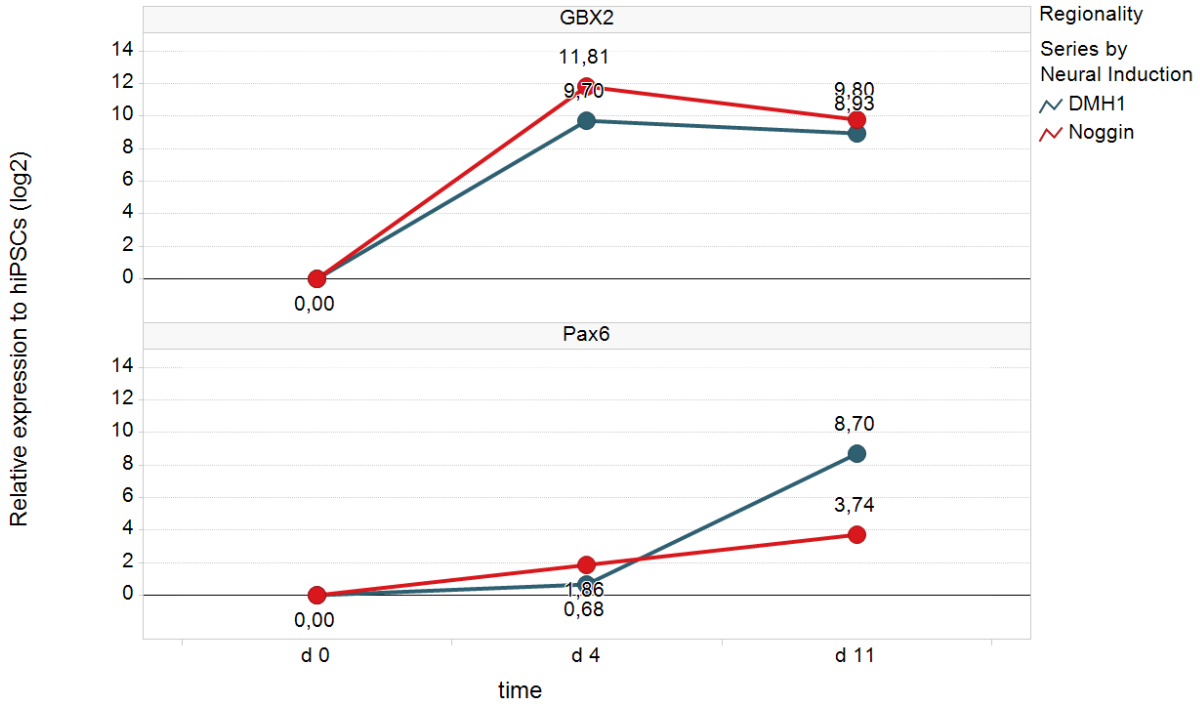

Figure 41 *Comparison of GBX2 expression and Pax6 expression between the two protocols. Pax6 expression by day 11 constitutes the first significant deviation between the two protocols. The expression of GBX2 follows the same trend in both protocols.*

Regarding the remaining regionality markers, it can be seen from Figure 42 that the Midbrain marker LMX1A was not upregulated. Moreover, the forebrain marker FoxG1 is downregulated by day 11.

OTX2 is a forebrain-midbrain marker and it is downregulated significantly by day 11 suggesting that the differentiated cell population may not have a considerable cell population associated with forebrain-midbrain identity.

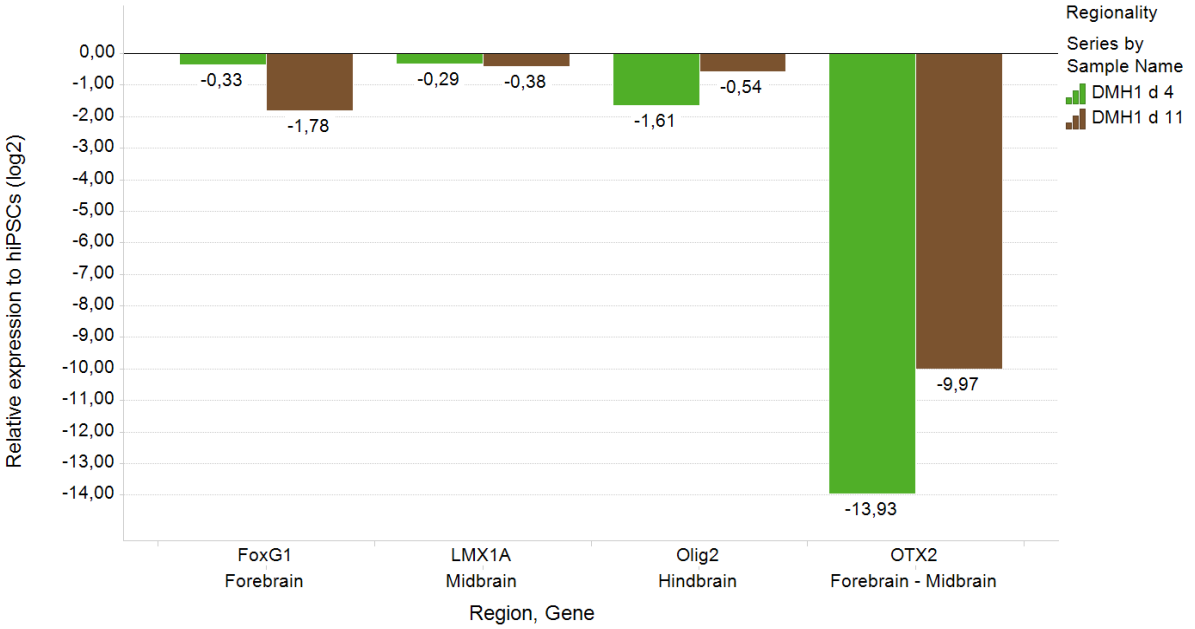

Figure 42 *Regionality markers for the optimized protocol (DMH1 5 µM and SB431542 2.5 µM). The LMX1A marker seems to remain stable while the forebrain marker FoxG1 is downregulated by day 11. A considerable downregulation of the forebrain midbrain marker OTX2 by day 4 and by day 11 is also observed.*

The fact the forebrain markers (FoxG1 – OTX2) and midbrain markers (OTX2 – LMX1A) were downregulated in combination with the fact that the hindbrain marker was highly upregulated suggests that the main identity of the generated cells is hindbrain.

Pax6 is expressed in the dorsal telencephalon (Kageyama 2013) and in the ventral hindbrain (Koch, Opitz et al. 2009). Since forebrain – midbrains markers are in fact downregulated, Pax6 upregulation by day11 is highly unlikely to be associated with the dorsal telencephalon (forebrain) and it is more likely associated with the ventral hindbrain.

Summarising, forebrain- midbrain markers are downregulated while the hindbrain marker GBX2 is upregulated suggesting a posterior shift. Moreover, PAX6 expression suggests that the generated cells have assumed a more ventral identity. These findings taking together indicate that the regional identity of the generated cells is ventral hindbrain.

Chapter 5: Discussion

5.1 Evaluation of the standard protocol

Seeding density had a strong impact on the expression of the midbrain marker LMX1A, the lower the seeding density on day 4 the higher the upregulation of the midbrain marker LMX1A, a finding that is on par with published data (Thwaites JW 2014) suggesting that the seeding density has in fact an impact on the expression of the midbrain marker LMX1A.

The default identity in neural induction in vitro (without introducing any patterning factors) is the forebrain (Lupo, Bertacchi et al. 2014) recapitulating the stages in brain development where the neural stem cells assume initially a forebrain identity and afterwards begin populating other parts of the brain. According to the findings in Chambers et al (2009) the forebrain marker FoxG1 was upregulated which is on par with the fact that the forebrain identity is the default identity of neural stem cells without introducing any patterning factors.

Pax6 upregulation was also evident, but since Pax6 expression is present in forebrain and hindbrain, a conclusion regarding the identity of the cell population cannot be reached based solely on Pax6 expression.

In this study, the hindbrain marker GBX2 was highly upregulated while the forebrain marker FoxG1 expression remained stable, unlike the findings in Chambers et al (2009) where FoxG1 was upregulated, suggesting that there is a possibility that the generated cells have assumed a more posterior identity (hindbrain).

A possible explanation of this posterior shift in expression could be attributed to the presence of CHIR99021 since the introduction of this compound was the only difference between the standard protocol in this study and the protocol used in Chambers et al (2009). CHIR99021 is an activator of the canonical Wnt pathway which is responsible for posteriorizing cell populations (Kiecker and Niehrs 2003, Moya, Cutts et al. 2014).

Looking at ΔCT values of the qPCR analysis revealed that FoxG1 is highly expressed in the hiPSCs. The fact that FoxG1 is already expressed in the hiPSCs strengthen the findings in literature that forebrain is the default regionality without introducing any patterning factors. In this study there seems to be a posterior shift in the regionality backed up by the upregulation of the hindbrain gene GBX2. Even though a signal from ICC for the forebrain marker FoxG1 was detected, it may be a false positive.

Nevertheless, further analysis is required to verify whether these speculations about the posterior shift (from forebrain to hindbrain regionality) holds.

5.2 Evaluation of the optimized protocol

When comparing the optimized and the standard noggin-containing protocol, DMH1 seemed to impair cell viability by day 4. Whether cells' primary focus was switched to differentiating instead of proliferating in the presence of DMH1 cannot be confirmed with the present data. However, this finding suggest that when trying to optimize protocols or exchange compounds, caution should also be taken on the initial seeding density since difference protocols generate cell populations proliferating at difference rates.

The substantial difference between the standard protocol and the optimized one lies in the considerable upregulation of Pax6 by day 11. Pax6 is expressed in the dorsal telencephalon (Kageyama 2013) and in the ventral hindbrain (Koch, Opitz et al. 2009).

In Chambers et al. (2009) Pax6 upregulation is attributed to the forebrain identity backed by the upregulation of the FoxG1 while in the optimized protocol the upregulation of Pax6 is an indicator of a ventral hindbrain identity backed by the upregulation of the hindbrain marker GBX2.

Moreover, the forebrain marker FoxG1 was downregulated by day 11 while the Forebrain – Midbrain marker OTX2 was downregulated considerably by day 11. Taking these findings together it can be speculated that the regional identity of the differentiated cells in the optimized protocol is mostly ventral hindbrain.

Contrastingly, the forebrain –midbrain marker OTX2 was upregulated in Chambers et al. (2009) contributing to the fact that the generated cell population in Chambers et al have the default forebrain identity while the generated cells with the optimized protocol have acquired a hindbrain identity.

OTX2 gene is responsible for the forebrain and midbrain patterning while GBX2 for the hindbrain patterning, the interplay between the genes OTX2 and GBX2 has been evaluated extensively in literature. OTX2 and GBX2 are responsible for different regions of the brain and they repress each other expression i.e. (Li and Joyner 2001, Nakamura 2001), which is evident in the findings in this study (see Figure 41 Figure 42).

The fact the regional identity of the generated cells is different between the standard and the optimized protocol used in this study suggests that the SM DMH1 has a ventralizing effect on the generated cells. This may be due to the fact that DMH1 selectively inhibits the BMP-4 receptors ALK 2 & 3 receptors and not the ALK6, while noggin by its mode of action presumably inhibits the activation of all the BMP-4 receptors.

Whether DMH1 can also posteriorize cell population cannot be ascertained since in the standard protocol CHIR99021 seemed to be the driving force behind the posterior shift of the generated cell population.

Hence, even though small molecules do pose as adequate candidates for BMP-4 inhibition, SMs should be also evaluated for their patterning capacity. For example, this optimized protocol containing DMH1 would not be ideal for when trying to generate dopaminergic neurons (midbrain) but more suitable for generating posterior identities e.g. motor neurons and, in fact, in Du, Chen et al. (2015) DMH1 has been used in order to generate motor neurons.

5.3 Factorial Experimental Design

FED experiments revolve around the movement of the set of levels which depends on the readouts in order to identify the optimum readout. The number of iterations of this process is not set and depends on how close your initial settings are to the optimum settings as well as how efficient is the process by which the next set of levels are identified.

The initial settings of FED experiment were selected according to literature. There are build-in programs in Modde that calculate the importance of each factor depending on the readouts and suggesting accordingly the potential changes in the levels of the factors that would contribute to better readouts. However in this study, the election of the levels after the initial settings was done by lowering the levels of factors usually to half its value/an order of magnitude. Moreover the levels of dorsomorphin were changed and the full potential of FED analysis cannot be reached by just changing the levels only of one factor.

Two of the three FED experiments exhibited Sox1 signal and not Pax6 and one exhibited Pax6 but not Sox1, these findings call for further experiments since in order to arrive to safe conclusions experiments should be repeated. Each experiment was performed only once in this study. Generally, repeatability of experiments is vital for accurate results therefore more experiments need to be done for the same settings to ensure accuracy of the results.

Pax6 and Sox1 are of the earliest markers to be expressed in the neuroectoderm. Sox1 expression precedes the expression of Pax6 in mouse embryogenesis while the opposite trend is evident in human (Simona Casarosa 2013). Therefore another type of Pax6 antibody should be explored since Pax6 is the first marker to be expressed in human and thus Pax6 would a more suitable candidate for these experiments.

Dorsomorphin appeared to have a toxic effect on cells at high levels (2.5 μM) while at lower levels (1 μM) it was only toxic in combination with other SMs. Dorsomorphin is not as selective in inhibiting BMP-4 receptors as DMH1 is, studies (Zhou, Su et al. 2010) have revealed that dorsomorphin may also inhibit TGFb1 receptors as well as having many "off target" effects, such as the inhibition of AMPK (adenosine monophosphate-activated protein kinase)(Zhou, Myers et al. 2001, Kim, Miller et al. 2004).

Consequently, dorsomorphin is not selective in BMP-4 inhibition and it should be avoided in future FED experiments since it may inhibit other pathways, rendering any conclusions regarding regionality and how regionality is coupled to the inhibition of specific receptors (ALK2-3 and ALK6) unreliable.

Regarding the FED model, it can be deduced that in order to generate reliable models different levels of each factor are vital, since inadequate amount of levels (<2) contributed to models with low predictive power in this study.

Chapter 6: Conclusion & Future Work

The standard protocol generated a mixed population of neural stem cells. Even though the hindbrain marker GBX2 was highly upregulated by day 11 it cannot be postulated that there is no presence of a forebrain population since the forebrain marker FoxG1 is expressed albeit not upregulated. Additional studies should be carried out to verify the identity of the generated cells using the standard protocol e.g. q PCR analysis for the forebrain-midbrain marker OXT2, ICC for the hindbrain gene GBX2 to verify protein translation.

The presence of CHIR99021 possibly altered the –expected– forebrain identity of the differentiated cells shifting them to more posterior identities. Therefore it would be of interest to carry out another differentiation without the presence of CHIR99021 and observe if there are any differences in the expression of FoxG1 and GBX2 genes.

Seeding density has an impact on the expression/repression of the midbrain marker LMX1A though it does not seem to affect the expression of neural stem cell markers.

The main differences between the standard noggin-containing and the optimized protocol can be summarized in three points (Table 7). Firstly, according to analysis of the ICC images, the standard protocol (noggin) yielded 35% $Sox1^+$ cells while the optimized protocol 95% $Sox1^+$ cells (DMH1). Secondly there is possibly no presence of midbrain cell populations in the optimized protocol while there is in the standard one. Lastly, Pax6 expression was highly upregulated in the optimized protocol while the same trend was not observed in the standard protocol. Taking together these findings for the optimized protocol it can be inferred that DMH1 apart from exchanging noggin for neuroectoderm differentiation, it may act as a patterning factor.

Future experiments regarding the optimized protocol would entail the evaluation of the impact the seeding density on day 4 would potentially have on regionality since in this study only one seeding density was evaluated for the optimized protocol. Moreover, it would be of interest to evaluate what effects the introduction of patterning factors such as purmorphamine and would have on the regionality. Purmorphamine is a pharmacological activator of the Shh pathway which is responsible for generating ventral identities (Suzuki and Vanderhaeghen 2015), hence, it would be interesting to evaluate the differences in the mode of action between DMH1 and purmorphamine since both seem to have a ventralizing effect.

		Forebrain Midbrain		Hindbrain	Forebrain - Hindbrain
	% Sox1+	FoxG1	LMX1A	GBX2	Pax6
Noggin	35	-0,46	5,38	9,80	3,74
DMH1	95	-1,78	-0,38	8,93	8,70

Table 7 *Summary of the main deviations/similarities between the two protocols regarding neural induction and regionality. Higher values denoted in green color while lower values in red, the values under the genes denote the relative expression to hiPSCs (log2). The capacity of the protocol to direct hiPSCs to a neuroectoderm fate ($Sox1^+$) was improved in the optimized protocol (DMH1) while the regional identity of the generated cell populations was different in the optimized protocol suggesting that DMH1 itself can be regarded as a patterning factor.*

Factorial experimental design is an efficient approach to evaluate many factors as well as assessing the interaction between them. The robustness of the readouts is important considering that in this study the same FED generated different type of readouts (shifts between Sox1 and Pax6 signal in the ICC). Moreover, the need for a range of levels within each factor is crucial in order to generate reliable FED models. Future FED experiments in this study would involve exploring different levels of DMH1.

Another possible venture would be the evaluation of the interaction of LDN193189 and bFGFi. The former exhibited promising results in neuralizing iPSCs from the FED # 3 (Figure 33) while the levels of the latter were not explored as much as in the case of Dorsomorphin. It would be interesting to evaluate whether LDN193189 has also a patterning effect – much like DMH1 – and draw conclusions about the correlation between ALK receptors and patterning cues since LDN193189 and DMH1 have different affinity for the ALK receptors.

References

Alberts B, J. A., Lewis J, et al. (2002). Molecular Biology of the Cell.4th edition. New York, Garland Science.

Bhattacharyya, S., A. Kumar, et al. (2012). "The voyage of stem cell toward terminal differentiation: a brief overview." Acta Biochimica et Biophysica Sinica **44**(6): 463-475.

Bioinformatics, S. S. I. "TGF-beta family signature and profile." 2015, from http://prosite.expasy.org/PDOC00223#technical.

Brown, L. and S. Brown (2009). "Zic2 is expressed in pluripotent cells in the blastocyst and adult brain expression overlaps with makers of neurogenesis." Gene Expression Patterns **9**(1): 43-49.

Burry, R. W. (2011). "Controls for immunocytochemistry: an update." J Histochem Cytochem **59**(1): 6-12.

Chambers, I. and S. R. Tomlinson (2009). "The transcriptional foundation of pluripotency." Development (Cambridge, England) **136**(14): 2311-2322.

Chambers, S. M., C. A. Fasano, et al. (2009). "Highly efficient neural conversion of human ES and iPS cells by dual inhibition of SMAD signaling." Nat Biotech **27**(3): 275-280.

Chambers, S. M., Y. Qi, et al. (2012). "Combined small-molecule inhibition accelerates developmental timing and converts human pluripotent stem cells into nociceptors." Nat Biotech **30**(7): 715-720.

Chizhikov, V. V. and K. J. Millen (2005). "Roof plate-dependent patterning of the vertebrate dorsal central nervous system." Developmental Biology **277**(2): 287-295.

Cuny, G. D., P. B. Yu, et al. (2008). "Structure-activity relationship study of bone morphogenetic protein (BMP) signaling inhibitors." Bioorg Med Chem Lett **18**(15): 4388-4392.

Downs, K. M. (2009). "The enigmatic primitive streak: prevailing notions and challenges concerning the body axis of mammals." BioEssays : news and reviews in molecular, cellular and developmental biology **31**(8): 892-902.

Du, Z.-W., H. Chen, et al. (2015). "Generation and expansion of highly pure motor neuron progenitors from human pluripotent stem cells." Nat Commun **6**.

Duane, T. (1993). Duane's Clinical Ophthalmology, Lippincott Williams & Wilkins.

Dupont, S., L. Zacchigna, et al. (2005). "Germ-Layer Specification and Control of Cell Growth by Ectodermin, a Smad4 Ubiquitin Ligase." Cell **121**(1): 87-99.

Elkabetz, Y., G. Panagiotakos, et al. (2008). "Human ES cell-derived neural rosettes reveal a functionally distinct early neural stem cell stage." Genes & Development **22**(2): 152-165.

Emdad, L., S. L. D'Souza, et al. (2012). "Efficient differentiation of human embryonic and induced pluripotent stem cells into functional astrocytes." Stem Cells Dev **21**(3): 404-410.

Ericson, J., J. Briscoe, et al. (1997). "Graded sonic hedgehog signaling and the specification of cell fate in the ventral neural tube." Cold Spring Harb Symp Quant Biol **62**: 451-466.

Espuny-Camacho, I., Kimmo A. Michelsen, et al. (2013). "Pyramidal Neurons Derived from Human Pluripotent Stem Cells Integrate Efficiently into Mouse Brain Circuits In Vivo." Neuron **77**(3): 440-456.

Falk, A., P. Koch, et al. (2012). "Capture of Neuroepithelial-Like Stem Cells from Pluripotent Stem Cells Provides a Versatile System for In Vitro Production of Human Neurons." PLoS ONE **7**(1): e29597.

Fusaki, N., H. Ban, et al. (2009). "Efficient induction of transgene-free human pluripotent stem cells using a vector based on Sendai virus, an RNA virus that does not integrate into the host genome." Proceedings of the Japan Academy, Series B **85**(8): 348-362.

Gilbert, S. (2006). Developmental Biology.8th Edition. Sunderland, Sinauer Associates, Inc.

Gilbert, S. F. (2014). Developmental Biology.10th Edition, Sinauer Associates, Inc.
Gordon, M. D. and R. Nusse (2006). "Wnt signaling: multiple pathways, multiple receptors, and multiple transcription factors." J Biol Chem **281**(32): 22429-22433.
Graham, V., J. Khudyakov, et al. (2003). "SOX2 functions to maintain neural progenitor identity." Neuron **39**(5): 749-765.
Greber, B., P. Coulon, et al. (2011). "FGF signalling inhibits neural induction in human embryonic stem cells." The EMBO Journal **30**(24): 4874-4884.
Groppe, J., J. Greenwald, et al. (2002). "Structural basis of BMP signalling inhibition by the cystine knot protein Noggin." Nature **420**(6916): 636-642.
Gure, A. O., E. Stockert, et al. (2000). "Serological identification of embryonic neural proteins as highly immunogenic tumor antigens in small cell lung cancer." Proc Natl Acad Sci U S A **97**(8): 4198-4203.
Habas, R. and I. B. Dawid (2005). "Dishevelled and Wnt signaling: is the nucleus the final frontier?" Journal of Biology **4**(1): 1-4.
Hao, J., J. N. Ho, et al. (2010). "In vivo structure-activity relationship study of dorsomorphin analogues identifies selective VEGF and BMP inhibitors." ACS Chem Biol **5**(2): 245-253.
Hemmati-Brivanlou, A. and D. Melton (1997). "Vertebrate embryonic cells will become nerve cells unless told otherwise." Cell **88**(1): 13-17.
Houtmeyers, R., J. Souopgui, et al. (2013). "The ZIC gene family encodes multi-functional proteins essential for patterning and morphogenesis." Cell Mol Life Sci **70**(20): 3791-3811.
Huang, X. and J.-P. Saint-Jeannet (2004). "Induction of the neural crest and the opportunities of life on the edge." Developmental Biology **275**(1): 1-11.
Hutton, S. R. and L. H. Pevny (2011). "SOX2 expression levels distinguish between neural progenitor populations of the developing dorsal telencephalon." Developmental Biology **352**(1): 40-47.
Ishmael, F. T. and C. Stellato (2008). "Principles and applications of polymerase chain reaction: basic science for the practicing physician." Annals of Allergy, Asthma & Immunology **101**(4): 437-443.
Jessell, T. M. (2000). "Neuronal specification in the spinal cord: inductive signals and transcriptional codes." Nat Rev Genet **1**(1): 20-29.
Judson, R. L., J. E. Babiarz, et al. (2009). "Embryonic stem cell-specific microRNAs promote induced pluripotency." Nat Biotech **27**(5): 459-461.
Kageyama, R., Yamamori, Tetsuo, Ed. (2013). Cortical Development: Neural Diversity and Neocortical Organization, Springer Japan.
Karim, M. S., G. T. Buzzard, et al. (2012). "Secreted, receptor-associated bone morphogenetic protein regulators reduce stochastic noise intrinsic to many extracellular morphogen distributions." Journal of The Royal Society Interface **9**(70): 1073-1083.
Keller, G. M. (1995). "In vitro differentiation of embryonic stem cells." Curr Opin Cell Biol **7**(6): 862-869.
Kiecker, C. and C. Niehrs (2003). The Role of Wnt Signaling in Vertebrate Head Induction and the Organizer-Gradient Model Dualism. Wnt Signalling in Development, Landes Bioscience, Kluwer Academic/Plenum Publishers**:** 71-89.
Kim, E. K., I. Miller, et al. (2004). "C75, a fatty acid synthase inhibitor, reduces food intake via hypothalamic AMP-activated protein kinase." J Biol Chem **279**(19): 19970-19976.
Koch, P., T. Opitz, et al. (2009). "A rosette-type, self-renewing human ES cell-derived neural stem cell with potential for in vitro instruction and synaptic integration." Proceedings of the National Academy of Sciences **106**(9): 3225-3230.
Koch, P., T. Opitz, et al. (2009). "A rosette-type, self-renewing human ES cell-derived neural stem cell with potential for in vitro instruction and synaptic integration." Proceedings of the National Academy of Sciences.
Komiya, Y. and R. Habas (2008). "Wnt signal transduction pathways." Organogenesis **4**(2): 68-75.

Krencik, R. and S.-C. Zhang (2011). "Directed differentiation of functional astroglial subtypes from human pluripotent stem cells." Nat. Protocols **6**(11): 1710-1717.
Kriks, S., J.-W. Shim, et al. (2011). "Dopamine neurons derived from human ES cells efficiently engraft in animal models of Parkinson/'s disease." Nature **480**(7378): 547-551.
Larsen, W. J. (2001). Human Embryology.3rd Edition.
Lee, H., G. A. Shamy, et al. (2007). "Directed differentiation and transplantation of human embryonic stem cell-derived motoneurons." Stem Cells **25**(8): 1931-1939.
Lee, K. J., P. Dietrich, et al. (2000). "Genetic ablation reveals that the roof plate is essential for dorsal interneuron specification." Nature **403**(6771): 734-740.
Lewis, W. (2007). Principles of Development.3rd Edition, Oxford University Press.
Li, J. Y. and A. L. Joyner (2001). "Otx2 and Gbx2 are required for refinement and not induction of mid-hindbrain gene expression." Development **128**(24): 4979-4991.
Li, W., W. Sun, et al. (2011). "Rapid induction and long-term self-renewal of primitive neural precursors from human embryonic stem cells by small molecule inhibitors." Proc Natl Acad Sci U S A **108**(20): 8299-8304.
Livak, K. J. and T. D. Schmittgen (2001). "Analysis of relative gene expression data using real-time quantitative PCR and the 2(-Delta Delta C(T)) Method." Methods **25**(4): 402-408.
Lu, J., H. Liu, et al. (2013). "Generation of Integration-free and Region-Specific Neural Progenitors from Primate Fibroblasts." Cell Reports **3**(5): 1580-1591.
Lupo, G., M. Bertacchi, et al. (2014). "From pluripotency to forebrain patterning: an in vitro journey astride embryonic stem cells." Cellular and Molecular Life Sciences **71**(15): 2917-2930.
Müller, T., H. Brohmann, et al. (2002). "The Homeodomain Factor Lbx1 Distinguishes Two Major Programs of Neuronal Differentiation in the Dorsal Spinal Cord." Neuron **34**(4): 551-562.
Maria Patestas, L. P. G. (2006). A Textbook of Neuroanatomy.1st Edition, Blackwell Science Ltd.
Maroof, Asif M., S. Keros, et al. (2013). "Directed Differentiation and Functional Maturation of Cortical Interneurons from Human Embryonic Stem Cells." Cell Stem Cell **12**(5): 559-572.
Massagué, J. and Q. Xi (2012). "TGF-β control of stem cell differentiation genes." FEBS Letters **586**(14): 1953-1958.
Masui, S., Y. Nakatake, et al. (2007). "Pluripotency governed by Sox2 via regulation of Oct3/4 expression in mouse embryonic stem cells." Nat Cell Biol **9**(6): 625-635.
Mayor, R. and E. Theveneau (2014). "The role of the non-canonical Wnt–planar cell polarity pathway in neural crest migration." Biochemical Journal **457**(1): 19-26.
Mercader, A. e. a. (2008). Human embryo culture, Academic Press.
Moya, N., J. Cutts, et al. (2014). "Endogenous WNT Signaling Regulates hPSC-Derived Neural Progenitor Cell Heterogeneity and Specifies Their Regional Identity." Stem Cell Reports **3**(6): 1015-1028.
Nakamura, H. (2001). "Regionalization of the optic tectum: combinations of gene expression that define the tectum." Trends Neurosci **24**(1): 32-39.
Nakano, T., H. Kodama, et al. (1994). "Generation of lymphohematopoietic cells from embryonic stem cells in culture." Science **265**(5175): 1098-1101.
Neely, M. D., M. J. Litt, et al. (2012). "DMH1, a Highly Selective Small Molecule BMP Inhibitor Promotes Neurogenesis of hiPSCs: Comparison of PAX6 and SOX1 Expression during Neural Induction." ACS Chemical Neuroscience **3**(6): 482-491.
Nusse, R. (2008). "Wnt signaling and stem cell control." Cell Res **18**(5): 523-527.
Park, D., A. P. Xiang, et al. (2010). "Nestin is required for the proper self-renewal of neural stem cells." Stem Cells **28**(12): 2162-2171.
Patten, I. and M. Placzek (2000). "The role of Sonic hedgehog in neural tube patterning." Cell Mol Life Sci **57**(12): 1695-1708.

Perrier, A. L., V. Tabar, et al. (2004). "Derivation of midbrain dopamine neurons from human embryonic stem cells." Proceedings of the National Academy of Sciences of the United States of America **101**(34): 12543-12548.
Pevny, L. H., S. Sockanathan, et al. (1998). "A role for SOX1 in neural determination." Development **125**(10): 1967-1978.
Quiñinao, C., A. Prochiantz, et al. (2015). "Local homeoprotein diffusion can stabilize boundaries generated by graded positional cues." Development **142**(10): 1860-1868.
Racaniello, V. (2015, 23th of April 2015). "Retroviral influence on human embryonic development." Retrieved 26th of January 2016, 2016, from http://www.virology.ws/2015/04/23/retroviral-influence-on-human-embryonic-development/.
Reinhardt, P., M. Glatza, et al. (2013). "Derivation and Expansion Using Only Small Molecules of Human Neural Progenitors for Neurodegenerative Disease Modeling." PLoS ONE **8**(3): e59252.
Reubinoff, B. E., P. Itsykson, et al. (2001). "Neural progenitors from human embryonic stem cells." Nat Biotech **19**(12): 1134-1140.
Ross, S. and C. S. Hill (2008). "How the Smads regulate transcription." The International Journal of Biochemistry & Cell Biology **40**(3): 383-408.
Sander, K. and P. E. Faessler (2001). "Introducing the Spemann-Mangold organizer: experiments and insights that generated a key concept in developmental biology." Int J Dev Biol **45**(1): 1-11.
Shrestha, S. (2010). "Neural Tube Defects (NTD)." Retrieved 10th of February, 2016, from http://medchrome.com/basic-science/anatomy/neural-tube-defects-ntd/.
Siegel, A. (2013). Ethics of Stem Cell Research. The Stanford Encyclopedia of Philosophy. E. N. Zalta.
Simona Casarosa, J. Z. a. L. C. (2013). Systems for ex-vivo Isolation and Culturing of Neural Stem Cells,Chapter 1. Neural Stem Cells - New Perspectives. L. Bonfanti, InTech**:** 428.
Smith, J. L. and G. C. Schoenwolf (1989). "Notochordal induction of cell wedging in the chick neural plate and its role in neural tube formation." J Exp Zool **250**(1): 49-62.
Smith, J. R., L. Vallier, et al. (2008). "Inhibition of Activin/Nodal signaling promotes specification of human embryonic stem cells into neuroectoderm." Developmental Biology **313**(1): 107-117.
Spence, J. R., C. N. Mayhew, et al. (2011). "Directed differentiation of human pluripotent stem cells into intestinal tissue in vitro." Nature **470**(7332): 105-109.
Stiles, J. (2008). The fundamentals of brain development: Integrating nature and nurture, Harvard University Press.
Stiles, J. and T. L. Jernigan (2010). "The Basics of Brain Development." Neuropsychology Review **20**(4): 327-348.
Surmacz, B., H. Fox, et al. (2012). "Directing differentiation of human embryonic stem cells toward anterior neural ectoderm using small molecules." Stem Cells **30**(9): 1875-1884.
Suzuki, I. K. and P. Vanderhaeghen (2015). "Is this a brain which I see before me? Modeling human neural development with pluripotent stem cells." Development **142**(18): 3138-3150.
Takahashi, K., K. Tanabe, et al. (2007). "Induction of Pluripotent Stem Cells from Adult Human Fibroblasts by Defined Factors." Cell **131**(5): 861-872.
Takahashi, K. and S. Yamanaka (2006). "Induction of Pluripotent Stem Cells from Mouse Embryonic and Adult Fibroblast Cultures by Defined Factors." Cell **126**(4): 663-676.
Thomson, M., Siyuan J. Liu, et al. (2011). "Pluripotency Factors in Embryonic Stem Cells Regulate Differentiation into Germ Layers." Cell **145**(6): 875-889.
Thwaites JW, R. L., Mason C, Dalby P, Habib N, Jaccard N, Szita N and Wall I. (2014). "Influence of Initial Seeding Density on Gene Expression during Neuronal Priming." Bioprocessing & Biotechniques.

van Amerongen, R. and R. Nusse (2009). "Towards an integrated view of Wnt signaling in development." Development **136**(19): 3205-3214.
Vazin, T., K. A. Ball, et al. (2014). "Efficient derivation of cortical glutamatergic neurons from human pluripotent stem cells: A model system to study neurotoxicity in Alzheimer's disease." Neurobiology of Disease **62**: 62-72.
Villapol, S., T. T. Logan, et al. (2013). Role of TGF-β Signaling in Neurogenic Regions After Brain Injury.
Wassarman, K. M., M. Lewandoski, et al. (1997). "Specification of the anterior hindbrain and establishment of a normal mid/hindbrain organizer is dependent on Gbx2 gene function." Development **124**(15): 2923-2934.
Wilson, P. A., G. Lagna, et al. (1997). "Concentration-dependent patterning of the Xenopus ectoderm by BMP4 and its signal transducer Smad1." Development **124**(16): 3177-3184.
Wolpert, L. (1969). "Positional information and the spatial pattern of cellular differentiation." Journal of Theoretical Biology **25**(1): 1-47.
Xu, L. (2006). "Regulation of Smad activities." Biochimica et Biophysica Acta (BBA) - Gene Structure and Expression **1759**(11–12): 503-513.
Yu, J., M. A. Vodyanik, et al. (2007). "Induced Pluripotent Stem Cell Lines Derived from Human Somatic Cells." Science **318**(5858): 1917-1920.
Zaret, K. S. (2001). "Hepatocyte differentiation: from the endoderm and beyond." Current Opinion in Genetics & Development **11**(5): 568-574.
Zhang, S.-C., M. Wernig, et al. (2001). "In vitro differentiation of transplantable neural precursors from human embryonic stem cells." Nat Biotech **19**(12): 1129-1133.
Zhou, G., R. Myers, et al. (2001). "Role of AMP-activated protein kinase in mechanism of metformin action." The Journal of Clinical Investigation **108**(8): 1167-1174.
Zhou, J., P. Su, et al. (2010). "High-Efficiency Induction of Neural Conversion in hESCs and hiPSCs with a Single Chemical Inhibitor of TGF-β Superfamily Receptors." Stem Cells (Dayton, Ohio) **28**(10): 1741-1750.
Zhou, T., C. Benda, et al. (2012). "Generation of human induced pluripotent stem cells from urine samples." Nat. Protocols **7**(12): 2080-2089.

Appendix 1 - Materials

Material	Catalog #	Supplier
12-well plates	3513	Corning
96-well plates	353219	Corning
8-strip PCR tubes	14-222-250	Fisher Scientific
8-strip PCR caps	14-222-265	Fisher Scientific

Appendix 2 - Reagents

Reagent	Catalog #	Supplier
DMEM/F12 + Glutamax	31331-028	Life Technologies
Neurobasal	21103-049	Life Technologies
β-mercaptoethanol	21985-023	Life Technologies
B27	0080085-SA	Life Technologies
N2	17502-048	Life Technologies
noggin	120-10C	Peprotech
SB43152	S4317	Sigma Aldrich
CHIR99021	4423	Stemgent
PDO0325901	04-0006	Stemgent
b-Fibroblast Growth Factor (b-FGF)	100-18B	Life Technologies
Epidermal Growth Factor (EGF)	E9644	Sigma Aldrich
Nutristem® hESC XF	05-100-1A	Biological Industries
Phosphate-buffered Saline w/ Ca^{2+},Mg^{2+}	14080-048	Life Technologies
Phosphate-buffered Saline w/o Ca^{2+},Mg^{2+}	14190-144	Life Technologies
TrypLE™ Select Enzyme	12536-029	Life Technologies
DAPI (4',6-diamino-2-phenylindole)	D3571	Life Technologies
LN-521™ hrLaminin 521	LN-521™	Biolamina
Paraformaldehyde 4%	9713.1000	VWR
Y-27632 (Rock Inhibitor)	688000	Calbiochem
Poly Ornithine	P3655	Sigma Aldrich
L2020	L2020	Sigma Aldrich
Triton X-100 (1%)	HFH-10	Life technologies
RNeasy mini kit	74106	Qiagen
High capacity cDNA Synthesis Kit	4374967	Applied Biosystems
Taqman® Fast Advanced Master Mix	4444558	Life Technologies

Appendix 3 - Seeding densities on day 4 for the standard protocol

Percentage	10^3 Cells/cm^2
20%	63
30%	95
40%	127
50%	159
60%	190